Some studies of the reactions of aromatic nitro compounds with nitrogen and carbon nucleophiles

Asghar, Basim Hussain

Some Studies of the Reactions of Aromatic Nitro-Compounds with Nitrogen and Carbon Nucleophiles

Basim Hussain Asghar

Thesis submitted for the qualification

Doctor of Philosophy (PhD.)

Supervised by: Dr. M. R. Crampton

Department of Chemistry

Ustinov College

University of Durham

July 2006

Contents

Abstract

Kinetic and equilibrium studies have been made of the reactions of a series of ring-substituted anilines with 1,3,5-trinitrobenzene (TNB) and with 4-nitrobenzofuroxan (4-NBF) in dimethyl sulfoxide (DMSO). There is evidence from ^{1}H NMR spectroscopy that in the presence of Dabco these reactions yield anionic σ-adducts. Kinetic studies are compatible with a two-step process involving initial nucleophilic attack by amine to give a zwitterionic intermediate which can transfer an acidic proton to Dabco. In the case of TNB the proton transfer step is rate-limiting due to the high rate of reversion of the zwitterion to reactants. Measurement of substituent effects shows that values of the equilibrium constant K_1 for the initial zwitterion formation decrease by a factor of *ca* 1000 as R, the ring substituent in the anilines, is changed from 4-OMe to 3-CN (ρ=-3.82), while values of K_{Dabco} for the proton transfer equilibrium increase by a similar factor (ρ=+3.62). Hence overall values of K_1K_{Dabco} show only a small variation with the nature of R.

Related studies with 4-NBF indicate that there is a balance between nucleophilic attack and proton transfer as the rate limiting step. This is due to the lower value for the rate of reversion of the zwitterion to reactants in the case of 4-NBF, relative to TNB. Values of K_{Dabco} are found to be larger for the 4-NBF reaction than for the TNB reaction, indicating greater electron withdrawing ability for the 4-NBF system than for TNB.

pK_a values in DMSO for the nine aniline derivatives used were measured using the proton transfer equilibrium with 2,4-dinitrophenol.

^{1}H NMR studies in d_6-DMSO show that the carbanions of nitromethane, nitroethane and 2-nitropropane add to 4-nitrobenzofurazan derivatives to give carbon-bonded σ-adducts. With time there is evidence for the base-catalysed elimination of nitrous acid from the adducts to yield anionic alkene derivatives. Kinetic and equilibrium results for the corresponding reactions in methanol have been measured. Three ring-substituted benzyl triflones were prepared and reactions of the carbanions formed from them with 4,6-dinitrobenzofuroxan, 1,3,5-trinitrobenzene and benzofurazan derivatives were examined. There is evidence for the initial formation of σ-adducts followed by rapid elimination of HSO_2CF_3. Rate constants for these reactions in methanol are reported.

Acknowledgments

All praise to God who guides us to knowledge and teaches us what we did not know. By his grace I have completed this work under the title "Some Studies of the Reactions of Aromatic Nitro-Compounds with Nitrogen and Carbon Nucleophiles".

I would like to thank my supervisor Dr. M. R. Crampton, Chemistry Department, University of Durham, who gave me all his time, advice, help, support and encouragement through this work. Thanks to all my colleagues and staff in the Department of Chemistry, University of Durham both in past and present for their help and support. I wish to express my thanks and gratitude to the University of Umm Al-Qura for giving me the opportunity to conduct this study and to the Ministry of Education, Kingdom of Saudi Arabia for financial support. I am especially grateful to Prof. Kamal Halwani, Dr. Abdullatif Ujaimi and Prof. Hussni Muathin, Department of Chemistry, University of Umm Al-Qura, Kingdom of Saudi Arabia for their help, advice and support. I must acknowledge Prof. Ezzat Hamed, Department of Chemistry, Alexandria University, Egypt for his encouragement and help before the start of this work. My sincere thanks to my wife Abrar Raies for her support and patience during this work. Especial thanks to my parents, my brothers, my sister, all my relatives for their continuous encouragement and support. Many thanks to my friends both past and present, especially to Mohammed Al-Hussini for his continued support until the end of this work.

بسم الله الرحمن الرحيم

الحمد لله رب العالمين. الحمدلله الذي بنعمته تتم الصالحات والصلاة والسلام على خاتم الانبياء والمرسلين وعلى اله وصحبه اجمعين وبعد:

الشكر لله اولا واخيرا على اتمامي لرسالة الدكتوراة في مجال الكيمياء العضوية الفيزيائية تحت عنوان "دراسة بعض تفاعلات مركبات النيترو الأروماتية مع النيتروجين والكربون النيكلوفيلية".

أحب أن أشكر مشرفي الدكتور مايكل كرامبتون قسم الكيمياء بجامعة درم بانجلترا على مساعدته ووقفته الدائمة معي ودعمه الكبير حتى تم انجاز هذا العمل.

الشكر الأكبر لوالدي ووالدتي الذين لم يقصروا في دعواتهم وتشجيعهم ودعمهم المستمر.

شكرا لزوجتي ام وسام لوقفتها وصبرها طوال فترة البعثة وفرحتي بقدوم وسام كانت في نفس اليوم اللي بدات فية الدراسة.

ايضا اقدم شكري لوزارة التعليم العالي جامعة ام القرى على الابتعاث والدعم.

الشكر للزملاء وخاصة الذين وقفوا معي من اساتذتي في جامعة ام القرى، قسم الكيمياء، أ.د كمال حلواني، د. عبداللطيف العجيمي، أ.د حسني مؤذن ومن جامعة الأسكندرية أ.د عزت عوض .

شكر خاص لأخوتي وجميع أقاربي ولاصدقائي ولكل من سأل وساندني وشجعني طوال فترة الدراسة والغربة.

Declaration

The work in this thesis was carried out in the Department of Chemistry at the University of Durham between 1st October 2003 and 30th September 2006. It has not been submitted for any other degree and is the author's own work, except where acknowledged by reference.

Copyright

Abbreviations

TNB	1,3,5-Trinitrobenzene
2.1, 3.2	Substituted aniline
DNP	2,4-Dinitrophenol
DMSO	Dimethyl sulfoxide
DNBF	4,6-Dinitrobenzofuroxan
4-NBF, 5.10	4-Nitrobenzofuroxan
4.2, 5.9	4-Nitrobenzofurazan
4.3, 5.11	7-Chloro-4-nitrobenzfurazan
4.4	7-Methoxy-4-nitrobenzofurazan
4.5	Nitromethane
4.6	Nitroethane
4.7	2-Nitropropane
5.1	Benzyl triflone
5.2	4-Trifluoromethylbenzyl triflone
5.3	4-Cyanomethylbenzyl triflone
δ / ppm	Chemical shift / parts per million
ε	Extinction coefficient
J / Hz	Coupling constant / Hertz
λ / nm	Wavelength / nanometer
MeOH	Methanol
MeONa	Sodium methoxide
m.p.	Melting point
NMR	Nuclear magnetic resonance
UV	Ultraviolet

Chapter One:

Introduction

Chapter One: Introduction

1.1 Nucleophilic Aromatic Substitution Reactions

1.1.1 The Mechanism of Nucleophilic Aromatic Substitution Reactions

The most common mechanism of Nucleophilic Aromatic Substitution is shown in Scheme 1.1[1], where Nu^- represents an anionic nucleophile, L^- represents a leaving group or nucleofuge, and the symbol EWG is used to show the presence of one or more electron-withdrawing groups in the aromatic ring. The first step is attack of Nu^- on the aromatic electrophile at the carbon centre undergoing the substitution to produce an intermediate cyclohexadienyl anion of some stability. This intermediate, (also known as a σ-adduct) contains an sp^3 hybridized carbon atom. The energy of the intermediate will be determined by the number and type of electron-withdrawing groups, the leaving group L, and the nature of the attacking nucleophile, Nu^-.

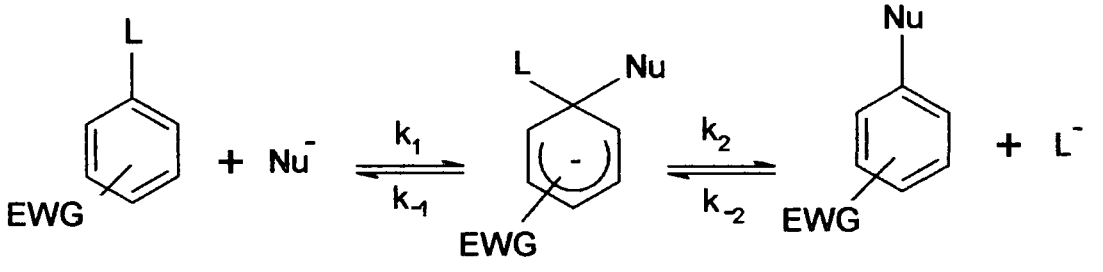

Intermediate

Scheme 1.1

The energy diagrams of Figure 1.1 show that depending on the relative energies of the two transition states, either the formation or the decomposition of the σ-adduct may be rate limiting[1].

Figure 1.1 Energy diagrams for nucleophilic aromatic substitution reactions of Scheme 1.1, (**a**) rate-limiting formation, and (**b**) rate limiting decomposition of the intermediates.

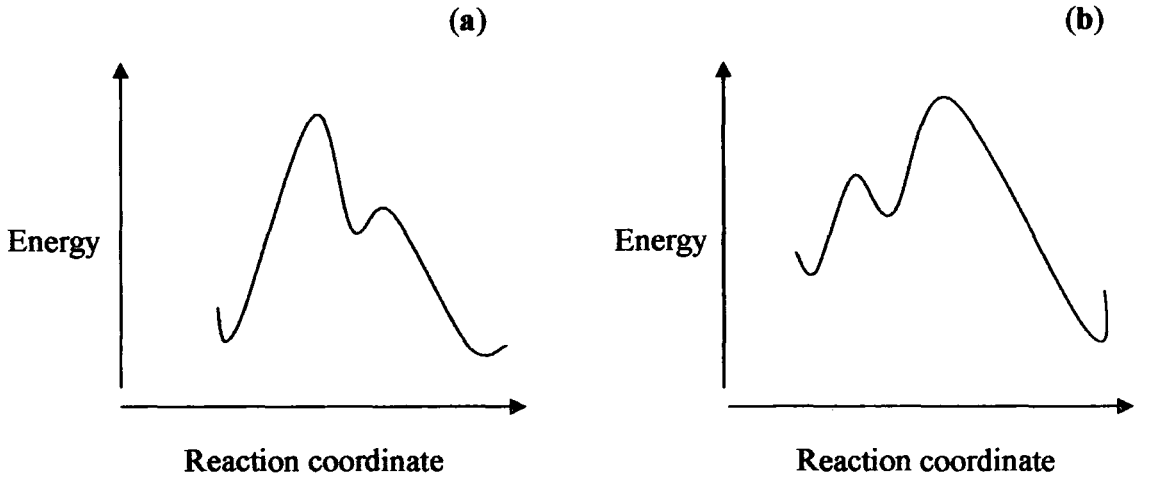

Case (**a**) is usually observed when L = Cl, Br so that a stable anion Cl^-, Br^- is formed. Case (**b**) occurs when the leaving group L^- is a poor nucleofuge, such as H^-, which is unstable in solution. In this case the intermediate may have a lifetime sufficiently long for it to be observed. When the attacking nucleophile is neutral (e.g., water, alcohol, amines), the initially formed σ-adduct is zwitterionic and contains an acidic proton, Scheme 1.2, which is removed by a base that can be the nucleophile itself.

As a result, conversion to products can occur by uncatalysed or base-catalysed pathways[1].

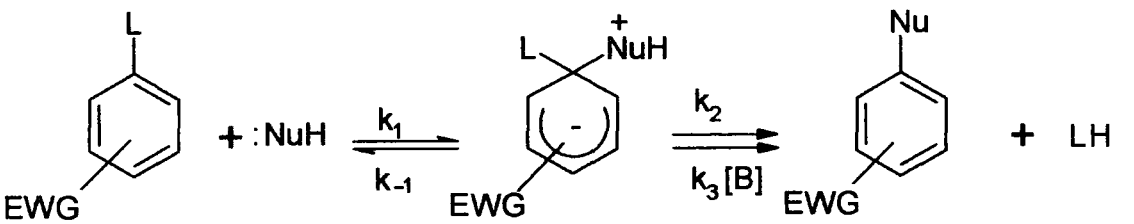

1.2

Scheme 1.2

1.1.2 σ-Adduct Intermediates

It was in 1900 that Jackson and Gazzolo first attributed quinoid resonance structures, **1.3** and **1.4**, to the product formed in the reaction between 2,4,6-trinitroanisole (TNA) and sodium methoxide[2].

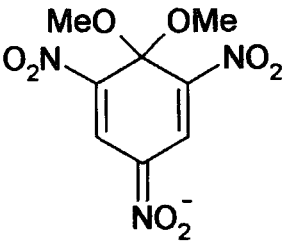

1.3

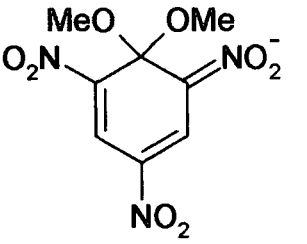

1.4

Convincing evidence for the covalently-bound structure **1.5** was provided by Meisenheimer who showed that the same product was produced by reaction of 2,4,6-trinitroanisole (TNA) with ethoxide ions and of 2,4,6-trinitrophenetole (TNP) with methoxide ion[3].

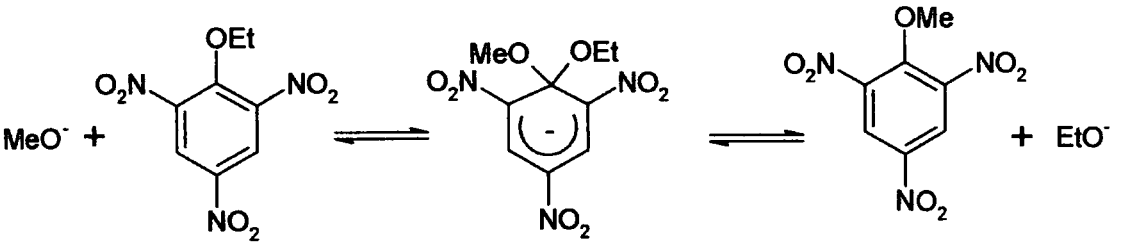

TNP **1.5** TNA

Scheme 1.3

Confirmation of the σ-adduct structure was obtained in 1964 with the availability of ^{1}H NMR spectroscopy[4].

Although the adducts formed are usually strongly coloured, it is often difficult to draw clear conclusions as to the nature of the adduct from the UV/visible spectra. In the case of TNA ^{1}H NMR measurements have shown that isomeric addition is possible. Thus the spectrum initially produced in the presence of methoxide is that of the 1,3-adduct **1.7** and this slowly rearranges to give the 1,1-adduct. In **1.7** the hydrogen at the position of attack shows a large change from δ 9.1 to δ 6.1 ppm corresponding to the change in hybridisation.

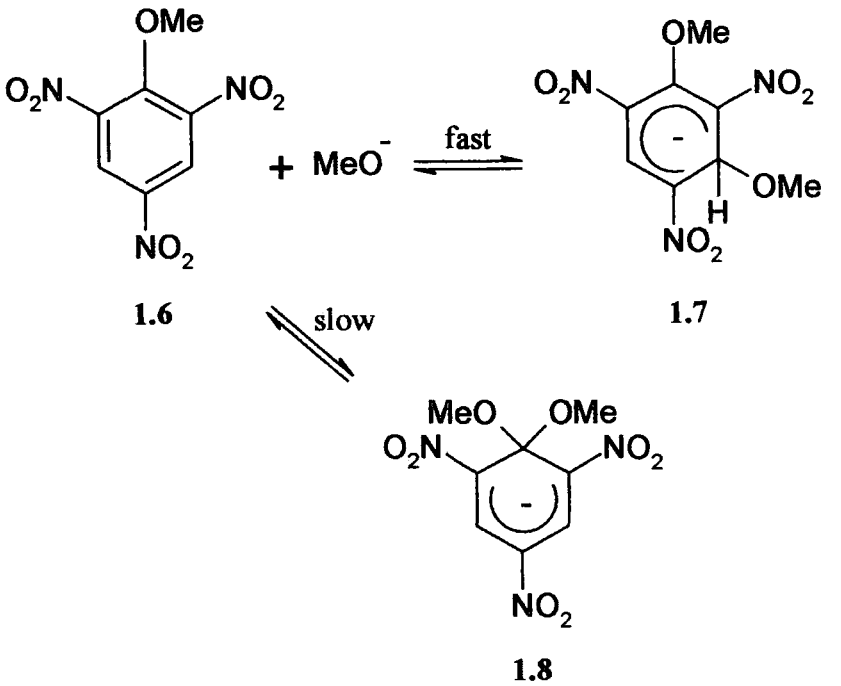

Scheme 1.4

Several others studies have shown that nucleophilic attack is generally faster at unsubstituted ring positions compared with attack at similarly activated substituted positions. For example as shown in Scheme 1.5 the observable species is **1.9** rather than **1.10**[5,6], where L = Cl, Br and Nu = OH^-, OMe^-.

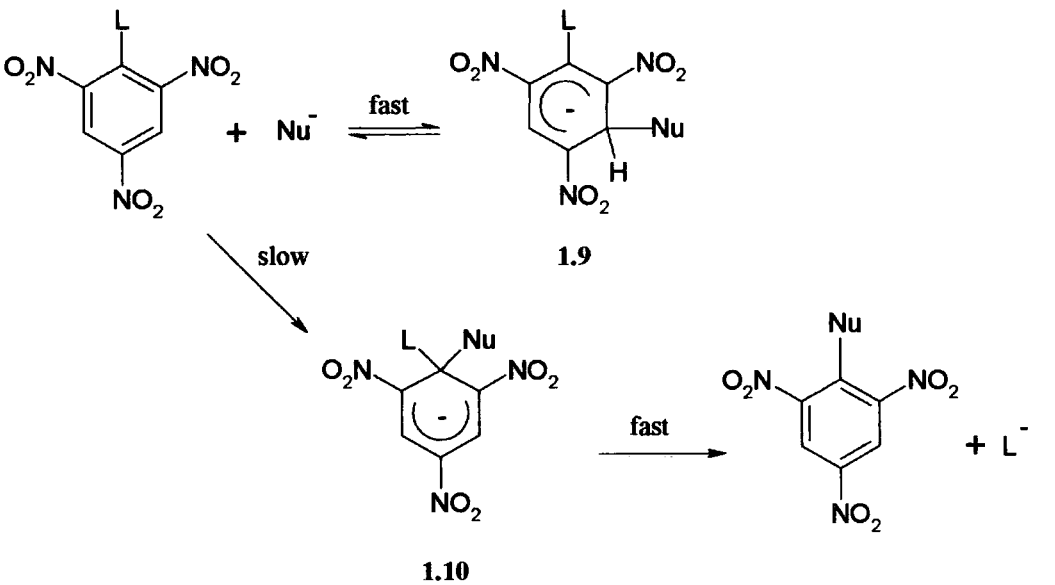

Scheme 1.5

1.1.3 Nitrogen Nucleophiles

Early work found evidence for a number of possible interactions between 1,3,5-trinitrobenzene (TNB) and aliphatic amines. Strong evidence that in dimethyl sulfoxide (DMSO) reaction involved the two stages shown in Scheme 1.6 was provided by ^{1}H NMR measurements and by conductivity measurements[7].

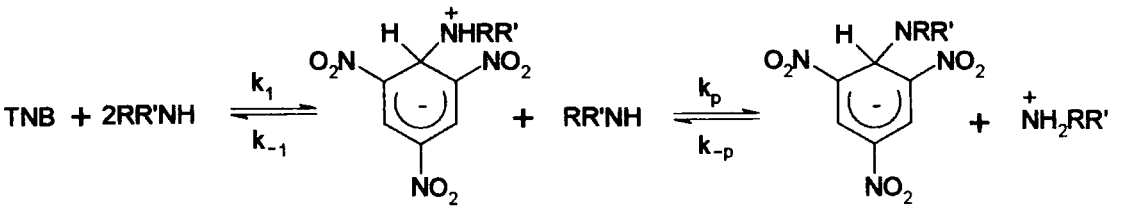

1.11 **1.12**

Scheme 1.6

Initial formation of the zwitterion **1.11** is followed by proton transfer to give the anionic adduct **1.12**. Initially in 1970 Bernasconi[8] reported a kinetic study of the reaction in water-dioxan in which the data were interpreted on the assumption that the proton transfer between **1.11** and **1.12** is always rapid[7]. However later work in both water-dioxan[9] and in DMSO[10] showed that proton transfer may be the rate-limiting step. In DMSO values of k_p were found to vary from 3×10^7 dm^3 mol^{-1} s^{-1} with butylamine to 5×10^4 dm^3 mol^{-1} s^{-1} with piperidine. This decrease in value was attributed to the greater steric hindrance involved with the secondary amine. Hence proton transfer is more likely to be rate determining with bulky amines.

When the parent nitro-compound contains a good leaving group, then nucleophilic displacement may occur. Here the mechanism is shown in Scheme 1.7 where k_2 represents uncatalysed decomposition of the zwitterionic intermediate **1.13** and k_3 [B] represents a base catalysed pathway. Z electron-withdrawing substituent(s) represents.

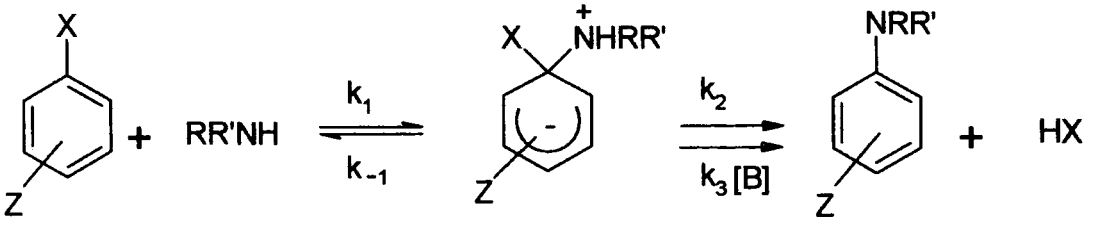

1.13

Scheme 1.7

There is evidence for two possible mechanisms of base catalysis. These are known as the SB-GA and RLPT mechanisms and are shown in Scheme 1.8[1]. Here SB-GA represents specific base-general acid and RLPT represents rate limiting proton-transfer.

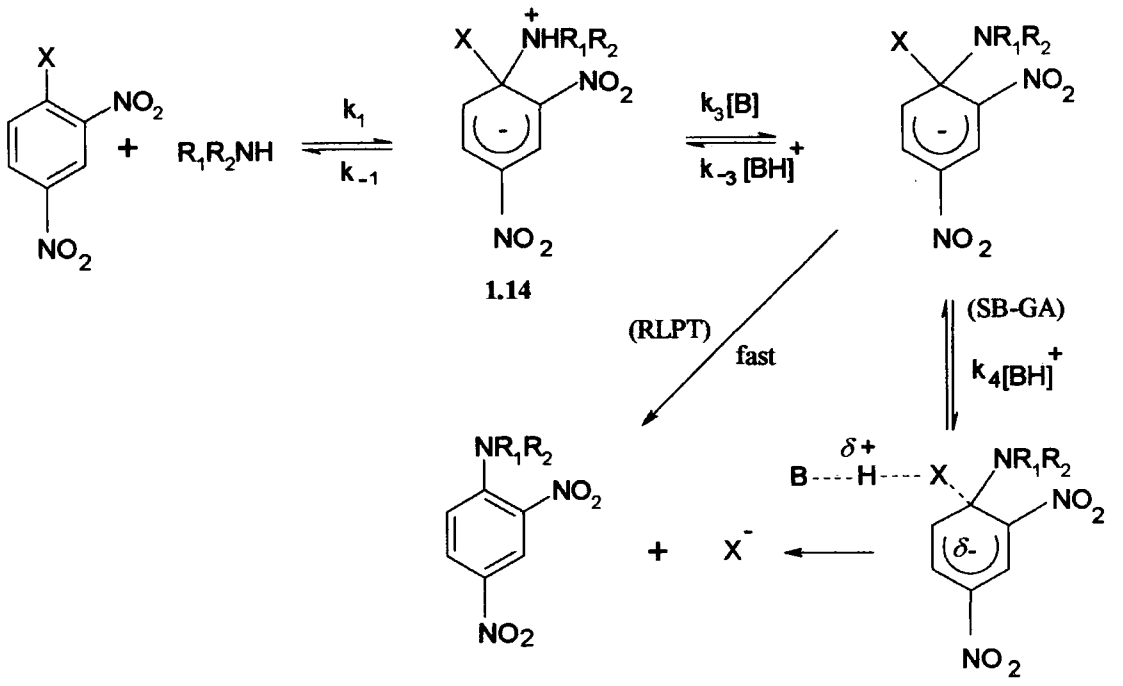

Scheme 1.8

The effect of the base is to deprotonate the initially formed zwitterion **1.14**, which may decay spontaneously (RLPT) or with the aid of general acid catalysis (SB-GA)[1]. The evidence is that the nature of the rate determining step may depend on the leaving group. Thus with good leaving groups, such as phenoxide[11], it is the proton transfer from the zwitterion which is rate limiting, while with poorer leaving groups, such as alkoxides, the SB-GA mechanism applies.

1.1.4 Aniline Derivatives

Aniline and its derivatives are very much weaker bases (pK_a = 3-5)[12] than are aliphatic amines (pK_a = 9-10)[10] and adducts have only been observed from TNB in the presence of a strong base.

Buncel and co workers showed by use of ^1H NMR spectroscopy, that reaction of the TNB–methoxide σ-adduct with aniline[13], or with ring-substituted anilines[14] resulted in the formation of TNB-anilide adducts such as **1.15**.

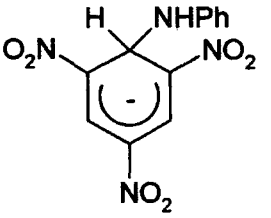

1.15

Mechanistic studies[15,16] showed that this was likely to involve a dissociative mechanism as shown in Scheme 1.9. The initial step involves dissociation to give free TNB which may then be attacked by aniline.

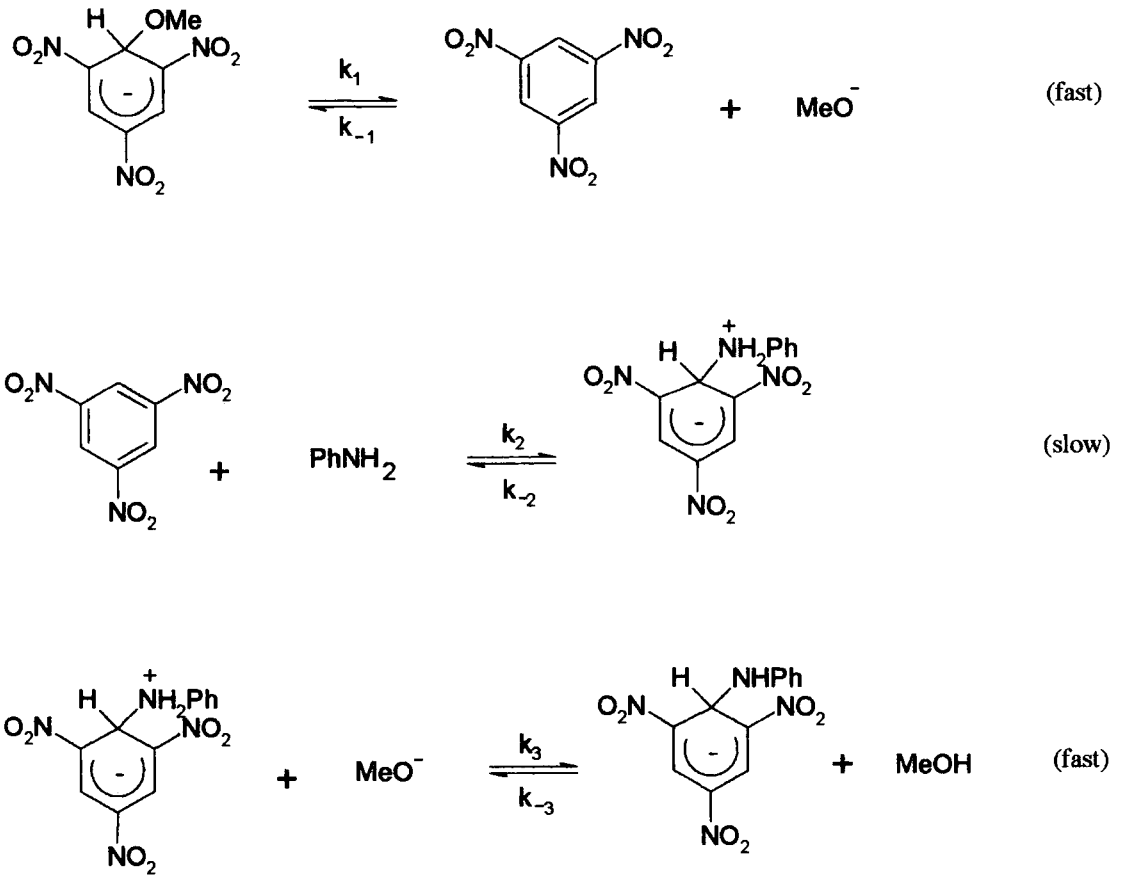

Scheme 1.9[16]

It was later found that **1.15** may be formed directly from TNB and aniline in DMSO in the presence of Dabco, to act as a proton acceptor. The reaction involves two steps, as shown in Scheme 1.10.

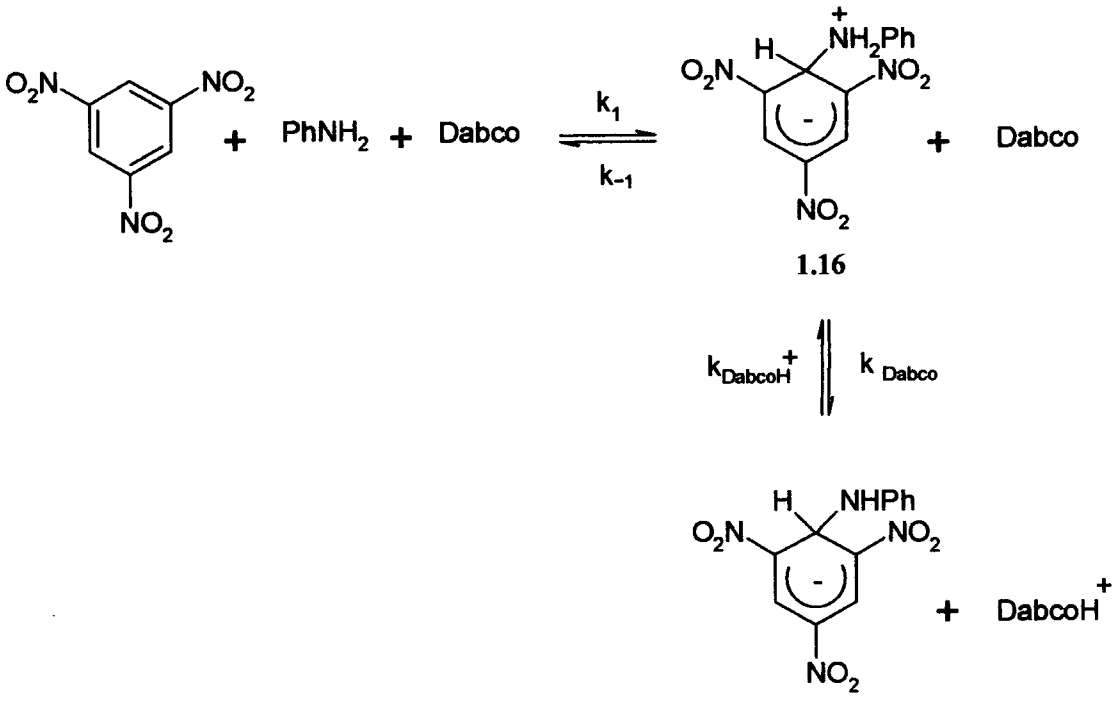

Scheme 1.10

The first step is thermodynamically unfavourable due to the weak basicity of aniline but the presence of a strong base makes the proton transfer step sufficiently favourable to allow formation of anionic adduct[18]. Nevertheless, kinetic studies[19,20] showed that the proton transfer from the zwitterion **1.16** is rate limiting, corresponding to the condition $k_{-1} > k_{Dabco}$ [Dabco].

Buncel et al were able to measure a value of *ca* 10 $dm^3\ mol^{-1}\ s^{-1}$ for $k_{DabcoH+}$ and assumed that the value of k_{Dabco} would be close to the diffusion-controlled limit[19] of 10^9 $dm^3\ mol^{-1}\ s^{-1}$. Proton transfer is rate limiting due to the instability of the zwitterion leading to a rapid rate for its decomposition back to reactants.

Further work[20] indicated only a small kinetic isotope effect, $\frac{k_H}{k_D} \sim 1.1$, when aniline was replaced with its deuterated derivative $PhND_2$. This was interpreted as evidence for a concerted mechanism of proton transfer involving the transition state **1.17**.

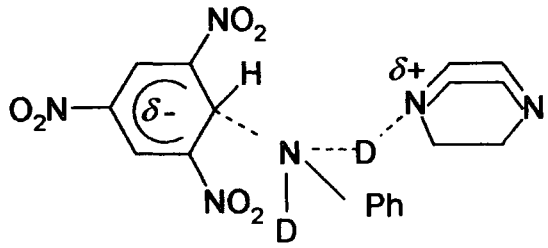

1.17

The reaction shown in Scheme 1.10 will be expected to show a salt effect since it results in the formation of ions from neutral reagents. Buncel et al[21] showed that in addition there was a specific effect in the presence of Et_4NCl, tetraethylammonium chloride, this was attributed to stabilisation of the $DabcoH^+$ ions by ion-pairing with chloride ion **1.18**.

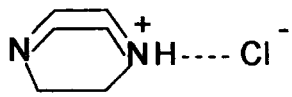

1.18

Values of the equilibrium constant K_1K_{Dabco} were found to increase by a factor of *ca* 100 in the presence of 1 mol dm^{-3} chloride.

There is also clear kinetic evidence for rate limiting proton transfer in the reaction of TNB with aliphatic amines[9,10,22]. Rate limiting proton transfer is also involved when substitution involves the specific base general acid catalysis mechanism (SB-GA), in which leaving group expulsion is the overall rate limiting step[18].

Scheme 1.11

Aniline and its substituted derivatives usually act as nitrogen nucleophiles. For example in the formation of σ-adducts from 1,3,5-trinitrobenzene (TNB) in dimethyl sulfoxide (DMSO) in the presence of a strong base. Nevertheless its ambident reactivity indicated in Scheme 1.11 has been shown in reaction with dinitrobenzofuroxan (DNBF)[23].

DNBF has been shown to have extremely high electrophilic reactivity, around 10 orders of magnitude higher than that of TNB[24] and with DNBF reaction occurs even in the absence of an additional strong base, such as Dabco. The reactions are shown in Scheme 1.12.

Formation of an N-bonded adduct is kinetically favoured but the C-bonded adduct is eventually more thermodynamically stable. The adduct **1.21** has been shown to be in equilibrium with its deprotonated form **1.23**[12].

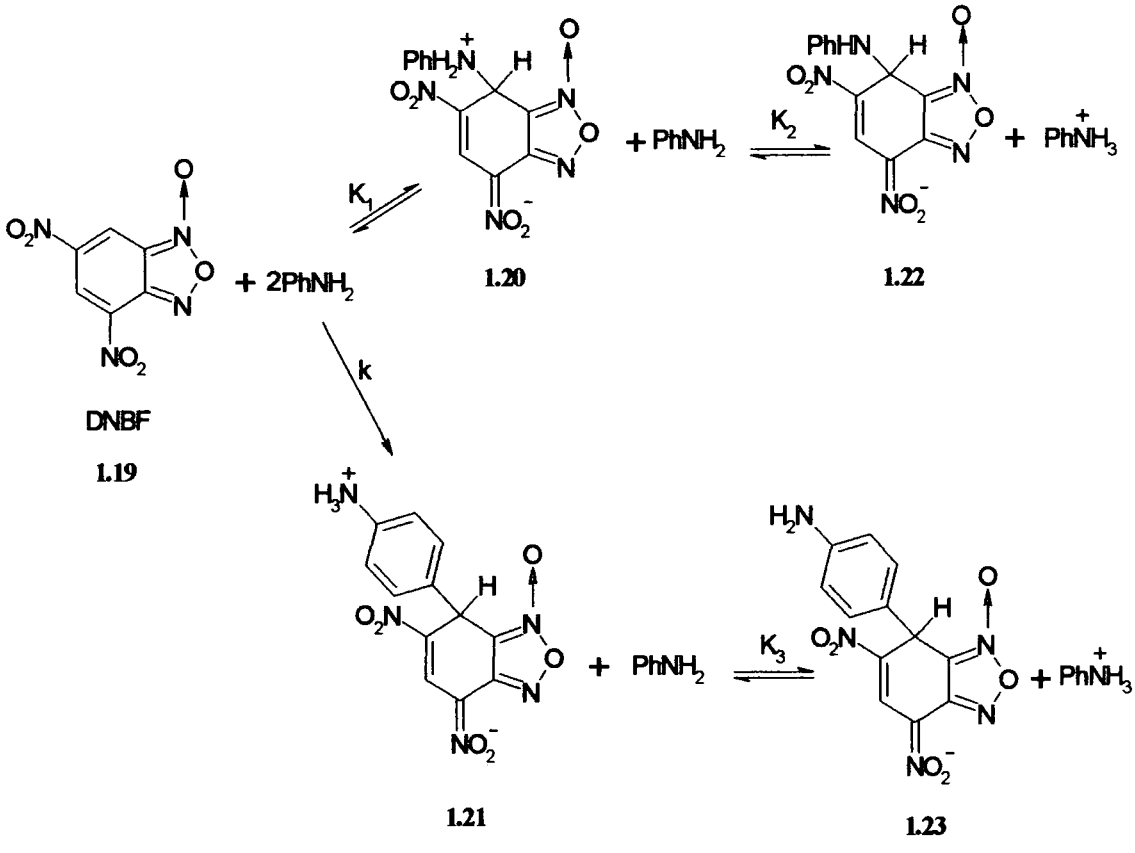

Scheme 1.12

1.2 Carbon-Nucleophiles

There have been many reports of the formation of carbon–bond σ-adducts[25,26,27,28]. These result from the reactions of a range of both anionic and neutral carbon nucleophiles[25]. Most studies have involved the determination of structures of the adducts formed and there are relatively few reports of detailed kinetic and equilibrium measurements. One problem here is the difficult in generating the nucleophiles under condition suitable for such studies.

One of the earliest nucleophiles examined was the cyanide ion[26]. Kinetic and equilibrium results in attack at an unsubstituted ring position in TNB to yield **1.24** have been reported in several different solvent systems.

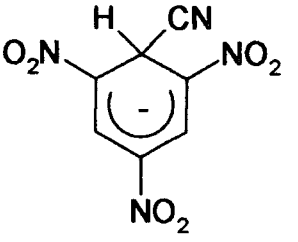

1.24

The reaction with 4-nitrobenzofuroxan was reported to give the adduct **1.25**[29]. However this assignment was made on the basis of UV data without corroboration from NMR measurements. In the light of present knowledge it seems likely that the process observed resulted from rapid attack at the 5-position of the 4-nitrobenzofuroxan[30].

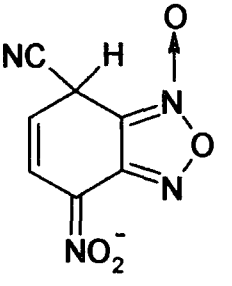

1.25

The pK_a value of HCN is 9.3[31] indicating that the cyanide ion is a relatively weak base in its reaction with protons. However in σ-adduct forming reactions involving carbon-carbon bond formation cyanide shows enhanced basicity. For example in methanol values of the equilibrium constant for reaction with TNB are reported as 39 $dm^3\ mol^{-1}$ for cyanide[32] and 23 $dm^3\ mol^{-1}$ for methoxide[33].

Enolate carbanions of various carbonyl derivatives such as ketones, aldehydes and esters have also been studied[34]. The reaction with TNB leads to adducts of general structure **1.26**, R_1R_2 = Alkyl; also enolate oxygen attack to give an oxygen–bonded adduct such as **1.27** has been observed. The ^1H NMR spectrum of **1.27** formed from TNB and the acetophenone enolate anion in acetonitrile-dimethoxyethane shows a band at 6.93 ppm for hydrogen at C_1. This is shifted considerably from the position of the corresponding hydrogen at 5.22 ppm in the carbon-bonded adduct[35].

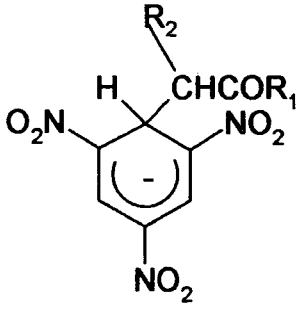

1.26

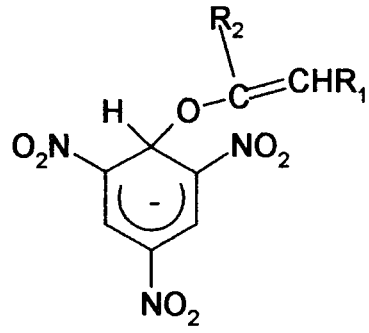

1.27

However adducts such as **1.27** are transient intermediates showing that the nucleophilic carbon of the enolate anion has much greater affinity than the enolate oxygen for the electrophilic carbon centre of the aromatic ring[35].

Formational of enolate complexes like **1.26** usually involves a two step process, as shown by equation 1.1 and equation 1.2 in which the carbanion is generated in a fast equilibrium prior to the rate-determining step[26].

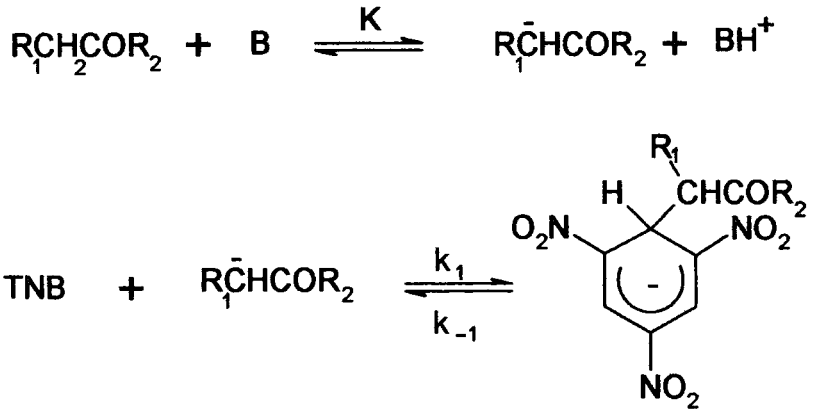

(1.1)

(1.2)

1.2.1 Ambident Nucleophiles

The ambident behaviour of phenoxide has been observed in σ-adduct formation as shown in Scheme 1.13 for the reaction with TNB[36,37]. While the formation of the aryloxide adduct **1.28** is reversible and occurs under kinetic control, that of the C-bonded adduct **1.30** is essentially irreversible due to the rearomatization of the quinoid type intermediate **1.29**. In general, the C-addition of the aromatic takes place preferentially at the 4-position of phenoxide ion but addition at the ortho position may occur with 4-substituted phenols[38].

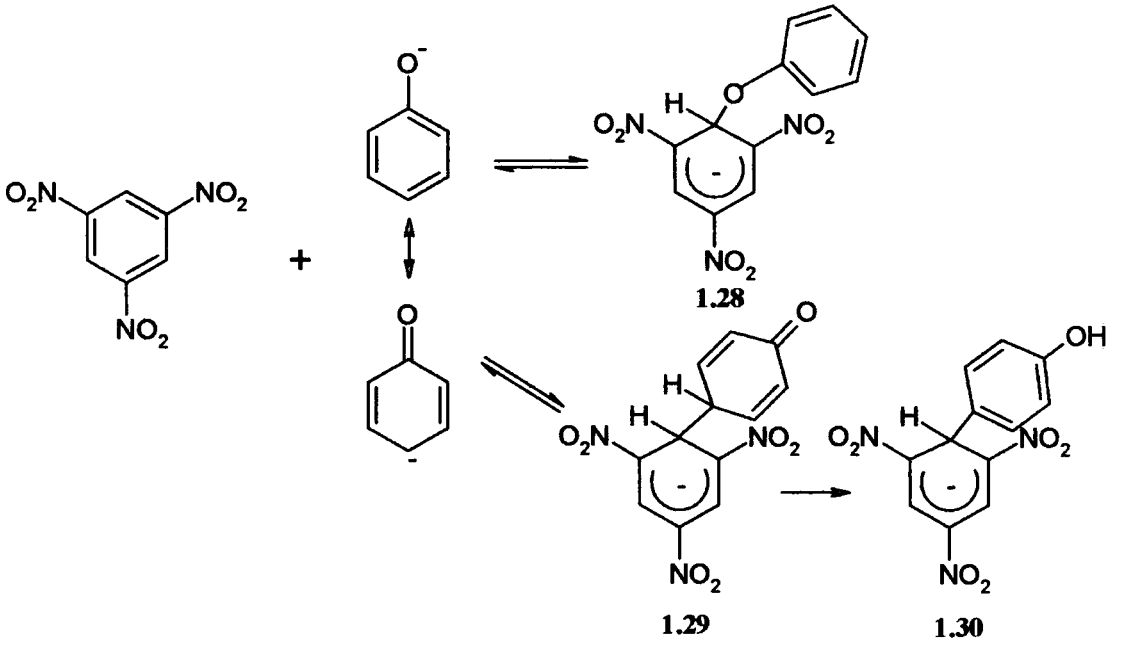

Scheme 1.13

Also, the ambident reactivity of aniline and its derivative was shown in Scheme 1.11.

1.2.2 Nitroalkanes

The earliest study of σ-adduct formation involving nitroalkane anions involved NMR measurement of their reaction with TNB in DMSO[39].

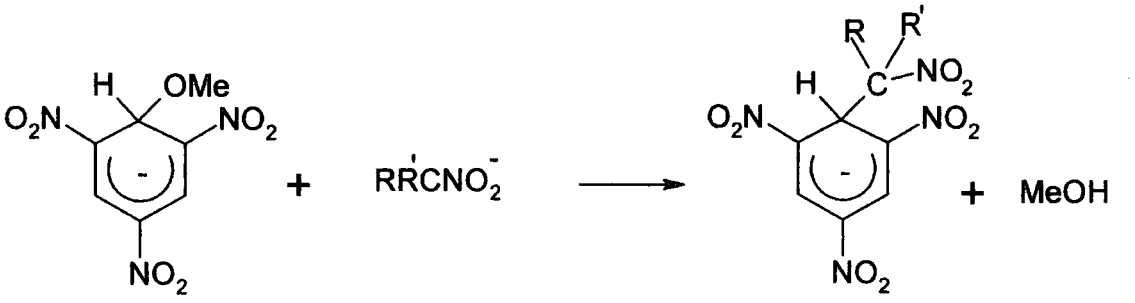

Scheme 1.14

Carbon-bound adducts were generated either by addition of triethylamine to TNB plus nitroalkane in DMSO or by addition of the nitroalkane to a solution of the methoxide adduct in DMSO, as shown in Scheme 1.14. Adducts were produced from nitromethane, nitroethane, 1-nitropropane and 2-nitropropane. The UV/visible maxima shift from 430 and 510 nm for methoxide adducts to 450 and 550 nm for the carbon adducts. The NMR spectrum of the adduct **1.31** from nitroethane gives resonances at δ 8.47 ppm, relative intensity 2, and 5.67 ppm, relative intensity 1, due to ring hydrogens, coupling J = 3.2 Hz was observed between H_b and H_c, although the resonances due to H_c and H_d were masked by solvent.

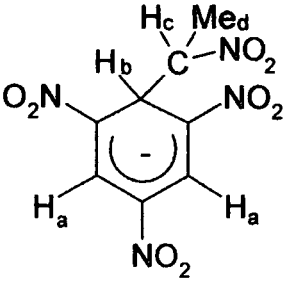

1.31

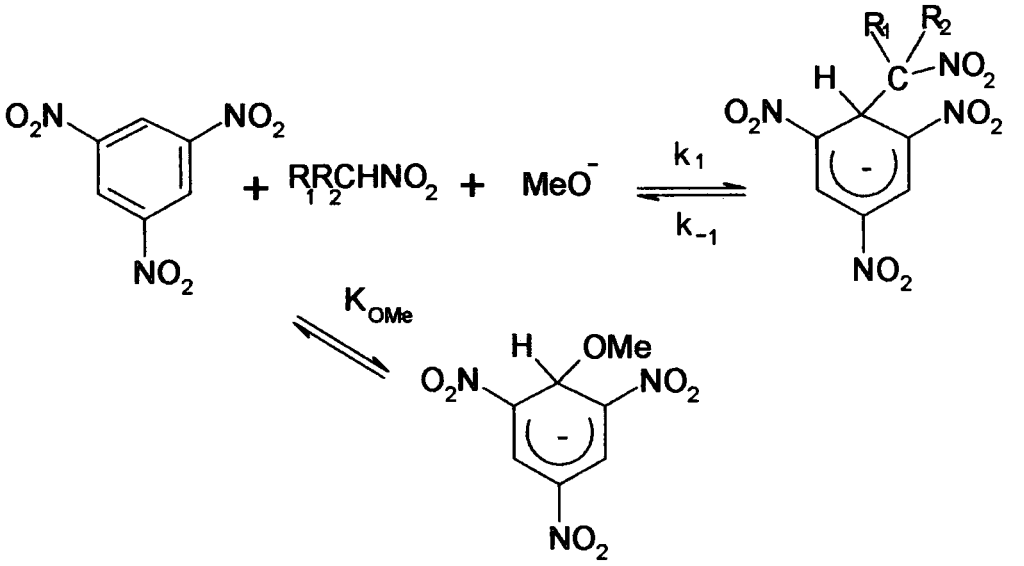

Scheme 1.15

Kinetic studies in methanol[40] were made by generating the nitroalkane anions using methoxide. Two processes were observed, a rapid reaction attributed to formation of the methoxide adduct and a slower reaction giving the carbon-adduct as shown in Scheme 1.15. The kinetic data for the slower process correspond to equation 1.3.

$$k_{obs} = \frac{k_1[R^1R^2CNO_2^-]}{1+K_{OMe}[OMe^-]} + k_{-1} \qquad \textbf{(1.3)}$$

Values obtained for k_1 and k_{-1} are given in the Table 1.1 where values for the methoxide reaction are given for comparison.

Table 1.1 Comparison of equilibrium and kinetic data for reactions in methanol.

Anion	pK_a	K_1 /dm^3 mol^{-1}	k_1 /dm^3 mol^{-1} s^{-1}	k_{-1} /s^{-1}
$CH_2NO_2^-$	15.6	7×10^4	800	0.011
$MeCHNO_2^-$	14.2	380	34	0.09
$Me_2CNO_2^-$	13.5	40	0.36	0.09
MeO^-	16.9	17	7050	305

Values of K_1 giving a measure of the carbon basicities of the nucleophiles, decrease in the order nitromethane>nitroethane>2-nitropropane and this is the same order as observed for proton basicities, as measured by pK_a values. However,

methoxide which has the highest proton basicity has a relatively low value for K_1 indicating that the carbon bases have considerably higher basicity than oxygen bases of similar proton basicity.

NMR studies have shown[41] that reaction of the superelectrophile 4,6-dinitrobenzofuroxan (DNBF) with carbanions of nitromethane, nitroethane, 1-nitropropane and 2-nitropropane in DMSO yield adducts at the 7-position. Kinetic measurement in water indicate that these adducts have high thermodynamic stabilities with values of equilibrium constant $\geq 10^9$ dm^3 mol^{-1}.

In the case of the nitroethane and 1-nitropropane systems, the complexation results in the formation of two chiral centres, at C-7 and C-8, leading to the observation of diastereoisomeric adducts **1.32** and **1.33** from 1-nitropropane.

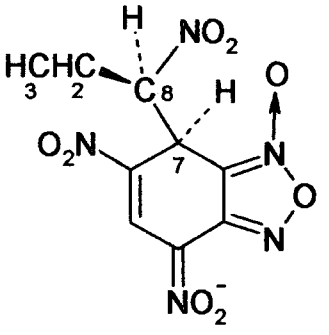

1.32

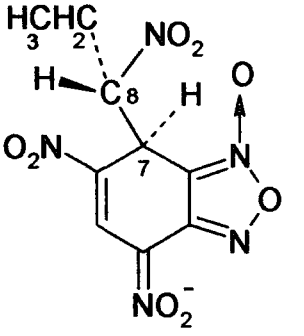

1.33

It is interesting that it was reported that the adducts underwent base catalysed elimination of nitrous acid to give alkene derivatives as shown in Scheme 1.16 for the 2-nitropropane adduct.

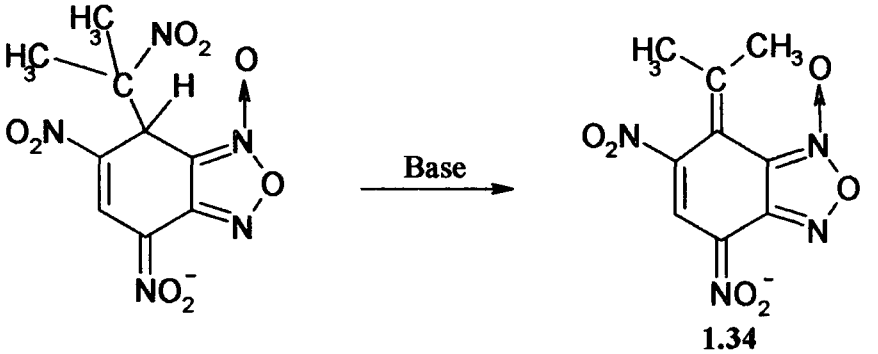

1.34

Scheme 1.16

The X-ray crystal structure of the 2-nitropropenide adduct has been reported[42] and shows a cis-configuration of the hydrogen and NO_2 substituents suggesting a syn-elimination process for the loss of nitrous acid.

1.2.3 Oxidation of Adducts

Terrier and co-workers found that protonation of **1.34**, which would result in formation of a neutral substitution product, is unsuccessful[41,43]. However electrochemical oxidation of the initially formed σ-adducts may result in the desired product. Thus it was found that electrochemical treatment of a series of nitropropenide adducts gave the neutral products as shown in Scheme 1.17. The results showed that the oxidation potentials involved were much higher than those for the corresponding process with nitrobenzene derivative.

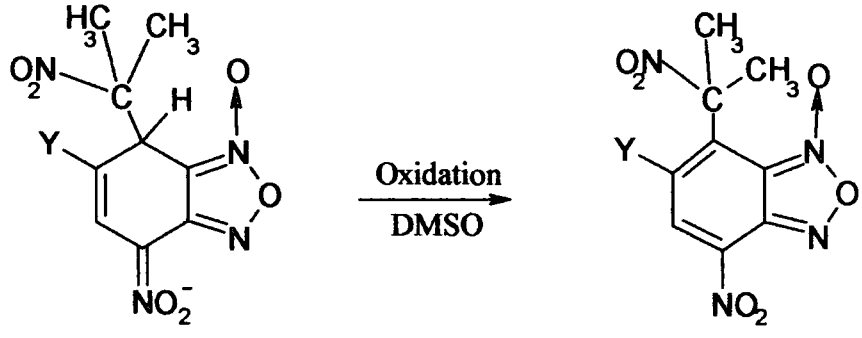

Y = NO_2, SO_2CF_3, CF_3, CN, H.

Scheme 1.17

It has also been shown[44] that powerful chemical oxidants including the Ce^{4+}/Ce^{3+} and MnO_4^-/Mn^{2+} couples, can effect oxidation of the σ-adducts. The products usually resulted from reaction at the 7-position of the benzofuroxan derivatives. However with 4-nitrobenzofuroxan isomeric addition of 2-nitropropenide at the 5- and 7-ring position was initially observed. However only the oxidised produced from the 7-adduct was isolated.

1.2.4 Vicarious Nucleophilic Substitution of Hydrogen (VS_NAr^H)

The direct nucleophilic substitution of hydrogen by nucleophiles is not a common process since the hydride ion H^- has low stability and is a poor leaving group[45]. However as shown in Scheme 1.17 oxidation of σ-adducts may result in formation of the substitution products. Also the base-catalysed elimination of nitrous acid from σ-adducts may, as shown in Scheme 1.16, result in loss of ring-hydrogen.

The latter is reminiscent of the vicarious mechanism of substitution pioneered by Makosza.

The vicarious substitution mechanism outlined in Scheme 1.18[46,47] involves the reaction of a nitro-activated aromatic compound with a carbanion stabilised by an electron-withdrawing group. Here rearomatization is afforded by eliminating a nucleofugal group, initially present at the reaction centre of the attacking nucleophile.

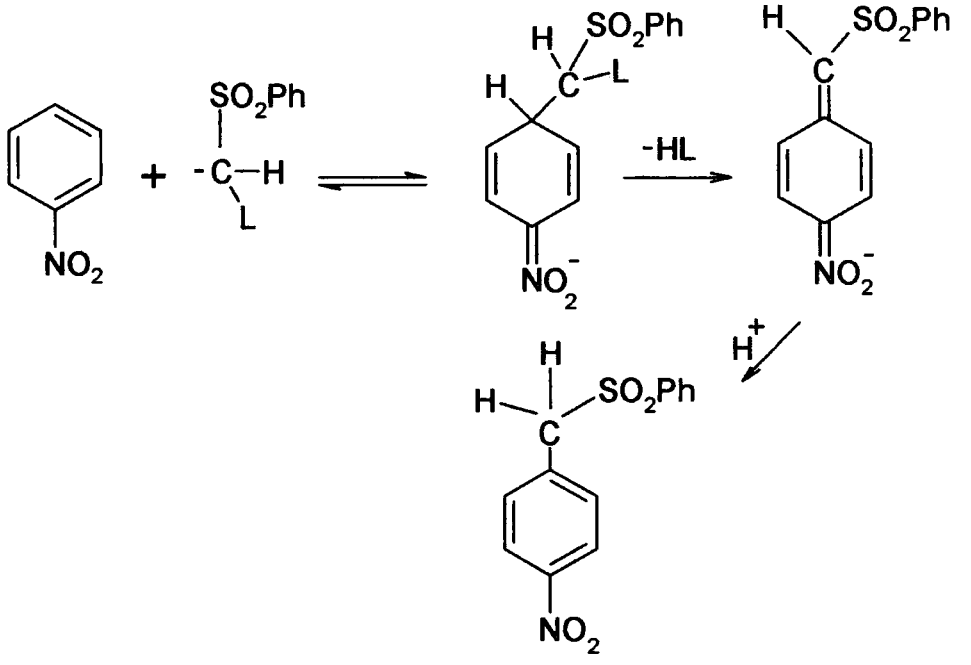

Scheme 1.18

There have been many studies of such substitutions of hydrogen involving addition of carbanions to nitroarenes. It has been shown that in nitroarenes possessing a good leaving group, for example Cl, Br, I, which would be susceptible to S_NA_r processes, vicarious nucleophilic substitution of hydrogen VS_NAr^H may occur

preferentially. Thus 4-Z substituted nitrobenzenes may undergo VS_NAr^H to produce substitution of the ortho-hydrogen atom, Scheme 1.19[48].

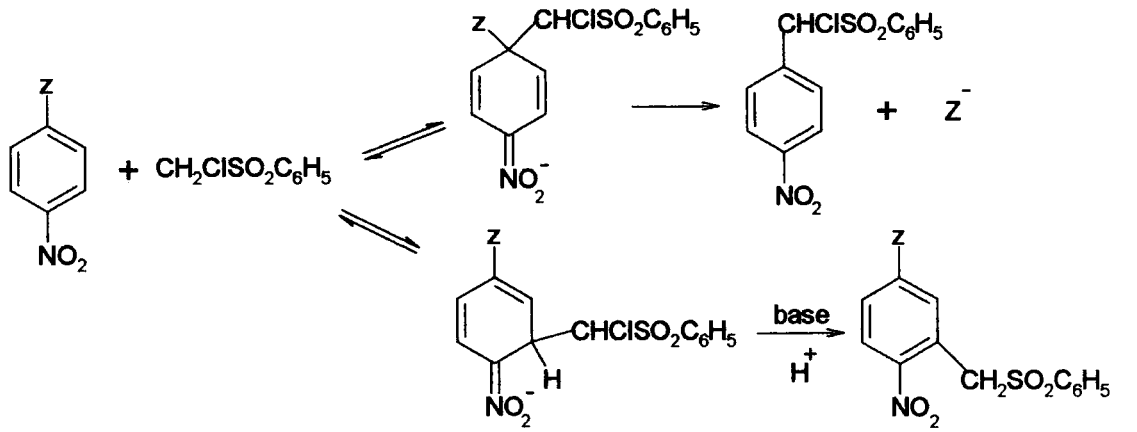

Z=Cl, Br, I, F, NO_2, CN.

Scheme 1.19

Kinetic studies[49] of the competitive S_NA_r substitution and VS_NAr^H substitution of a fluoro-substituted nitrobenzene, have confirmed that the elimination process in the vicarious pathway is base catalysed

Recently spectroscopic evidence[50] was reported for the formation of the intermediate **1.35** during the vicarious substitution reaction of 4-nitroanisole.

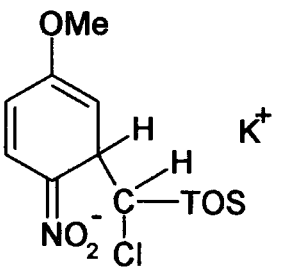

1.35

1.2.5 Comparison of The Acidifying Effects of SO_2CF_3 and NO_2 Groups

There have been several reports regarding the relative electron-withdrawing effect of the SO_2CF_3 and NO_2 groups. On the basis of the pK_a values of 4-X and 3-X substituted benzoic acids the SO_2CF_3 group is notably more electron-withdrawing.

Thus Hammett sigma values are reported as $\sigma_m = 0.76$ and $\sigma_p = 0.96$ for X = SO_2CF_3 and $\sigma_m = 0.74$, $\sigma_p = 0.78$ for X = NO_2[51,52].

In nucleophilic aromatic substitutions and in σ-adduct forming processes the SO_2CF_3 group is found to be more activating than a NO_2 group[25,26]. As an example, the methoxide adduct **1.36** of 1,3,5-trifluoromethylsulfonylbenzene is 10^6 time more stable thermodynamically than the trinitrobenzene adduct **1.37** in methanol[53].

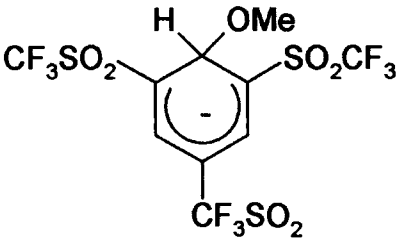

1.36

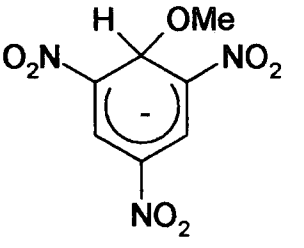

1.37

Comparisons of the activating effects of the SO_2CF_3 and NO_2 groups on the ionisation of carbon acids indicate the profound effect of the solvent used. Thus Bordwell[54] has shown that in DMSO trifluoromethylsulfonylmethane **1.38**, and benzyltriflone **1.40**, are each less acidic by two pK_a units than the corresponding nitro-derivatives **1.39** and **1.41**. By contrast in the gas phase **1.38** is more acidic than **1.39** by about 7 pK_a units[55].

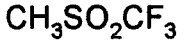

1.38

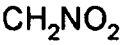

1.39

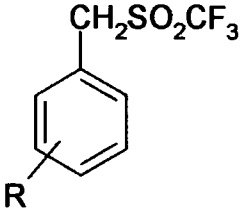

1.40

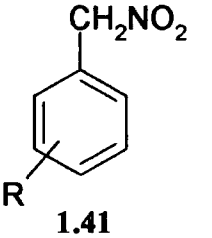

1.41

In an interesting study Buncel, Terrier et al studied[56] the effects of changing the solvent composition in water-DMSO mixtures on the acidities of **1.38**, **1.39** and of a series of substituted benzyl derivatives.

Figure 1.2 Effect of solvent composition (H_2O-Me_2SO) on the acidities of **1.40** and **1.41**.

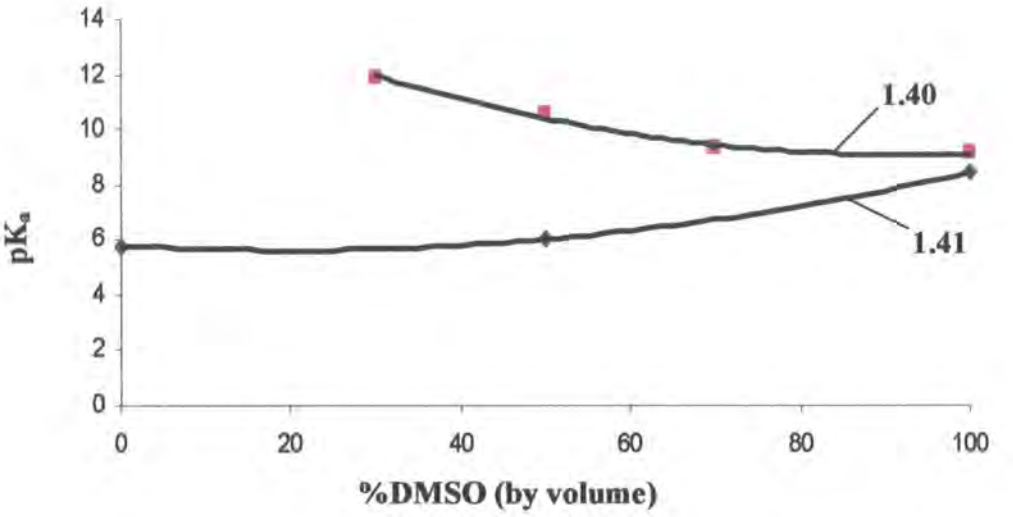

The acidity of 4-nitrobenzyltriflone **1.40**, (4-NO_2) decreases going from DMSO to water while that of 4-nitrophenylnitromethane **1.41**, (4-NO_2) increases as shown in Figure 1.2. The latter effect is readily attributed to the excellent solvation of the NO_2^- group by the hydrogen-bonding solvent, water, as shown in Scheme 1.20.

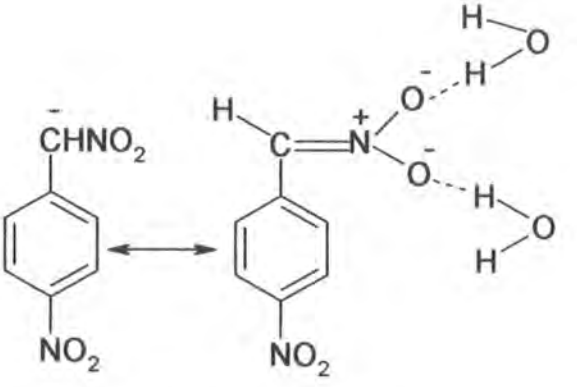

Scheme 1.20

The results indicate that the anion from **1.40** is better solvated in DMSO than in water suggesting that the SO_2CF_3 group when directly attached to the carbanionic centre acts mainly through a polarizability effect which is favoured in DMSO.

Nevertheless when the SO_2CF_3 group acts as a ring substituent it is significantly more stabilising than a NO_2 group due to its ability to stabilise an adjacent negative charge **1.42**.

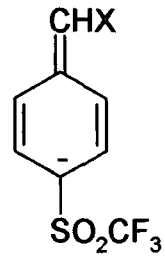

1.42

Kinetic studies of the ionisation of benzyltriflone in water-DMSO mixtures indicate a low Marcus intrinsic barrier associated with proton transfer. For example in 50/50 (v/v) DMSO/water the values of $\log_{10} k_o$ are 5 for benzyltriflone and -1 for phenylnitromethane, where k_o represent the intrinsic rate constant[57].

The height of the intrinsic barrier reflects the degree of solvent and electron re-organisation required during reaction. Hence the low barrier associated with the benzyltriflone is consistent with a carbanion where the negative charge remains largely on the C_α carbon atom, **1.43**, where it is stabilised by a polarizability effect.

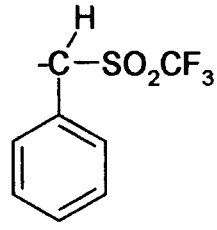

1.43

1.3 Reactions of Nitrobenzofuroxan and Nitrobenzofurazan

In the early part of the 20th century, there was much discussion over the structure of benzofuroxan derivatives, and the now generally accepted structure **1.44**, was suggested by Green and Rowe in 1912[58].

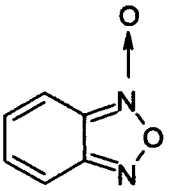

1.44

Several studies of the reactions of 4-nitrobenzofuroxan and 4-nitrobenzofurazan with nucleophiles, have been reported. One reason for this interest involves their ability to act as in vitro inhibitors of nucleic acid and protein biosynthesis in animal cells[59,60]. This action, which probably involves σ-adduct formation, may be useful in treating tumours.

Dinitrobenzofuroxan (DNBF) **1.19**, was first prepared by Drost in 1899 and was named m-dinitro-o-dinitrosobenzene. The structure of this compound was confirmed in the early 1960's by NMR (Harris and co workers)[61], and by UV and IR (Boulton and co workers)[62], and has been recently re-investigated by Terrier and co workers[63]. Other nitrobenzofurazan and nitrobenzofuroxan derivatives have been synthesised[64] and characterised using NMR spectroscopy[61,65,66], and X-ray crystallography[67].

The reactions with sulfite ions in water of 4-nitrobenzofuroxan[68] have been examined by ^{1}H NMR spectroscopy and stopped-flow spectrophotometry. The initial reaction occurs at the 5-position to give a σ-adduct which has considerably higher thermodynamic stability than the corresponding adduct from 1,3,5 trinitrobenzene.

Sulfite readily forms σ-adducts by reaction as a sulfur nucleophile with electron-deficient aromatics.

Similarly the NMR spectrum of 4-nitrobenzofurazan in the presence of sulfite indicates initial addition at the 5-position to give **1.45** which very slowly, over a matter of days, converts to the adduct **1.46**[68]. The spectra of the isomeric adducts can be distinguished principally from the shift of H_6 which is found to have a higher value

in 5-adducts than in 7-adducts. The results are compatible with the processes shown in Scheme 1.21.

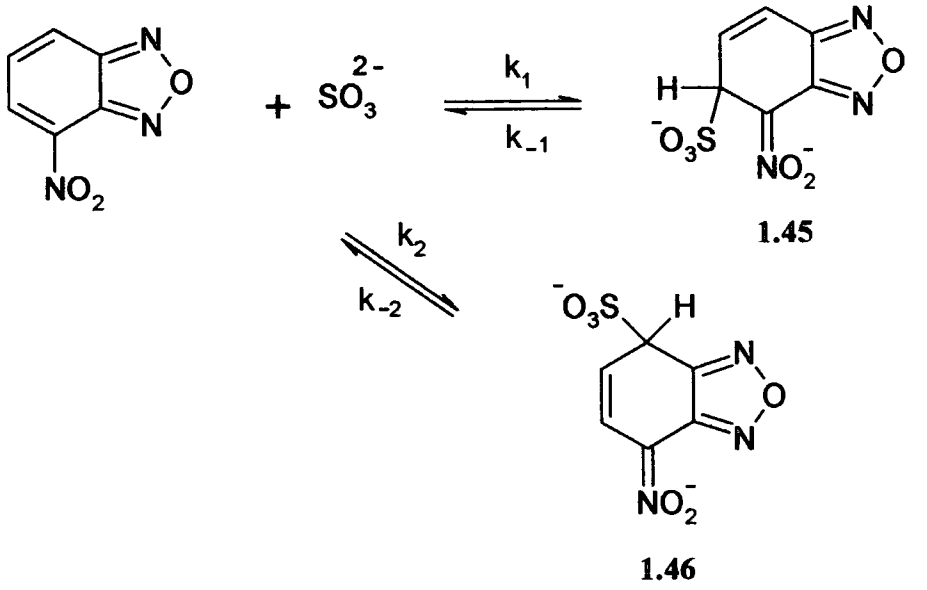

1.45

1.46

Scheme 1.21

The reaction of 4,6-dinitrobenzofuroxan DNBF with sulfite ions in water results in the formation of a 1:1 adduct with high thermodynamic stability, K_1 = 1.3×10^{13} dm^3 mol^{-1}, and in a 1:2 adduct which can exist in trans and cis-isomeric forms as shown in Scheme 1.22[24].

The reaction of 1,3,5-trinitrobenzene TNB with sulfite ions in water[69] results in formation of a 1:1 adduct, K_1 = 280 dm^3 mol^{-1}. Comparison of the corresponding values for formation of 1:1 adduct from TNB and DNBF, shows that the stability of the 1:1 adduct from DNBF is *ca* 10^{11} higher than that of the TNB-SO_3^{2-} adduct giving further evidence of the high electrophilicty of DNBF[24].

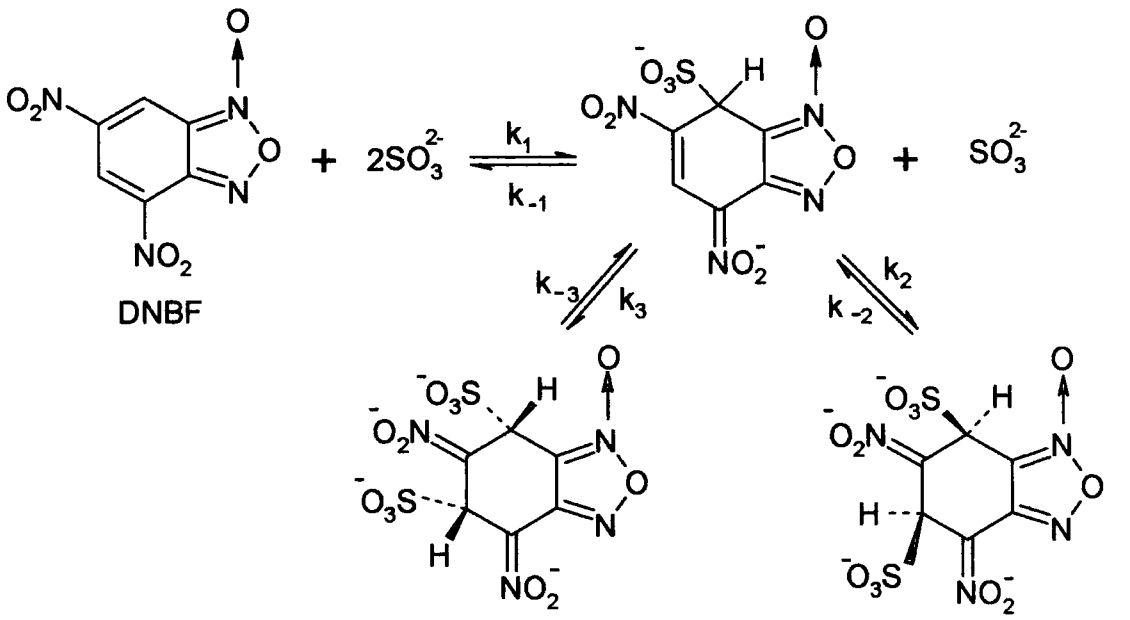

Scheme 1.22

^{1}H NMR studies[66] have also shown that the reactions of 4-nitrobenzofurazan **1.47**, and 4-nitrobenzofuroxan **1.48**, with methoxide ions resulted in rapid attack at the 5-position followed by slower isomerisation to the thermodynamically more stable 7-adducts. The kinetics of the reactions in methanol have been studied by Terrier et al[30] and the values obtained for adducts at the 5-position and 7-position are given in the Table 1.2.

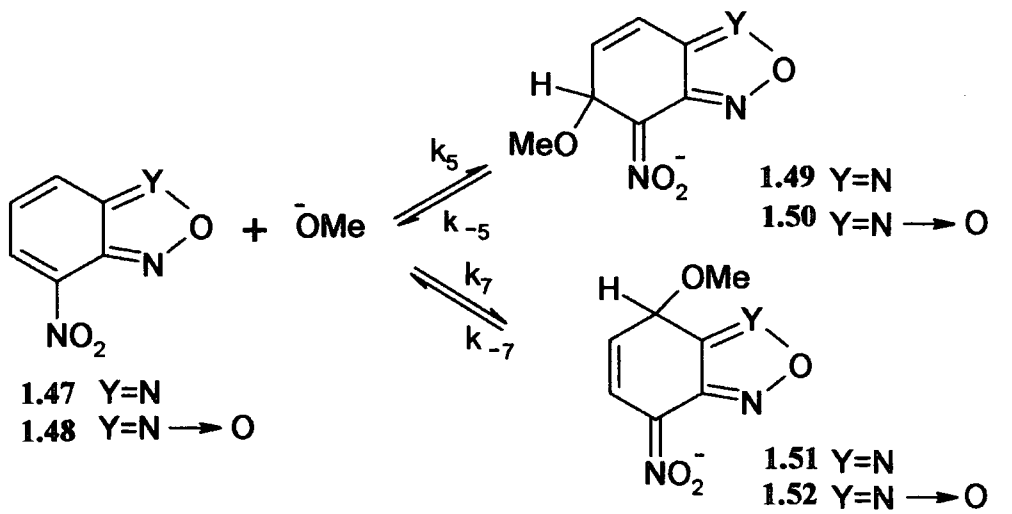

Scheme 1.23

The Table 1.2 shows that the most stable adducts are **1.51**, **1.52** and this result suggests that the para-nitro group is more efficient than the ortho-nitro group in delocalizing the negative charge of **1.51**, **1.52**.

Table 1.2 Kinetic and equilibrium data for reactions shown in Scheme 1.23.

	1.47	**1.48**	**1.53**	**1.54**
$k_5/dm^3 mol^{-1} s^{-1}$	1200	1950	5100	350
k_{-5}/s^{-1}	8.5	4.6	1.8	16
$K_5/dm^3 mol^{-1}$	140	430	2800	22
$k_7/dm^3 mol^{-1}s^{-1}$	6	28	7.7	14.5
k_{-7}/s^{-1}	0.0020	0.0033	/	0.0071
$K_7/dm^3 mol^{-1}$	3000	8000	/	2050
λ_{max}/nm (parent)	320	403	/	/
λ_{max}/nm (adduct)	330	340	/	/

In another study with 4-nitrobenzofurazan derivatives[70] substituted at the 7-position, reaction was again found to be more rapid at the 5-position. For 7-chloro-4-nitrobenzofurazan **1.53**, the slow reaction at the 7-position resulted in substitution of chlorine while with 7-methoxy-4-nitrobenzofurazan **1.54**, the slower reaction yielded a stable σ-adduct. Data are included in the Table 1.2.

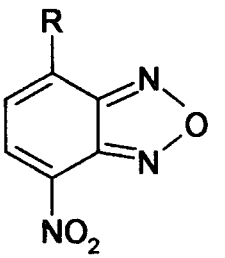

1.53 R=Cl

1.54 R=OMe

In contrast with methoxide addition the 7-aryloxy adducts are preferred both kinetically and thermodynamically to the 5-adducts[71].

NMR and kinetic studies of the reaction of 4- nitrobenzofuroxan with amines indicate rapid attack at the 5-position followed by slower reaction to give the thermodynamically more stable 7-adducts[72].

A recent paper has examined the kinetics of the reaction of 7-chloro-4-nitrobenzofurazan **1.53**, and also 3-methyl-1-(4-nitrobenzofurazanyl)-imidazolium ion **1.55** with a series of substituted anilines in water-DMSO mixture. In both reactions substitution of the 7-substituent is observed and the kinetics indicated that initial nucleophilic attack is rate limiting. Interestingly the Brønsted plots of log k versus pK_a for aniline had slopes of *ca* 1 for **1.53** and 1.4 for **1.55**. A possible explanation for these high values which indicate considerable charge development on the amino nitrogen is a two step single electron transfer mechanism. The fast step would involve electron transfer from the aniline donor to the nitrobenzofurazan acceptor and the slow step coupling of the resulting cation and anion radicals[73].

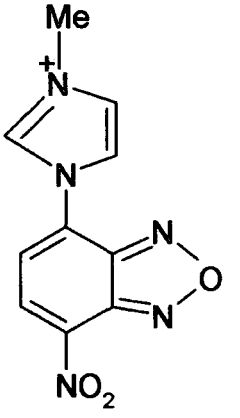

1.55

1.4 Solvent Effects

Changing the solvent in which a reaction is carried out often exerts a profound effect on the rate and may even result in a change in its mechanistic pathway[74].

A good example of the sensitivity of reaction rate to solvent is provided by the aromatic nucleophilic substitution reaction of the azide ion with 4-fluoronitrobenzene,[75] Scheme 1.24 and Table 1.3.

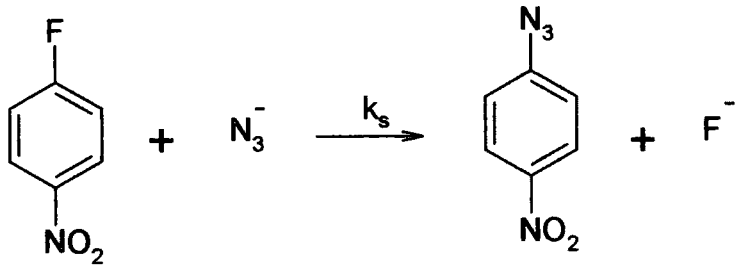

Scheme 1.24

Table 1.3 Rate constants in solvents at 25 °C.

Solvent	H_2O[a]	MeOH	Me_2SO	$HCONMe_2$	$(Me_2N)_3PO$
k_s/k_{H_2O}	1	1.6	1.3×10^4	4.3×10^4	2.0×10^6

a. $k_{H_2O} = 4.0\times10^{-8}\ dm^3\ mol^{-1}\ s^{-1}$.

In all cases, there is a large rate increase when the solvent is changed from water to dimethylsulfoxide DMSO and other dipolar aprotic solvents.

Also in σ-adduct forming reactions involving anionic nucleophiles values of the equilibrium constant increase dramatically on going from protic to dipolar aprotic solvent. The value for reaction of TNB and methoxide is *ca* 10^8 higher in DMSO than in methanol while for reaction with thiophenoxide ion the increase[76] is *ca* 10^5.

Methanol is good at stabilising anions with localised negative charge by hydrogen-bonding interaction; methoxide will be stabilised better than thiophenoxide where the charge is more dispersed. In contrast DMSO is good at stabilising large polarisable species such as the σ-adduct products but will not stabilise localised anions. Hence on transfer from methanol to DMSO the equilibrium constant for the TNB/methoxide adduct is strongly increased; while the value for the TNB/thiophenoxide adduct is increased but less dramatically.

1.5 The Hammett Equation

The investigation of the effects of substituents in an aromatic ring may provide information about reaction mechanism and about the structures of activated complexes. Hammett showed how the effects of substituents can be quantified. He succeeded in giving numerical values to ring substituents in order to measure their effect on the reactivity of the substrate[77].

The Hammett equation is given in equation 1.4; for a given substituent X, K_o is the equilibrium constant for reaction when X = H, K the equilibrium constant for X.

σ is a constant characteristic of X that is a measure of the ability of the substituent X to modify the acid strength of benzoic acid.

The σ values are the sum of resonance and inductive effects of a group X attached to a benzene ring. A positive σ-value indicates an acid strengthening substituent, and corresponds to an electron attracting effect. A negative σ-value indicates an acid weakening substituent, usually one with an electron-donating effect.

$$\log \frac{K}{K_o} = \sigma\rho \qquad (1.4)$$

The equation was based on the study of ionisation of substituted benzoic acid in water at 25 °C, Scheme 1.25.

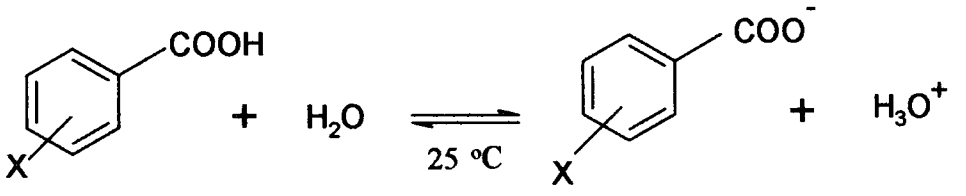

Scheme 1.25

The value of ρ was set at 1.00 for this reaction and σ_m and σ_p values calculated accordingly. In general for other reactions the constant ρ measures the susceptibility of the reaction to electronic effects. Reaction with a positive ρ value show increased equilibrium constants when electron-withdrawing groups are present, while the equilibrium constants of reactions with negative ρ value are increased in the presence of electron-donating groups. A value of zero would mean a polar substituent has no effect on the equilibrium constant[78].

The Hammett treatment usually fails for substituents at the ortho position because of steric hindrance effects.

Where direct resonance interaction is possible between the group X and the reacting position in the benzene ring, two new sets of σ values have been calculated.

When electron-withdrawing groups interact with a developing negative charge, σ^- values are used and when an electron-donating group interacts with a developing positive charge σ^+ values are applied. A selection of σ values is given in Table 1.4.

Table 1.4 σ values for a selection of substituents.

Group	σ_p	σ_m	σ_p^+	σ^-
H	0	0	0	/
Me	-0.14	-0.06	-0.31	/
MeO	-0.28	0.1	-0.78	/
Cl	0.22	0.37	0.11	/
NO_2	0.78	0.71	/	1.27
CN	0.7	0.61	/	0.88

The same concept may be used when studying rate constants for reaction where the Hammett equation is 1.5.

$$\log\frac{k}{k_o} = \sigma\rho \qquad \textbf{(1.5)}$$

Figure 1.3

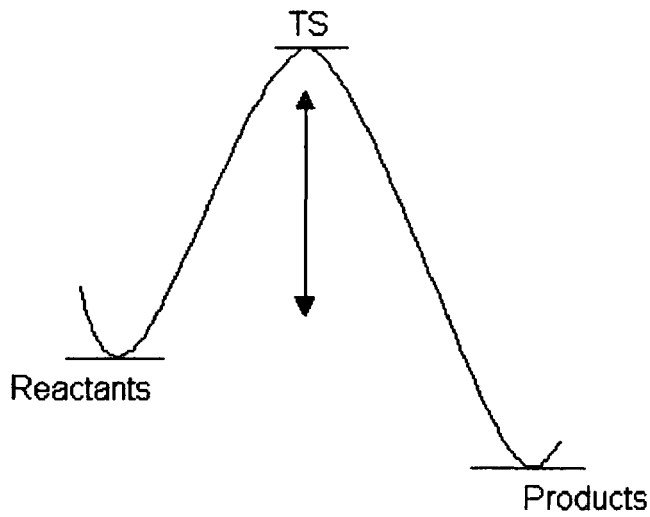

Here the rate constants are a measure of energy barrier between reactants and products, as shown in Figure 1.3 and the ρ value will be determined by the effects of substituents on this barrier.

1.6 Aims of the Project

The aims of the project were to investigate quantitatively the reactions of several activated aromatic compounds with several different types of nucleophiles. It was planned to determine the structures of the adducts formed using spectroscopic methods and to measure rate and equilibrium constants using UV/visible spectrophotometry.

Initially reactions with the nitrogen base aniline were investigated. It has been shown previously that in the reactions of TNB with aniline in the presence of Dabco proton transfer may be rate limiting. It was hoped that the present work would enable the values of rate constants for proton transfer reactions to be measured. Here measurements are reported for reactions of a series of ring-substituted anilines with TNB and with 4-nitrobenzofuroxan in DMSO. Dabco has been used as a strong base to enable adduct formation with aniline to be observed. In this context the claims by Forlani et al that TNB will react with Dabco to form a zwitterionic adduct have been investigated[79,80,81]. Measurements were made in DMSO and although the pK_a value of the anilinium ion in this solvent is known to be 3.8, the values for ring-substituted anilines have not previously been determined. Hence equilibrium measurements, using the proton transfer reaction with 2,4-dinitrophenol have been used to determine such values.

Carbon-carbon bond formation is an important process in organic chemistry, so that it was planned to study the reactions of activated aromatic compounds with some carbon bases. There is current interest in the formation of carbanions stabilised by trifluoromethylsulfonyl groups and it was hoped to study their reactivity in σ-adducts forming reactions. Some quantitative information is already available[40] for carbanions stabilised by nitro groups. So it was hoped to make a comparison of the two differently activated carbanions.

1.7 References

[1] F. Terrier, 'Nucleophilic Aromatic Displacement', 1991, VCH.

[2] C. L. Jackson and F. H. Gazzolo, J. Am. Chem. Soc., 1900, **23**, 376.

[3] J. Meisenheimer. Liebigs Ann. Chem., 1902, **323**, 205.

[4] M. R. Crampton and V. Gold, J. Chem. Soc., 1964, 4293.

[5] K. L. Servis, J. Am. Chem. Soc., 1965, **87**, 5495.

[6] K. L. Servis, J. Am. Chem. Soc., 1967, **89**, 1508.

[7] M. R. Crampton and V. Gold, J. Chem. Soc. B, 1967, 23.

[8] C. F. Bernasconi, J. Am. Chem. Soc., 1970, **92**, 2417.

[9] C. F. Bernasconi, M. C. Muller and P. Schmid, J. Org. Chem., 1979, **44**, 3189.

[10] M. R. Crampton and B. Gibson, J. Chem. Soc., Perkin Trans. 2, 1981, 533.

[11] R. A Chamberlin and M. R. Crampton, J. Chem. Soc., Perkin Trans. 2, 1995, 1831.

[12] M. R. Crampton and L. C. Rabbitt, J. Chem. Soc., Perkin Trans. 2, 1999, 1669.

[13] E. Buncel and J. G. K. Webb, Can. J. Chem., 1972, **50**, 129.

[14] E. Buncel and J. G. K. Webb, Can. J. Chem., 1974, **52**, 630.

[15] E. Buncel and J. G. K. Webb, Tetrahedron Lett., 1976, 4417.

[16] E. Buncel and J. G. K. Webb and J. F. Wiltshire, J. Am. Chem. Soc., 1977, **99**, 4429.

[17] E. Buncel and H. W. Leung, J. Chem. Soc., Commun., 1975, 19.

[18] M.R. Crampton and I. Robotham, Can. J. Chem., 1998, **76**, 627.

[19] E. Buncel and W. Eggimann, J. Am. Chem. Soc., 1977, **99**, 5958.

[20] E. Buncel, W. Eggimann and H. W. Leung, J. Chem. Soc., Chem. Commun., 1977, 55.

[21] E. Buncel and W. Eggimann, J. Chem. Soc., Perkin Trans. 2, 1978, 673.

[22] C. F. Bernasconi, Acc. Chem.Res., 1978, **11**, 147.

[23] E. Buncel, R. A. Manderville and J. M. Dust, J. Chem. Soc., Perkin Trans. 2, 1997, 1019.

[24] M. R. Crampton and L. C. Rabbitt, J. Chem. Soc., Perkin Trans. 2, 2000, 2169.

[25] E. Buncel, M. R. Crampton, M. J. Strauss and F. Terrier, 'Electron Deficient Aromatic and Heteroaromatic-Base Interactions', 1984, Elsevier.

[26] F. Terrier, Chem. Rev., 1982, **82**, 77.

[27] M. R. Crampton, T. P. .Kee and J. R. Wilcock, Can. J. Chem., 1986, **64**,1714.

[28] J. H. Atherton, M. R. Crampton, G. L. Duffield and J. A. Stevens, J. Chem. Soc., Perkin Trans. 2, 1995, 443.

[29] M. E. Moir and A. R. Norris, Can. J. chem., 1980, **58**, 16911.

[30] F. Terrier, A.-P. Chatrousse and F. Millot, J. Org. Chem., 1980, **45**, 2666.

[31] E. P. Serjeant and B. Dempsey (eds.), 'Ionization Constants of Organic Acids in Solution', IUPAC Chemical Data series No. 23, Pergamon Press, Oxford, UK, 1979.

[32] E. Buncel, A. R. Norris, W. Proudlock, K. E. Russell, Can. J. Chem., 1969, **47**, 4129.

[33] C. F. Bernasconi, J. Am. Chem. Soc., 1970, **92**, 4682.

[34] G. A. Artamkina, M. P.Egarov and I. P. Beletskaya, Chem. Rev., 1982, **82**, 427.

[35] E. Buncel, J. M. Dust and R. A. Manderville, J. Am. Chem. Soc., 1996, **118**, 6072.

[36] C. F. Bernasconi and M. C. Muller, J. Am. Chem. Soc., 1978, **100**, 5530.

[37] E. Buncel, R. Y, Moir, A.R. Norris, Can. J. Chem., 1981, **59**, 2470.

[38] S. M. Shein, O. G. Byval'kevich and A. D. Khmelinskaya, zh. Org. Khim., 1976, **12**, 134.

[39] C. A. Fyfe, Can. J. Chem., 1968, **46**, 3047.

[40] J. P. L. Cox, M. R. Crampton and P. Wight, J. Chem. Soc., Perkin Trans. 2, 1988, 25.

[41] F. Terrier, R. Goumont, M.-J. Pouet and J.-C. Halle, J. Chem. Soc., Perkin Trans. 2, 1995, 1629.

[42] F. Terrier, J. Lelievre, A. P. Chatrousse, T. Boubaker, B. Bachet and A. Cousson, J. Chem. Soc., Perkin Trans. 2, 1992, 361.

[43] F. Terrier, D. Croisat, A. P. Chatrousse, M. J. Pouet, J. C. Halle and G. Jacob, J. Org. Chem., 1992, **57**, 3684.

[44] R. Goumont, E. Jan, M. Makosza and F. Terrier, Org. Biomol. Chem., 2003, **1**, 2192.

[45] J. Miller, 'Aromatic Nucleophilic Substitution', Elsevier, Amstrdam, 1968.

[46] M. Makosza and J. Winiarski, Acc. Chem. Res., 1987, **20**, 282.

[47] M. Makosza, 'Current Trends in Organic Synthesis', Pergamon Press, New York, 1983.

[48] M. Makosza, J. Golinski and J. Baran, J. Org. Chem., 1984, **49**, 1488.

[49] M. Makosza, T. Lemek, A. Kwast and F. Terrier, J. Org. Chem., 2002, **67**, 394.

[50] T. Lemek, M. Makosza, D. S. Stephenson and H. Mayr, Angew. Chem. Int. Ed., 2003, **42**, 2793.

[51] L. M. Yagupol'skii, A. Y. Il'chenko, N.B. Kondratenko, Usp. Khim., 1974, **43**, 64.

[52] W. Seppard, J. Am. Chem. Soc., 1963, **85**, 1314.

[53] F. Terrier, A. P. Chatrousse, E. Kizilian, V. N. Ignatev and L. M. Yagupolskii, Bull. Soc. Chem. Fr., 1989, 627.

[54] F. G. Bordwell, N. R. Vanier, W. S. Matthews, J. B. Hendrickson and P. L. Skipper, J. Am. Chem. Soc., 1975, **97**, 7160.

[55] A. I. Koppel, R. W.Taft, F. Anvia, S-Z. Zhu, L. Q. Hu, K-S. Sung, D. D. Desmarteau, L. M. Yagupolskii, V. M. Vlasov, R. Notario and P. C. Maria, J. Am. Chem. Soc., 1994, **116**, 3047.

[56] R. Goumont, E. Kizilian, E. Buncel and F. Terrier, Org. Biomol. Chem., 2003, **1**, 1741.

[57] F. Terrier, E. Magnier, E. Kizilian, C. Wakselman and E. Buncel, J. Am. Chem. Soc., 2005, **127**, 5563.

[58] A. G. Green and F. M. Rowe, J. Chem. Soc., 1912, **101**, 2452.

[59] P. B. Ghosh and M. W. Whitehouse, J. Medicinal Chem., 1968, **11**, 305.

[60] P. B. Ghosh, B. Ternai and M. W. Whitehouse, J. Medicinal Chem., 1972, **15**, 255.

[61] R. K. Harris, A. R. Katritzky, S. Oksne, A. S. Bailey and W. G. Paterson, J. Chem. Soc., 1963, 197.

[62] A. J. Boulton and P. B. Ghosh, Adv. Heterocycl. Chem., 1969, **10**, 1.

[63] F. Terrier, J-C. Halle, P. MacCormack and M-J. Pouet, Can. J. Chem., 1989, **67**, 503.

[64] R. J. Gaughran, J. P. Picard and J. V. R. Kaufman, J. Am. Chem. Soc., 1954, **76**, 2233.

[65] E. Buncel, N. Chuaqui-Offermans and A. R. Norris, J. Chem. Soc., Perkin Trans. 1, 1977, 415.

[66] F. Terrier, F. Millot, A-P. Chatrousse, M-J. Pouet and M-P. Simonnin, Org. Mag. Res., 1976, **8**, 56.

[67] G. G. Messmer and G. J. Palenik, Chem. Commun., 1969, 470.

[68] M. R. Crampton, L. M. Pearce and L. C. Rabbitt, J. Chem. Soc., Perkin Trans. 2, 2002, 257.

[69] C. F. Bernasconi and R. G. Bergstrom, J. Am. Chem. Soc., 1973, **95**, 3603.

[70] L. D. Nunno and S. Florio and P. E. Todesco, J. Chem. Soc., Perkin Trans. 2, 1975, 1469.

[71] R. A. Manderville and E. Buncel, J. Chem. Soc., Perkin Trans. 2, 1993, 1887.

[72] M. R. Crampton, J. Delaney and L. C. Rabbitt, J. Chem. Soc., Perkin Trans. 2, 1999, 2473.

[73] F. Terrier, M. Mokhtari, R. Goumont, J.-C. Halle and E. Buncel, Org. Biomol. Chem., 2003, **1**, 1757.

[74] P. Sykes, 'A guidebook to Mechanism in Organic Chemistry', Longman, London, 1975.

[75] B. G. Cox,'Modern Liquid Phase Kinetics', Oxford University press Inc., New York, 1994.

[76] M. R. Crampton, J. Chem. Soc. B, 1968, 1208.

[77] L. P. Hammett, J. Am. Chem. Soc., 1937, **59**, 96.

[78] H. Maskill, 'Structure and Reactivity in Organic Chemistry', Oxford, New York, 1999.

[79] C. Boga and L. Forlani, J. Chem. Soc., Perkin Trans. 2, 2001, 1408.

[80] C. Boga and L. Forlani, J. Chem. Soc., Perkin Trans. 2, 1998, 2155.

[81] L. Forlani, M. Sintoni and P. E. Todesco, J. Chem. Res., 1986, 344.

Chapter Two:

pK_a Values of Substituted Anilinium Ions in DMSO

Chapter Two: pK_a Values of Substituted Anilinium Ions in DMSO

2.1 Introduction

In chapter 3 kinetic and equilibrium results are reported for the reactions of 1,3,5-trinitrobenzene and also 4-nitrobenzofuroxan with a series of substituted anilines in the presence of Dabco, or in some cases of quinuclidine, in DMSO. The aims were to investigate the effects of both the structure of the nitro-compound and of substituents in the aniline on rate constants for proton transfer and on the nature of the rate-determining step. The pK_a values for the substituted anilinium ions in DMSO were measured since they are relevant to the work.

2.2 Determination of pK_a Values

The pK_a values for a number of amines in DMSO have been reported previously[1]. The value for aniline is 3.82, and for Dabco 9.06. However values for substituted anilines in DMSO have not been reported previously.

In the present work, as previously[1], a spectrophotometric method using 2,4-dinitrophenol (DNP) as indicator was used. The pK_a value of DNP is known[2] to be 5.12±0.04 in DMSO.

pK_a values for nine anilinium ions corresponding to the anilines **2.1a-i** were measured.

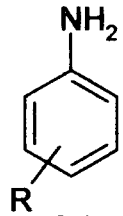

2.1

a 4-OMe

b 4-Me

c H

d 4-Cl

e 3-Cl

f 3-CN

g 2-Me

h 2-Et

i R=H, N-Me

2.2.1 Results

Measurements of absorbance were made at 430 nm which is the absorption maximum of the 2,4-dinitrophenolate ion. It was necessary to make a small correction for the absorbance due to the substituted anilines at this wavelength. Wherever possible measurements were made with solutions containing 0.01 mol dm^{-3} of the appropriate aniline hydrochloride. For the less basic anilines, where concentrations of hydrochloride lower than 0.01 mol dm^{-3} were required, the ionic strength was maintained at 0.01 mol dm^{-3} with tetramethylammonium chloride.

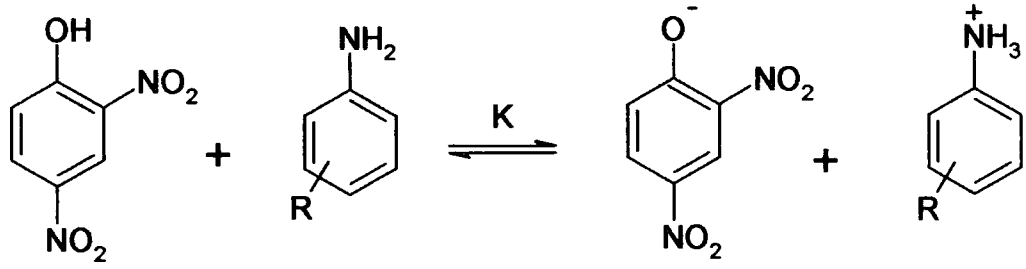

DNP 2.1 2.2

Scheme 2.1

Scheme 2.1 and equation 2.1 define an equilibrium constant, K, for the overall conversion of DNP into its deprotonated from **2.2** by the respective aniline.

Absorbance measurements yielded the value of the equilibrium constant, K, for the equilibrium given in equation 2.1.

The main absorbing species at 430 nm is the anion **2.2** so that equation 2.1 may be written as 2.2.

$$K = \frac{[\mathbf{2.2}][AnH^+]}{[DNP][An]} \qquad (2.1)$$

$$K = \frac{(Abs - A_o)[AnH^+]}{(A_\infty - Abs)[An]} \qquad (2.2)$$

$$\log_{10}K = pK_a(AnH^+) - pK_a(DNP) \qquad (2.3)$$

A_o = Obtained without aniline, absorbance measurement for DNP only.

A_∞ = Obtained without aniline salt, corresponds to complete conversion to **2.2**.

[An] = Aniline concentration, mol dm^{-3}.

$[AnH^+]$ = Aniline hydrochloride concentration, mol dm^{-3}.

Equation 2.3 relates the value of $\log_{10} K$ to the pK_a values of the aniline used and DNP. Representative results for DNP in solutions containing 4-methylaniline **2.1b** and **2.1b HCl** are shown in Figure 2.1 and Table 2.1.

A correction was included for the absorbance of **2.1b** at 430 nm; a 0.6 mol dm^{-3} solution had an absorbance of 0.028.

Figure 2.1 UV/visible spectra of DNP (4×10^{-5} mol dm^{-3}) in DMSO containing 4-methylaniline and 4-methylaniline hydrochloride corresponding to conditions given in Table 2.1.

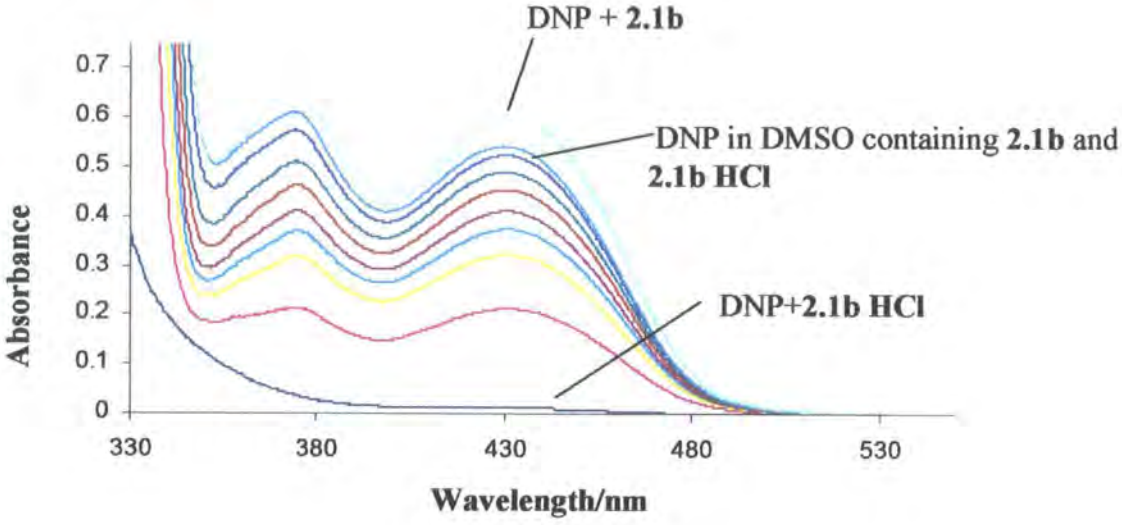

Table 2.1 Absorbance data for DNP (4×10^{-5} mol dm^{-3}) in DMSO containing various concentrations of 4-methylaniline **2.1b** at 25 °C.

[2.1b]/mol dm^{-3}	[2.1b HCl]/mol dm^{-3}	Abs	$Abs_{/corrected}$[a]	K[b]
0	0.01	0.0124	0.0124	/
0.025	0.01	0.213	0.212	0.22
0.05	0.01	0.322	0.320	0.24
0.075	0.01	0.373	0.370	0.23
0.10	0.01	0.410	0.405	0.22
0.15	0.01	0.453	0.446	0.22
0.20	0.01	0.488	0.479	0.23
0.30	0.01	0.523	0.509	0.23
0.40	0.01	0.542	0.523	0.23
0.40	0	0.595	0.580	/
0.60	0	0.606	0.580	/

a. $Abs_{/Corrected} = Abs_{/Measured} - Abs_{/Aniline}$.

$$Abs_{/Corrected} = Abs_{/Measured} - \frac{0.028\times[\mathbf{2.1b}]}{0.6}.$$

b. $$K = \frac{[Abs - 0.0124][AnH^+]}{[0.58 - Abs][An]}.$$

Values for reaction with other anilines are given in Tables 2.2-2.9. Values for K and pK_a are collected in Table 2.10 with use of equation 2.3.

Table 2.2 Absorbance data for DNP (4×10^{-5} mol dm^{-3}) in DMSO containing various concentrations of 4-methoxyaniline **2.1a** at 25 °C.

[2.1a]/mol dm^{-3}	[2.1a HCl]/mol dm^{-3}	Abs	$Abs_{/corrected}$[a]	K[b]
0.005	0.01	0.179	0.175	0.86
0.01	0.01	0.280	0.271	0.92
0.015	0.01	0.346	0.333	0.98
0.02	0.01	0.386	0.368	0.98
0.03	0.01	0.436	0.409	0.94
0.04	0.01	0.465	0.429	0.86
0.05	0.01	0.498	0.453	0.91
0.10	0	0.655	0.565	/
0.16	0	0.682	0.538	/
0	0.01	0.013	0.013	/

a. $Abs_{/Corrected} = Abs_{/Measured} - Abs_{/Aniline}$.

$$Abs_{/Corrected} = Abs_{/Measured} - \frac{0.09\times[\mathbf{2.1a}]}{0.1}.$$

b. $$K = \frac{[Abs - 0.013][AnH^+]}{[0.55 - Abs][An]}.$$

Table 2.3 Absorbance data for DNP (4×10^{-5} mol dm^{-3}) in DMSO containing various concentrations of aniline **2.1c** at 25 °C.

[2.1c]/mol dm^{-3}	[2.1c HCl]/mol dm^{-3}	Abs	$Abs_{/corrected}$[a]	K[b]
0.05	0.01	0.15	0.147	0.050
0.10	0.01	0.26	0.252	0.054
0.15	0.01	0.31	0.301	0.049
0.20	0.01	0.36	0.353	0.050
0.25	0.01	0.40	0.389	0.049
0.30	0.01	0.43	0.415	0.047
0.40	0	0.74	0.719	/
0.60	0	0.72	0.688	/
0	0.01	0.009	0.009	/

a. $Abs_{/Corrected} = Abs_{/Measured} - Abs_{/Aniline}$.

$$Abs_{/Corrected} = Abs_{/Measured} - \frac{0.033\times[\mathbf{2.1c}]}{0.6}.$$

b. $$K = \frac{[Abs - 0.009][AnH^+]}{[0.7 - Abs][An]}.$$

Table 2.4 Absorbance data for DNP (4×10^{-5} mol dm^{-3}) in DMSO containing various concentrations of 4-chloroaniline **2.1d** at 25 °C.

[2.1d]/mol dm^{-3}	[2.1d HCl]/mol dm^{-3} [a]	Abs	$Abs_{/corrected}$ [b]	K [c]
0.10	0.01	0.051	0.032	0.0055
0.20	0.01	0.091	0.053	0.0050
0.30	0.01	0.1305	0.073	0.0049
0.40	0.01	0.169	0.092	0.0049
0.05	0.001	0.145	0.135	0.0064
0.075	0.001	0.189	0.175	0.0061
0.10	0.001	0.223	0.204	0.0058
0.60	0	0.667	0.552	/
0	0.01	0.0032	0.0032	/

a. Ionic strength kept at 0.01mol dm^{-3} using tetramethylammonium chloride.

b. $Abs_{/Corrected} = Abs_{/Measured} - Abs_{/Aniline}$.

$$Abs_{/Corrected} = Abs_{/Measured} - \frac{0.115\times[\mathbf{2.1d}]}{0.6}.$$

c. $$K = \frac{[Abs - 0.0032][AnH^+]}{[0.55 - Abs][An]}.$$

Table 2.5 Absorbance data for DNP (4×10^{-5} mol dm^{-3}) in DMSO containing various concentrations of 3-chloroaniline **2.1e** at 25 °C.

[2.1e]/mol dm^{-3}	[2.1e HCl]/mol dm^{-3} [a]	Abs	$Abs_{/corrected}$ [b]	$K/10^{-3}$ [c]
0.05	0.001	0.08	0.080	1.9
0.10	0.001	0.13	0.128	1.8
0.20	0.001	0.21	0.207	1.7
0.30	0.001	0.28	0.266	1.6
0.40	0.001	0.32	0.304	1.5
0.50	0.001	0.37	0.354	1.6
0.60	0.001	0.40	0.381	1.5
0.30	0	0.79	0.787	/
0.60	0	0.81	0.788	/
0	0.001	0.01	0.010	/

a. Ionic strength kept at 0.01mol dm^{-3} using tetramethylammonium chloride.

b. $Abs_{/Corrected} = Abs_{/Measured} - Abs_{/Aniline}$.

$$Abs_{/Corrected} = Abs_{/Measured} - \frac{0.0225\times[\mathbf{2.1e}]}{0.6}.$$

c. $$K = \frac{[Abs - 0.01][AnH^+]}{[0.79 - Abs][An]}.$$

Table 2.6 Absorbance data for DNP ($4x10^{-5}$ mol dm^{-3}) in DMSO containing various concentrations of 3-cyanoaniline **2.1f** at 25 °C.

[2.1f]/mol dm^{-3}	[2.1f HCl]/mol dm^{-3}[a]	Abs	$Abs_{/corrected}$[b]	$K/10^{-4}$[c]
0.05	0.001	0.038	0.019	2.10
0.10	0.001	0.063	0.025	1.87
0.20	0.001	0.115	0.038	1.90
0.30	0.001	0.160	0.045	1.59
0.40	0.001	0.210	0.056	1.62
0.50	0.001	0.258	0.066	1.60
0.60	0.001	0.304	0.073	1.53
0.30	0	0.867	0.752	/
0.60	0	0.980	0.749	/
0	0.001	0.011	0.011	/

a. Ionic strength kept at 0.01mol dm^{-3} using tetramethylammonium chloride.

b. $Abs_{/Corrected} = Abs_{/Measured} - Abs_{/Aniline}$.

$$Abs_{/Corrected} = Abs_{/Measured} - \frac{0.231 \times [\mathbf{2.1f}]}{0.6}.$$

c. $$K = \frac{[Abs - 0.0109][AnH^+]}{[0.75 - Abs][An]}.$$

Table 2.7 Absorbance data for DNP (4×10^{-5} mol dm^{-3}) in DMSO containing various concentrations of 2-methylaniline **2.1g** at 25 °C.

[2.1g]/mol dm^{-3}	[2.1g HCl]/mol dm^{-3}	Abs	$Abs_{/corrected}$[a]	K[b]
0	0.01	0.0121	0.0121	/
0.025	0.01	0.1047	0.0995	0.0495
0.05	0.01	0.180	0.169	0.0493
0.075	0.01	0.2438	0.228	0.0498
0.10	0.01	0.2970	0.275	0.0496
0.15	0.01	0.3701	0.337	0.0463
0.20	0.01	0.4415	0.399	0.0465
0.30	0.01	0.5498	0.485	0.0493
0.40	0.01	0.6183	0.531	0.0473
0.30	0	0.8621	0.797	/
0.60	0	0.9433	0.813	/

a. $Abs_{/Corrected} = Abs_{/Measured} - Abs_{/Aniline}$.

$$Abs_{/Corrected} = Abs_{/Measured} - \frac{0.087 \times [\mathbf{2.1g}]}{0.4}.$$

b. $$K = \frac{[Abs - 0.012][AnH^+]}{[0.805 - Abs][An]}.$$

Table 2.8 Absorbance data for DNP (4×10^{-5} mol dm^{-3}) in DMSO containing various concentrations of 2-ethylaniline **2.1h** at 25 °C.

[2.1h]/mol dm^{-3}	[2.1h HCl]/mol dm^{-3}	Abs	$Abs_{/corrected}$ [a]	K [b]
0	0.01	0.0096	0.0096	/
0.025	0.01	0.1002	0.094	0.0446
0.05	0.01	0.1799	0.167	0.0461
0.075	0.01	0.2438	0.225	0.0459
0.10	0.01	0.2867	0.262	0.0429
0.15	0.01	0.3732	0.336	0.0423
0.20	0.01	0.437	0.388	0.0409
0.30	0.01	0.5459	0.472	0.0407
0.40	0.01	0.6319	0.533	0.0413
0.30	0	0.9174	0.843	/
0.60	0	1.0065	0.858	/

a. $Abs_{/Corrected} = Abs_{/Measured} - Abs_{/Aniline}$.

$$Abs_{/Corrected} = Abs_{/Measured} - \frac{0.099\times[\mathbf{2.1h}]}{0.4}.$$

b. $$K = \frac{[Abs - 0.0096][AnH^+]}{[0.85 - Abs][An]}.$$

Table 2.9 Absorbance data for DNP (4×10^{-5} mol dm^{-3}) in DMSO containing various concentrations of N-methylaniline **2.1i** at 25 °C.

[2.1i]/mol dm^{-3}	[2.1i HCl]/mol dm^{-3}	Abs	$Abs_{/corrected}$ [a]	K [b]
0	0.01	0.0083	0.0083	/
0.025	0.01	0.0333	0.0203	0.0058
0.05	0.01	0.0586	0.0326	0.0065
0.075	0.01	0.0789	0.0399	0.0058
0.10	0.01	0.1057	0.0537	0.0065
0.15	0.01	0.1503	0.0723	0.0063
0.20	0.01	0.1911	0.0871	0.0060
0.30	0.01	0.2785	0.1225	0.0062
0.40	0.01	0.3667	0.1587	0.0065
0.30	0	0.8698	0.7138	/
0.60	0	1.0645	0.7525	/

a. $Abs_{/Corrected} = Abs_{/Measured} - Abs_{/Aniline}$.

$$Abs_{/Corrected} = Abs_{/Measured} - \frac{0.208\times[\mathbf{2.1i}]}{0.4}.$$

b. $$K = \frac{[Abs - 0.01][AnH^+]}{[0.73 - Abs][An]}.$$

2.2.2 Summary and Discussion

Table 2.10 Values for K and pK_a of substituted anilinium ions in DMSO.

Anilines	R	K[a]	pK_a (DMSO)[b]	pK_a (water)[3]
2.1a	**4-OMe**	0.920±0.045	5.08±0.02	5.36
2.1b	**4-Me**	0.23±0.007	4.48±0.02	5.08
2.1c	**H**	$(5.0\pm0.2)\times10^{-2}$	3.82±0.02	4.58
2.1d	**4-Cl**	$(5.5\pm0.6)\times10^{-3}$	2.86±0.04	4.15
2.1e	**3-Cl**	$(1.66\pm0.14)\times10^{-3}$	2.34±0.04	3.46
2.1f	**3-CN**	$(1.74\pm0.18)\times10^{-4}$	1.36±0.04	2.75
2.1g	**2-Me**	0.048±0.002	3.80±0.05	4.39
2.1h	**2-Et**	0.043±0.002	3.75±0.05	4.37
2.1i	**H, N-Me**	$(6.2\pm0.3)\times10^{-3}$	2.91±0.05	4.85

a. The error is the standard deviation in the measured values of K.

b. Calculated from equation 2.3 with pK_a (DNP) = 5.12.

Figure 2.2 Hammett σ correlation with pK_a.

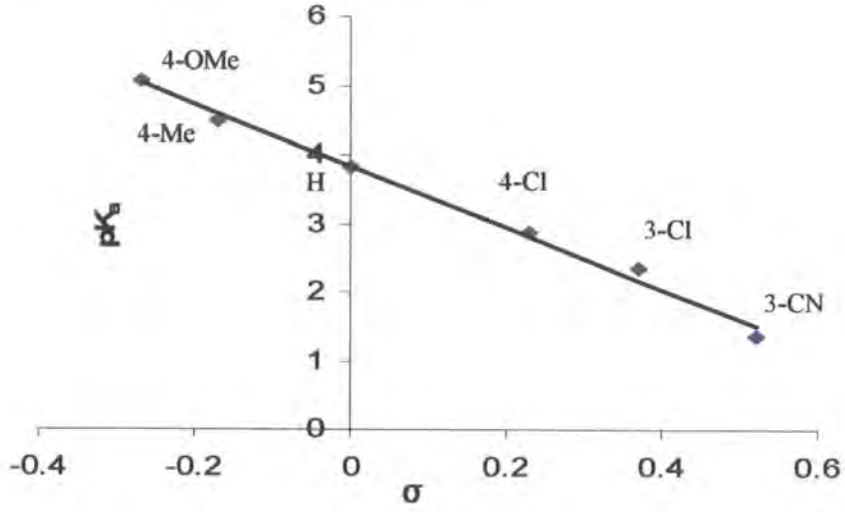

The values in Table 2.10 for the anilines with substituents at the meta- and para- positions are plotted versus Hammett σ values[4] in Figure 2.2. The plot of pK_a values gives a ρ value of -4.46. The related plot of $\log_{10} K_a$ versus σ would correspondingly give a ρ value of +4.46. This corresponds to the decrease in positive charge on the anilinium ion accompanying dissociation. The high acidity the N-methylanilinium ion in DMSO deserves comment. It is known[1,5] that DMSO is an extremely good hydrogen-bond acceptor so that stabilisation of the cationic species will decrease as the number of NH^+ hydrogens available for hydrogen-bonding

decreases. The reduced number, relative to anilinium, of such acidic hydrogens in the N-methylanilinium ion is likely to be an important factor here. Some steric inhibition of solvation by DMSO of the 2-substituted anilinium ions may also be expected.

2.3 pK_a for the Quinuclidinium Ion

Table 2.11 Absorbance data for 2,4,6-trinitrodiphenylamine (5×10^{-5} mol dm^{-3}) in DMSO containing various concentrations of quinuclidine at 25 °C.

[Quin]/mol dm^{-3}	[Quin HCl]/mol dm^{-3}	$[Quin]_{eq}$/mol dm^{-3}	Abs	K[a]
0	0.01	0	0.225	/
0.00040	0.01	0.00036	0.750	95
0.00060	0.01	0.00056	0.812	114
0.00080	0.01	0.00075	0.827	104
0.00100	0.01	0.00095	0.853	129
0.00450	0	0.00450	0.904	/

a. $K = \dfrac{[Abs - 0.225][QuinH^+]}{[0.904 - Abs][Quin]_{eq}}$.

The pK_a value for the quinuclidinium ion in DMSO was measured using 2,4,6-trinitrodiphenylamine[1] pK_a = 8.01 as the indicator. The reaction involved is shown in Scheme 2.2.

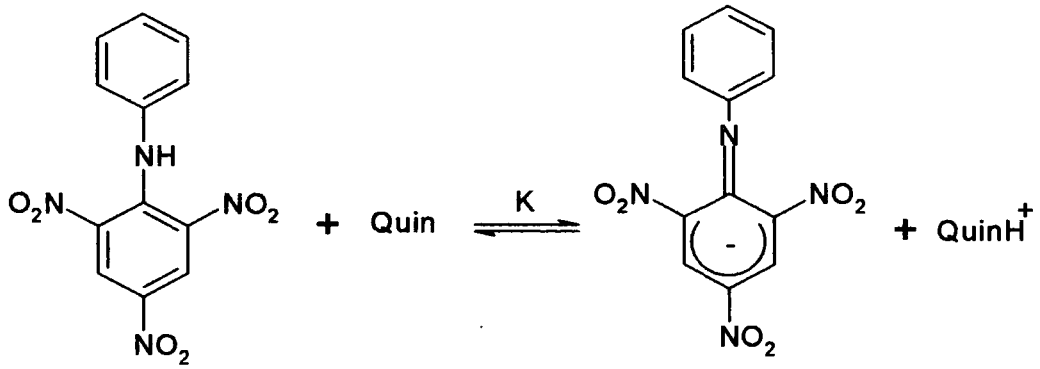

Scheme 2.2

Measurements were made at 450 nm, the maximum for the anionic form. Results are in Table 2.11. It was necessary to work with low concentration of quinuclidine in order to balance the position of equilibrium. Hence concentrations of quinuclidine at equilibrium were used in order to calculate values of K. The value

obtained for K was 110±10. The pK_a value for the quinuclidinium ion was calculated using equation 2.4 to be 10.05±0.05.

$$pK_a(QuinH^+) = \log_{10}K + pK_a(Indicator) \qquad (2.4)$$
$$= 2.04 + 8.01$$
$$= 10.05 \pm 0.05.$$

2.4 References

[1] M. R. Crampton and I. A. Robotham, J. Chem. Research, (S), 1997, 22.

[2] F. G. Bordwell, J. C. Branca, D. L. Hughes and W. N. Olmstead, J. Org. Chem., 1980, **45**, 3305.

[3] D. D. Perrin, 'Dissociation Constants of Organic Bases in Aqueous Solution', Butterworths, London, 1972.

[4] G. B. Barlin and D. P. Perrin, Chem. Soc., Quart. Rev., 1966, **20**, 75.

[5] M. J. Kamlet and R. W. Taft, J. Am. Chem. Soc., 1976, **98**, 377.

Chapter Three:

Reaction of Substituted Anilines with 1,3,5-Trinitrobenzene and 4-Nitrobenzofuroxan

Chapter Three: Reaction of Substituted Anilines with 1,3,5-Trinitrobenzene and 4-Nitrobenzofuroxan

3.1 Introduction

As noted in chapter 1 the reaction of 1,3,5-trinitrobenzene with aliphatic amines[1,2] in DMSO, results in the spontaneous formation of anionic σ-adducts. Kinetic studies are consistent with the two step process shown in Scheme 3.1, and have shown that the proton-transfer step may be rate-limiting[3,4], even though this step is thermodynamically favourable.

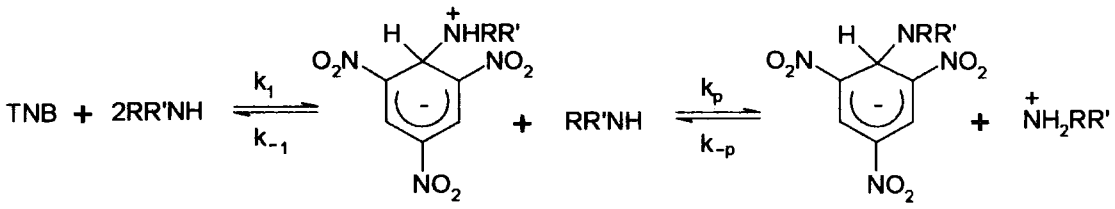

Scheme 3.1

Aniline is a very much weaker base than aliphatic amines and reaction with TNB does not occur. However Buncel and co-workers have shown that in the presence of a strong base, such as Dabco, to act as a proton accepter reaction may be observed[5,6]. Kinetic studies have shown that the proton transfer step may be rate-limiting[7,8]. One limitation in Buncel's work is that measurements were made without the addition of any acid salt, such as Dabcohydrochloride. This led to complicated kinetics with first order kinetics in the forward direction but second order in the reverse direction.

In this chapter kinetic and equilibrium results are reported for the reactions of 1,3,5-trinitrobenzene and 4-nitrobenzofuroxan with a series of substituted anilines in the presence of Dabco, or in some cases of quinuclidine, in DMSO. Measurements were made in the presence of Dabco and its hydrochloride salt allowing a more complete evaluation of the competing processes than was achieved in earlier studies.

It was also necessary to consider the recent claim[16,17] that the reaction of TNB with Dabco in DMSO yields a zwitterionic σ-adduct in spectroscopically observable amounts.

4-Nitrobenzofuroxan, is known to react with anionic nucleophiles, such as methoxide[10,11] or sulfite[12], to yield adducts at the 5- or 7-ring positions. Its reaction with aliphatic amines in DMSO may also yield σ-adducts and kinetic studies have shown that here too proton-transfer may be rate-limiting[13]. Reactions of 4-nitrobenzofuroxan with aromatic amines, which have not previously been investigated, are reported here.

3.2 Reaction of 1,3,5-Trinitrobenzene (TNB) with Aniline in DMSO

3.2.1 Initial Studies

UV/visible spectra of TNB, Dabco and aniline in DMSO measured separately showed little absorption above 350 nm. TNB (1×10^{-4} mol dm^{-3}) and aniline (0.1 mol dm^{-3}) together showed very weak absorption λ_{max} = 448 and 540 nm.

TNB (1×10^{-4} mol dm^{-3}) and Dabco (0.1 mol dm^{-3}) resulted in bands at λ_{max} = 449 nm, (Absorbance = 1.1) and at λ_{max} = 530 nm (Absorbance = 0.69). However spectra with TNB (1×10^{-4} mol dm^{-3}) and Dabco (0.1 mol dm^{-3}) containing Dabcohydrochloride (0.01 mol dm^{-3}) showed very much reduced absorption as seen in Figure 3.1.

Figure 3.1 Visible spectra of TNB (1×10^{-4} mol dm^{-3}), Dabco (0.1 mol dm^{-3}) and $DabcoH^+$ (0.01 mol dm^{-3}) in DMSO taken 10 min. to 1 h. after mixing.

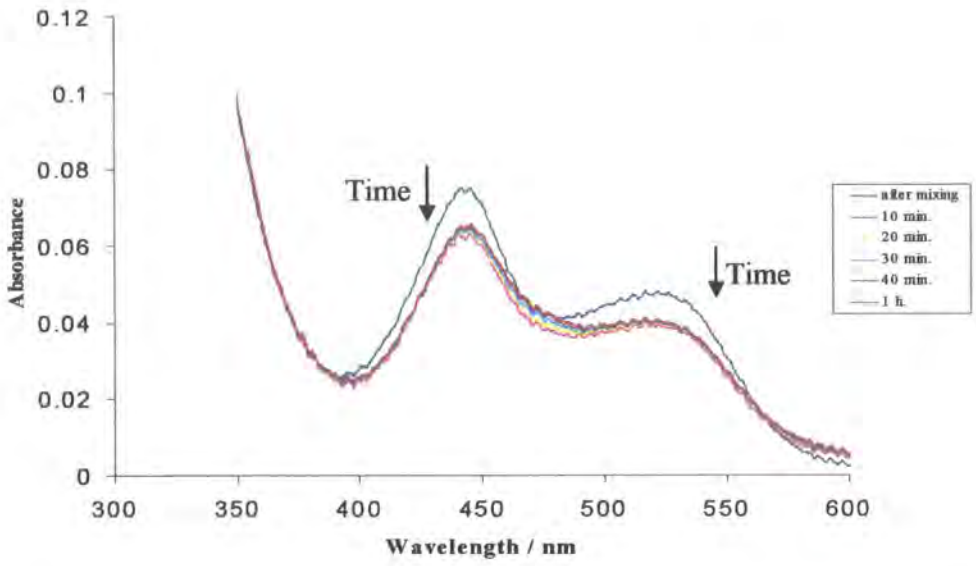

This decrease in absorbance in the presence of $DabcoH^+$ indicates that the reaction involved is not directly between TNB and Dabco, which would produce a zwitterion as shown in Scheme 3.2 and should be independent of the presence of $DabcoH^+$.

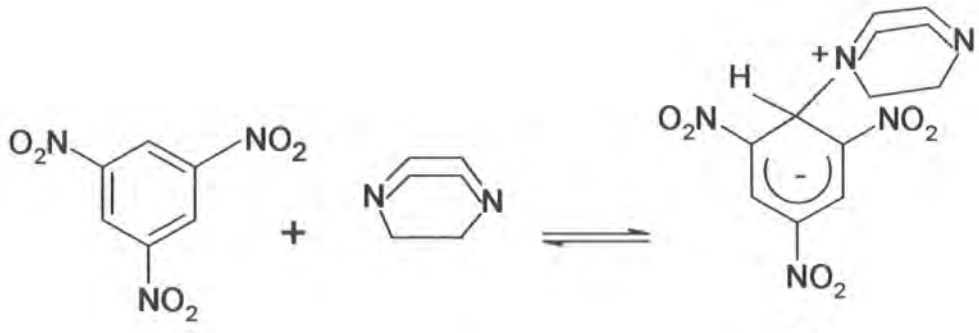

3.1

Scheme 3.2

The process observed probably involves the interaction of TNB with some amine impurity in the Dabco where a reaction of the type shown Scheme 3.3 below is possible.

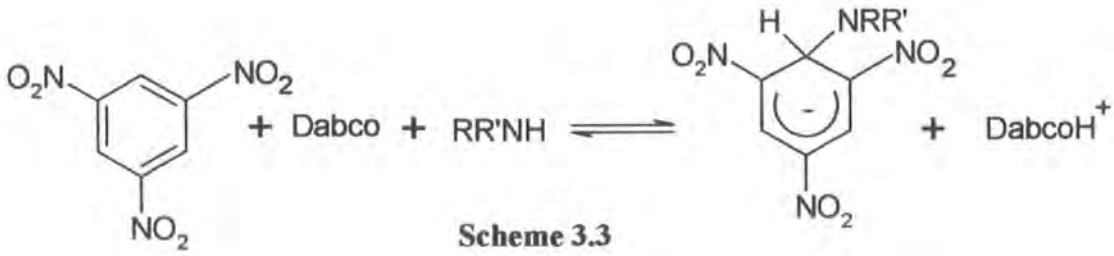

Scheme 3.3

In the presence of aniline and Dabco, TNB shows a strong absorbance λ_{max} = 445 nm ($\varepsilon = 3\times10^4$ dm^3 mol cm^{-1}) and 529 nm ($\varepsilon = 1.8\times10^4$ dm^3 mol cm^{-1}) attributed as previously[6,14,15], to formation of the aniline adduct **3.3**. The spectrum is shown in Figure 3.2.

Figure 3.2 Visible spectra of TNB (1×10^{-4} mol dm^{-3}), Dabco (0.1 mol dm^{-3}) and aniline in DMSO taken 10 min. to 1 h. after mixing.

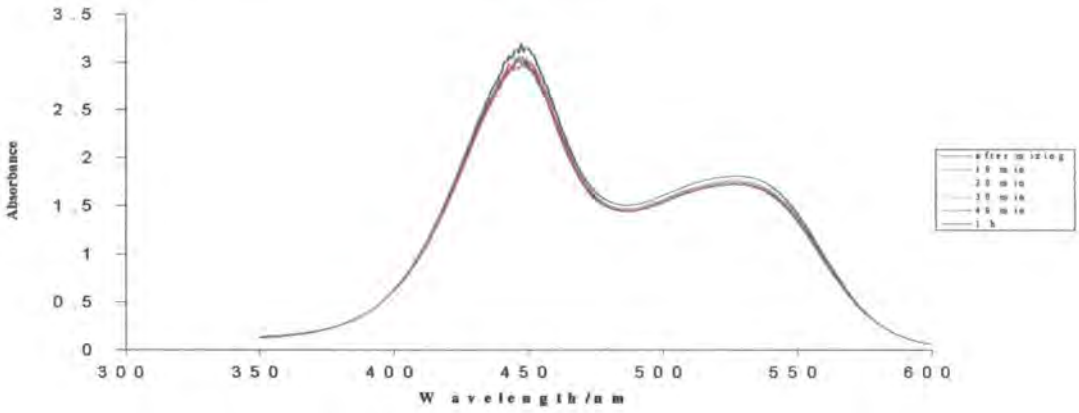

Measurements have been made involving the reactions of TNB and of nitrobenzofuroxan with a series of aniline derivatives **3.2**.

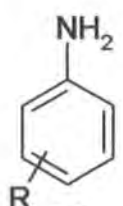

3.2

a 4-OMe
b 4-Me
c H
d 4-Cl
e 3-Cl
f 3-CN
g 2-Me
h 2-Et
i R=H, N-Me

In order to confirm the nature of the adduct ^1H NMR measurements were made.

3.2.2 ^1H NMR Measurements

Measurements were made with aniline and with a series of ring-substituted anilines in d_6 DMSO.

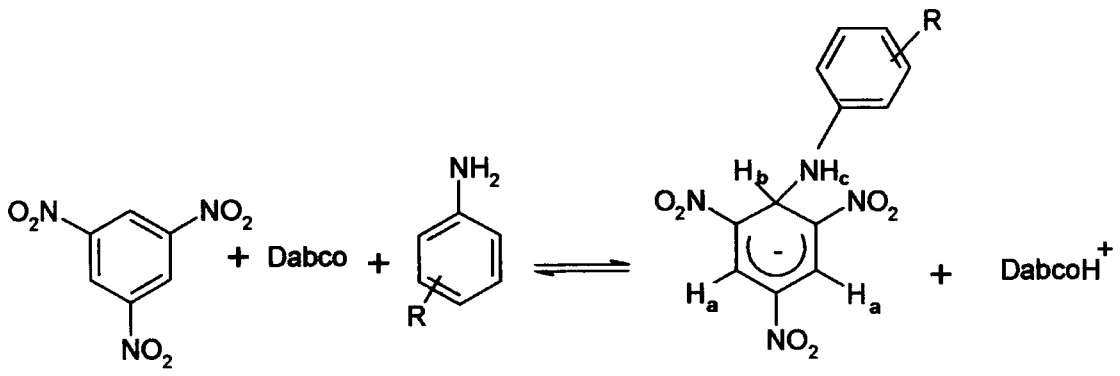

3.2 3.3

Scheme3.4

^1H NMR spectra of TNB (0.025 mol dm^{-3}) with **3.2a** (0.225 mol dm^{-3}) in the presence of Dabco (0.075 mol dm^{-3}) in $^2H_6$ DMSO were recorded immediately after mixing. The shifts indicate the formation of the thermodynamically stable adducts resulting from reaction at the 2-position as shown in Scheme 3.4.

For the reagents measured separately in $^2H_6$ DMSO bands are observed for TNB (δ 9.16 ppm, s), 4-methoxyaniline (6.51 and 6.64 ppm, doublets J = 8.8 Hz, ring hydrogen; 3.62 ppm, s, OMe) 4.5 ppm (broad, NH) and Dabco (2.65 ppm, s).

In the spectrum, Figure 3.3, of the mixture of the three components, bands are observed due to the unchanged reactants but new bands are also observed. The singlet at δ 8.34 ppm is attributed to H_a in the adduct, while the doublets J = 8.8 Hz at 6.08 and 5.51 ppm are due to H_b and H_c respectively.

Figure 3.3 ^{1}H NMR spectrum for adduct **3.3a** formed from 1,3,5-trinitrobenzene (TNB) (0.025 mol dm^{-3}) with 4-methoxyaniline (0.225 mol dm^{-3}) and Dabco (0.075 mol dm^{-3}) in $^{2}H_6$ DMSO.

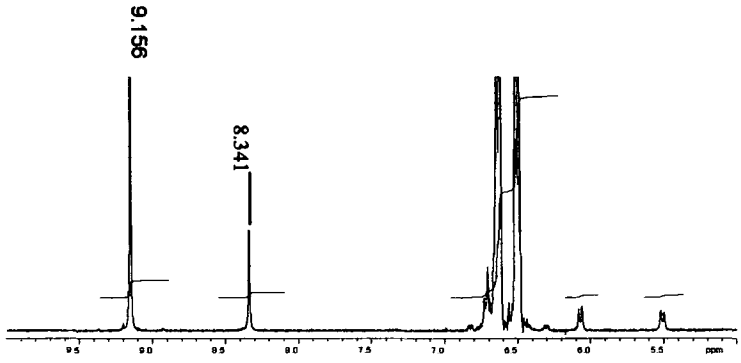

The observation of C-H to N-H coupling indicates that the amine hydrogen does not exchange rapidly with other labile hydrogens.

After the addition of a trace of D_2O to the mixture the band at δ 5.51 was lost due to deuteration, and the band at δ 6.08 collapsed to a singlet. This is expected since C-H to N-D coupling is much weaker than C-H to N-H coupling. The change in δ value from 9.16 to 6.08 ppm, for H_b is consistent with the change in hybridization from sp^2 aromatic to sp^3.

The spectrum in Figure 3.3 shows only a relatively small extent of conversion of TNB to the adduct indicating that the equilibrium constant for adduct formation is low.

Similarly spectra were measured in the presence of other anilines **3.2b-f** and the shift values for the adducts formed **3.3a-f** are collected in Table 3.1. In each case the resonance for the N-H hydrogen was identified by its disappearance in the presence of D_2O.

Table 3.1 ^{1}H NMR data for adducts **3.3** formed from 1,3,5-trinitrobenzene (TNB) (0.025 mol dm^{-3}) with anilines (0.225 mol dm^{-3}) and Dabco (0.075 mol dm^{-3}) in $^{2}H_6$ DMSO.

Adduct 3.3	^{1}H NMR Shifts/ppm			
	H_a	H_b	H_c	J_{bc}/Hz
a 4-OMe	8.34	6.08	5.51	8.8
b 4-Me	8.34	6.14	5.7	8.8
c H	8.35	6.21	5.88	9.2
d 4-Cl	8.36	6.18	6.12	8.8
e 3-Cl	8.37	6.20	6.26	9.2
f 3-CN	8.36	6.25	6.46	9.2

Table 3.2 The values of δ NH with σ.

Adducts 3.3	σ	δ NH/ppm
4-methoxyaniline	-0.27	5.51
4-methylaniline	-0.17	5.7
aniline	0	5.88
4-chlororaniline	0.23	6.12
3-chloroaniline	0.37	6.26
3-cyanoaniline	0.66	6.46

Figure 3.4 Hammett σ correlation with δ NH.

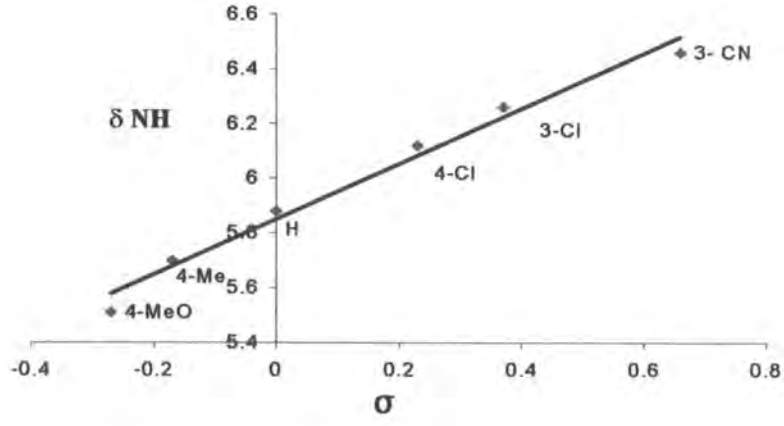

The values of δ NH given in Table 3.2, show a reasonably good correlation with Hammett σ values as shown in Figure 3.4. The positive slope is consistent with increasing acidity of the NH hydrogen as the electron density of the NH hydrogen decreases as the substituents are made more electron withdrawing.

3.2.3 TNB and Dabco in DMSO

Boga and Forlani[16,17] have reported a strong interaction K = 70 dm^3 mol^{-1} between TNB and Dabco in DMSO to give the zwitterionic adduct as shown in Scheme **3.2**.

The UV/visible measurements show that this is unlikely since the reaction is inhibited by $DabcoH^+$. Confirmation of the lack of reaction of TNB and Dabco was obtained from NMR measurements. The spectrum, Figure 3.5 of TNB (0.025 mol dm^{-3}), in the presence of Dabco (0.067 mol dm^{-3}) shows only extremely weak bands at δ 8.33 and 6.19 ppm attributable to adduct formation. The relative intensities, per hydrogen, of the TNB and adduct bands are 33 and 0.3 respectively. Hence the value calculated for K, the equilibrium constant is *ca* 0.14 dm^3 mol^{-1}.

$$K = \frac{[\text{Adduct}]}{[\text{TNB}][\text{Dabco}]}$$

$$= \frac{0.3}{33 \times 0.067} = 0.14 \text{ dm}^3 \text{ mol}^{-1}.$$

It is very likely that the bands observed result not from the direct interaction of TNB and Dabco but from the presence of an amine impurity in the Dabco.

Figure 3.5 ^{1}H NMR spectrum of adduct **3.1** formed from TNB (0.025 mol dm^{-3}) in the presence of Dabco (0.067 mol dm^{-3}) in $^{2}H_6$ DMSO.

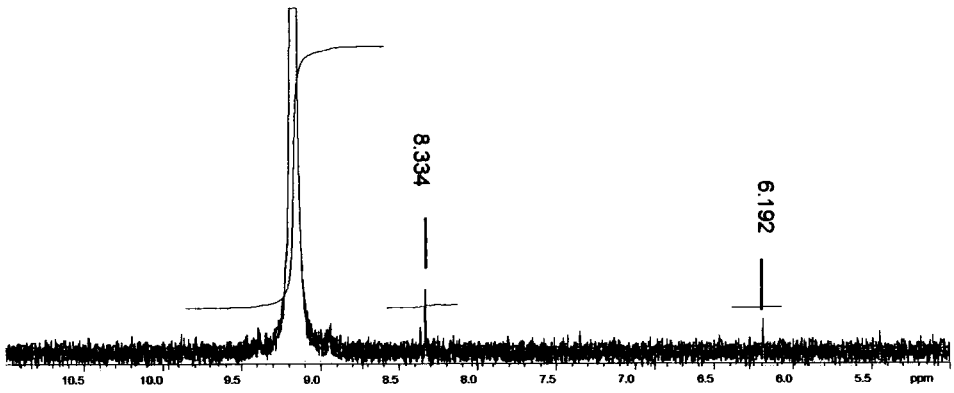

3.2.4 Kinetic and Equilibrium Studies

Rate and equilibrium measurements were made for the reaction of TNB with anilines **3.2a-i** in DMSO in the presence of Dabco at 25 °C. Absorbance measurements were made at 446 nm and/or 530 nm, the absorption maxima of the adducts formed. The TNB concentration was kept at 4×10^{-5} mol dm^{-3}, and was very much lower than those of the other components. Under these conditions first order kinetic traces were observed. All measurements were made in the presence of 0.01 mol dm^{-3} Dabcohydrochloride. This inhibited any reaction between TNB and Dabco, and effectively kept the ionic strength of the solution constant. The variations with both Dabco concentration and aniline concentration of rate constants and absorbance values at completion of reaction were measured.

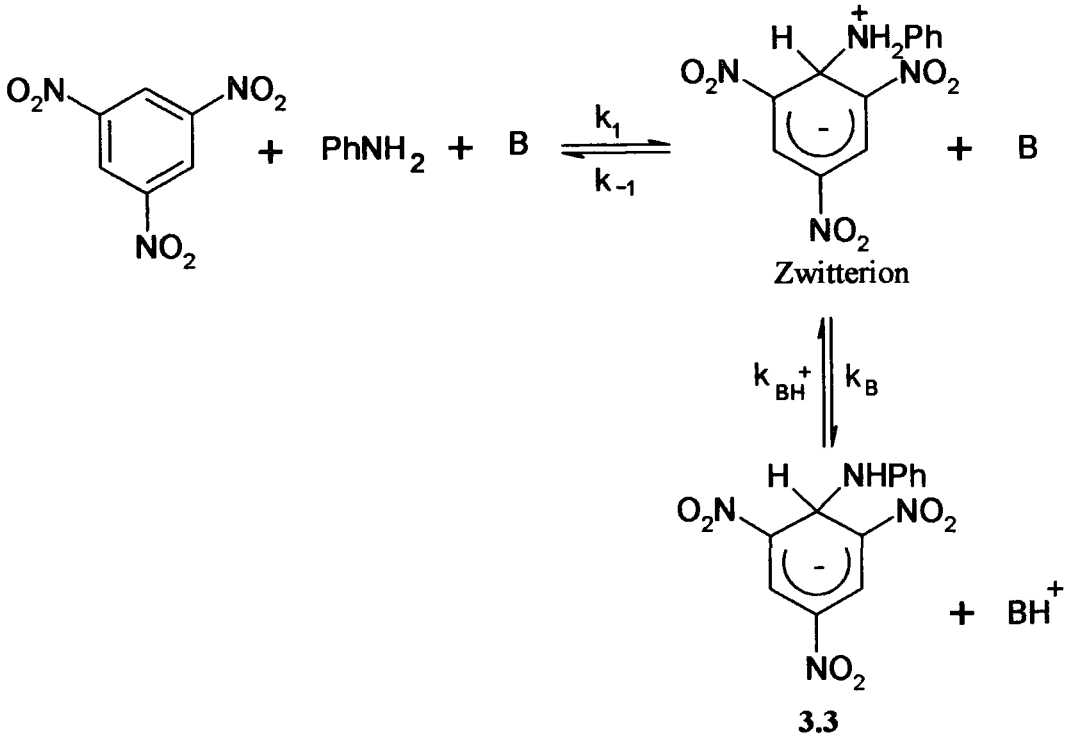

3.3

Scheme 3.5

The results are interpreted in terms of Scheme 3.5 where B may be Dabco or may be a second molecule of aniline.

The overall equilibrium constant is given in equation 3.1 which becomes equation 3.2 when the base considered is Dabco.

$$K_{obs} = \frac{[\mathbf{3.3}][BH^+]}{[TNB][PhNH_2][B]} \qquad (3.1)$$

$$K_{obs} = \frac{k_1}{k_{-1}} \frac{k_B}{k_{BH^+}}$$

$$K_{obs} = K_1 K_{Dabco} = \frac{[\mathbf{3.3}][DabcoH^+]}{[TNB][PhNH_2][Dabco]} = \frac{k_1}{k_{-1}} \frac{k_{Dabco}}{k_{DabcoH^+}} \qquad (3.2)$$

Since **3.3** is the only absorbing species in the visible region values of K_{obs}(= K_1K_{Dabco}) could be calculated using equation 3.2.

Measurements with Dabco and aniline in the absence of Dabcohydrochloride, where conversion to adduct was almost complete, allowed the calculation of the extinction coefficient of the adduct.

$$Abs = \varepsilon cl \qquad (3.3)$$

Then measurements in solutions containing Dabcohydrochloride gave values of the concentration of **3.3** in other solutions.

Then: $[TNB] = 4\times10^{-5}\,mol\,dm^{-3} - [\mathbf{3.3}]$

Representative data for reaction with 4-methoxyaniline **3.2a** and with aniline **3.2c** are given in Tables 3.3 and 3.4.

The result shows that when the [Dabcohydrochloride] is constant at 0.01 mol dm^{-3}, the values of K_1K_{Dabco} are essentially constant. Values are collected in Table 3.5. When the [Dabcohydrochloride] is increased values of K_{obs} also increase. This is likely to be due to a specific effect of chloride ion which stabilises the $DabcoH^+$ ion by association[18] (Scheme 3.6).

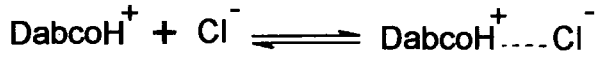

Scheme 3.6

Table 3.3

[4-methoxyaniline]/ mol dm^{-3}	[Dabco]/ mol dm^{-3}	[$DabcoH^+$]/ mol dm^{-3}	Abs λ = 530	K_{obs}/ $dm^3\,mol^{-1}$
0.1	0.1	/	0.78	/
0.2	0.1	/	0.79	/
0.2	0.05	/	0.78	/
0.1	0.1	0.01	0.228	0.409
0.1	0.1	0.01	0.276	0.546
0.2	0.1	0.01	0.406	0.544
0.3	0.1	0.01	0.506	0.616
0.1	0.06	0.01	0.201	0.579
0.1	0.04	0.01	0.160	0.646
0.2	0.05	0.005	0.388	0.492
0.2	0.05	0.008	0.322	0.564
0.2	0.05	0.015	0.269	0.789
0.1	0.05	0.02	0.138	0.860

Table 3.4

[aniline]/ mol dm^{-3}	[Dabco]/ mol dm^{-3}	[DabcoH$^+$]/ mol dm^{-3}	Abs λ = 446	K_{obs}/ dm^3 mol^{-1}
0.1	0.1	/	1.31	/
0.2	0.1	/	1.32	/
0.2	0.05	/	1.31	/
0.1	0.1	0.01	0.345	0.357
0.1	0.1	0.01	0.359	0.375
0.2	0.1	0.01	0.538	0.348
0.3	0.1	0.01	0.672	0.352
0.4	0.1	0.01	0.724	0.31
0.1	0.06	0.01	0.255	0.398
0.1	0.04	0.01	0.176	0.388
0.2	0.05	0.005	0.475	0.285
0.2	0.05	0.008	0.379	0.325
0.2	0.05	0.015	0.275	0.398
0.1	0.05	0.02	0.145	0.498

Table 3.5 Values obtained with [Dabcohydrochloride] = 0.01 mol dm^{-3}.

Anilines	K_1K_{Dabco}/ dm^3 mol^{-1}
3.2a	0.55±0.1
3.2b	0.5±0.1
3.2c	0.36±0.03
3.2d	0.43±0.04
3.2e	0.50±0.03
3.2f	0.22±0.02

It is worth noting that an equilibrium constant could also be defined solely in terms of the aniline concentration. The pK_a values for the protonated forms of aniline and Dabco in DMSO are known[19] to be 3.82 and 9.06 respectively. Hence the value of the equilibrium constant K_a' for equation 3.4 is given by equation 3.5.

$$\text{Aniline} + \text{DabcoH}^+ \rightleftharpoons \text{AnilineH}^+ + \text{Dabco} \qquad (3.4)$$

$$K_a' = \frac{K_a^{\text{DabcoH}^+}}{K_a^{\text{AnilineH}^+}} = 5.8\times10^{-6} = \frac{K_{An}}{K_{Dabco}} \qquad (3.5)$$

When aniline is considered as the base as well as the nucleophile, then equation 3.1 takes the form of equation 3.6.

$$K_{obs} = K_1 K_{An} = \frac{[\mathbf{3.3}][AnilineH^+]}{[TNB][Aniline]^2} = \frac{k_1 k_{An}}{k_{-1} k_{AnH^+}} \qquad \textbf{(3.6)}$$

Hence using equation 3.5 it is seen that equation 3.7 is true.

$$K_1 K_{An} = K_1 K_{Dabco} \times 5.8 \times 10^{-6} \qquad \textbf{(3.7)}$$

The very low values expected for K_1K_{An} explain why little adduct formation is observed in the absence of Dabco.

Kinetic

Kinetic measurements were conveniently made using the stopped-flow method at 446 nm. All measurements were made with concentration of TNB very much lower than those of the aniline derivative, Dabco or Dabcohydrochloride. The latter concentration was kept constant at 0.01 mol dm^{-3} for all experiments. Under these conditions first order kinetics were observed and representative traces are shown in Figures 3.6 and 3.7. The Figure 3.6 shows the experimental trace, together with that calculated with k = 11.30±0.02 s^{-1} superimposed, and k = 1.60±0.003 s^{-1} for Figure 3.7.

Figure 3.6 Stopped flow trace for reaction of TNB (4×10^{-5} mol dm^{-3}), Dabco (0.1 mol dm^{-3}), Dabcohydrochloride (0.01 mol dm^{-3}) and 4-methoxyaniline (0.05 mol dm^{-3}), λ = 530 nm.

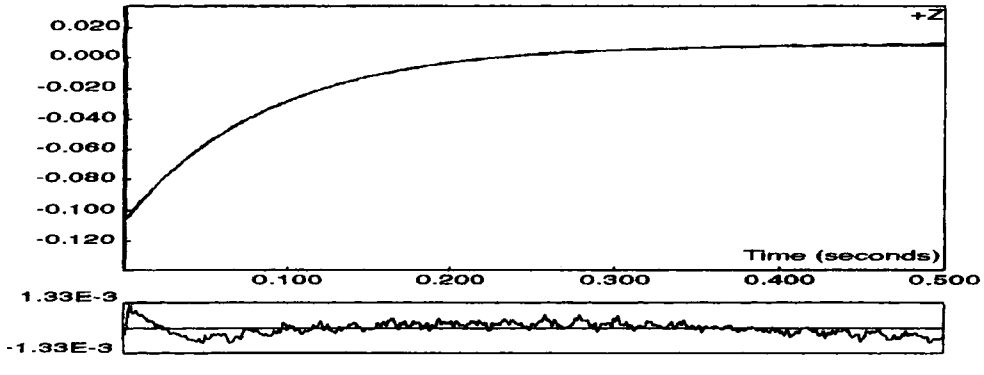

Figure 3.7 Stopped flow trace for reaction of TNB (4×10^{-5} mol dm^{-3}), Dabco (0.1 mol dm^{-3}), Dabcohydrochloride (0.01 mol dm^{-3}) and aniline (0.1 mol dm^{-3}), $\lambda = 446$ nm.

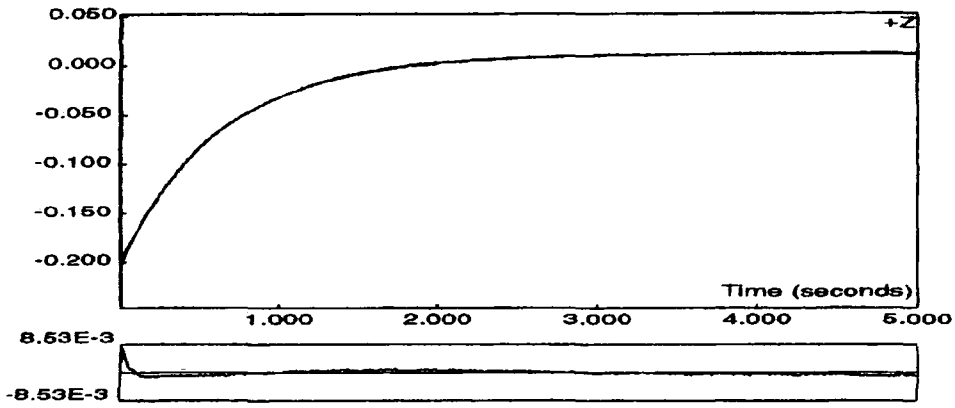

Treatment of the zwitterion as a steady-state intermediate leads to the rate expression given in equation 3.8 which simplifies to equation 3.9 (for details see appendix I).

$$k_{obs} = \frac{k_1[PhNH_2]k_B[B]}{k_{-1} + k_B[B]} + \frac{k_{BH^+}[BH^+]k_{-1}}{k_{-1} + k_B[B]} \qquad \textbf{(3.8)}$$

$$k_{obs} = \frac{k_1[PhNH_2]k_B[B] + k_{BH^+}[BH^+]k_{-1}}{k_{-1} + k_B[B]} \qquad \textbf{(3.9)}$$

If $k_{-1} \rangg k_B[B]$, corresponding to rate limiting proton transfer, then equation 3.10 follows.

$$k_{obs} = \frac{k_1}{k_{-1}}[PhNH_2]k_B[B] + k_{BH^+}[BH^+] \qquad \textbf{(3.10)}$$

Since $K_1 = \frac{k_1}{k_{-1}}$ this reduces to equation 3.11.

$$k_{obs} = K_1[PhNH_2]k_B[B] + k_{BH^+}[BH^+] \qquad \textbf{(3.11)}$$

Plots according to equation 3.11 are shown in Figure 3.8 for reactions at constant concentration, 0.1 mol dm^{-3}, of 4-methoxyaniline and in Figure 3.9 at constant concentration, 0.1 mol dm^{-3}, of Dabco. The plots are similar but have slopes corresponding to K_1k_{Dabco} which are not exactly the same. Similarly the intercepts corresponding to $k_{DabcoH}{}^{+}[DabcoH^{+}]$ are not exactly equal.

Figure 3.8

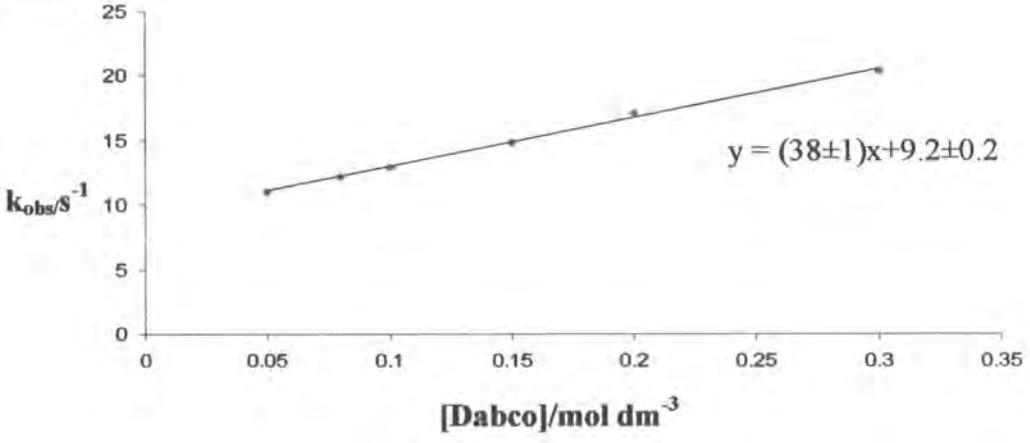

Figure 3.9

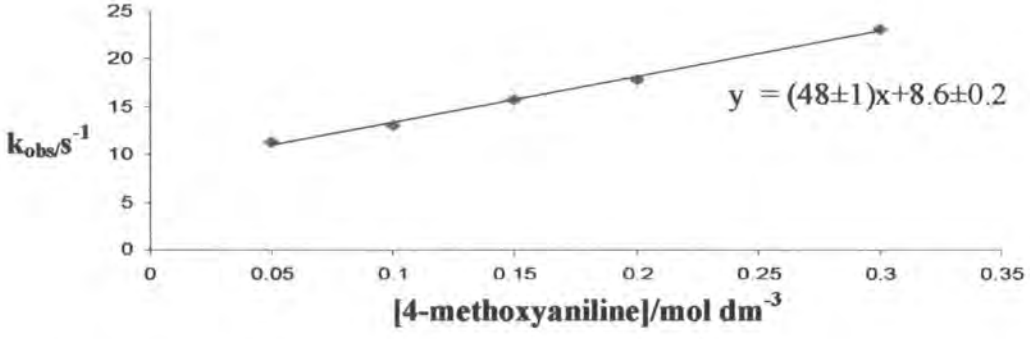

If, as Buncel[18] assumed, only Dabco is effective as a base in the proton transfer stage of the reaction then values of slopes and intercept should be equal within the error of the experiment.

These results indicate that it is necessary to include the possibility of aniline itself also acting as the base in the proton transfer step. In a related system Crampton and Robotham[8] showed that aniline, even though a much weaker base, might also contribute to the proton transfer equilibration. Thus, the zwitterion in Scheme 3.5 is expected to be more acidic than the corresponding anilinium ion. This results from the fact that the trinitrocyclohexadienate group, even though it is negatively charged, is

electron withdrawing relative to hydrogen[3,4]. Hence the zwitterion will be more acidic than the corresponding anilinium ion so that the proton transfer step zwitterion $\rightleftharpoons$ **3.3** will be thermodynamically favoured even when the reaction involves aniline as B and the corresponding anilinium ion as BH^+. Taking account of the possibility of this additional proton transfer process leads to equation 3.12.

$$k_{obs} = K_1[An](k_{Dabco}[Dabco] + k_{An}[An]) + k_{DabcoH^+}[DabcoH^+] + k_{AnH^+}[AnH^+] \quad \textbf{(3.12)}$$

Since $\frac{K_{An}}{K_{Dabco}}$ has a constant value it is possible to reduce the number of variables in equation 3.12 to give equation 3.13 as shown below.

$$\frac{k_{Dabco}[Dabco][Zwitterion]}{k_{DabcoH^+}[DabcoH^+][\mathbf{3.3}]} = \frac{k_{An}[An][Zwitterion]}{k_{AnH^+}[AnH^+][\mathbf{3.3}]}$$

$$\frac{k_{AnH^+}[AnH^+]}{k_{DabcoH^+}[DabcoH^+]} = \frac{k_{An}[An]}{k_{Dabco}[Dabco]}$$

$$k_{AnH^+}[AnH^+] = \frac{k_{An}[An]}{k_{Dabco}[Dabco]} k_{DabcoH^+}[DabcoH^+]$$

Substitution in equation 3.12 gives.

$$k_{obs} = K_1[An](k_{Dabco}[Dabco] + k_{An}[An]) + k_{DabcoH^+}[DabcoH^+](1 + \frac{k_{An}[An]}{k_{Dabco}[Dabco]})$$

$$k_{obs} = K_1[An]k_{Dabco}[Dabco](1 + \frac{k_{An}[An]}{k_{Dabco}[Dabco]}) + k_{DabcoH^+}[DabcoH^+](1 + \frac{k_{An}[An]}{k_{Dabco}[Dabco]})$$

$$k_{obs} = K_1[An]k_{Dabco}([Dabco] + \frac{k_{An}}{k_{Dabco}}[An]) + k_{DabcoH^+}[DabcoH^+](1 + \frac{k_{An}[An]}{k_{Dabco}[Dabco]}) \quad \textbf{(3.13)}$$

There are three variable parameters in equation 3.13, which were represented as shown below when fitting the experimental data.

$K_1 k_{Dabco} = a$

$k_{DabcoH}{}^{+}[DabcoH^{+}] = b$

$k_{An} / k_{Dabco} = c$

Then equation 3.13 is equivalent to equation 3.14.

$$k_{calc} = a[An]([Dab\ co] + c[An]) + b(1 + c\frac{[An]}{[Dabco]}) \qquad \textbf{(3.14)}$$

Representative data for reaction of [TNB] = 4×10^{-5} mol dm^{-3} with 3-chloroaniline **3.2e** in the presence of [$DabcoH^{+}$] = 0.01 mol $dm^{-3}$are in Table 3.6, and data for 4-methoxyaniline are in Table 3.7. Values of a,b and c, were varied so as to optimise the fit, judged by the standard deviation σ, between observed and calculated values.

$$\sigma = \sqrt{\frac{\sum(k_{obs} - k_{calc})^2}{n}}$$

All reported data were measured with [TNB] = 4×10^{-5} mol dm^{-3} and [Dabcohydrochloride] = 0.01 mol dm^{-3}.

Table 3.6

[3-chloroaniline]/ mol dm^{-3}	[Dabco]/ mol dm^{-3}	k_{obs}/s^{-1}	k_{calc}/s^{-1}	k_{calc}/s^{-1}	k_{calc}/s^{-1}	k_{calc}/s^{-1}	k_{calc}/s^{-1}
0.05	0.1	0.047	0.043	0.044	0.043	0.045	0.045
0.1	0.1	0.055	0.052	0.053	0.050	0.055	0.054
0.15	0.1	0.06	0.061	0.062	0.057	0.065	0.063
0.2	0.1	0.071	0.071	0.072	0.064	0.076	0.073
0.3	0.1	0.088	0.092	0.093	0.078	0.099	0.093
0.1	0.05	0.048	0.049	0.049	0.043	0.051	0.048
0.1	0.1	0.052	0.052	0.053	0.050	0.055	0.054
0.1	0.15	0.058	0.057	0.058	0.057	0.060	0.060
0.1	0.2	0.063	0.062	0.064	0.064	0.067	0.068
0.1	0.3	0.072	0.073	0.077	0.078	0.080	0.082
(k_{calc}/s^{-1}) calculated from equation 3.14 with		**a** =	1.2	1.3	1.4	1.4	1.5
		b =	0.035	0.036	0.036	0.036	0.036
		c =	0.1	0.08	0	0.09	0.05
		σ =	2×10^{-3}	3×10^{-3}	5.16×10^{-3}	5.23×10^{-3}	4×10^{-3}

Table 3.7

[4-methoxyaniline]/ mol dm^{-3}	[Dabco]/ mol dm^{-3}	k_{obs}/s^{-1}	k_{calc}/s^{-1}	k_{calc}/s^{-1}	k_{calc}/s^{-1}	k_{calc}/s^{-1}	k_{calc}/s^{-1}
0.05	0.1	11.3	10.9	11.0	11.3	10.9	10.6
0.1	0.1	13.1	13.1	13.3	13.7	13.1	12.7
0.15	0.1	15.8	15.4	15.7	16.1	15.4	14.9
0.2	0.1	17.9	17.7	18.3	18.7	17.8	17.3
0.3	0.1	23.1	22.6	23.6	24.2	22.9	22.2
0.1	0.05	11	11.6	11.8	12.1	11.7	11.3
0.1	0.08	12.2	12.4	12.7	13.0	12.5	12.1
0.1	0.1	12.9	13.1	13.3	13.7	13.1	12.7
0.1	0.15	14.8	14.9	15.1	15.5	14.8	14.4
0.1	0.2	17.1	16.7	17.0	17.4	16.6	16.1
0.1	0.3	20.3	20.5	20.8	21.4	20.2	19.6
(k_{calc}/s^{-1}) calculated from equation 3.14 with		**a** =	380	390	400	370	360
		b =	8.8	8.8	9	8.8	8.5
		c =	0.04	0.05	0.05	0.05	0.05
		σ =	0.33	0.43	0.75	0.34	0.64

It was found that a non-zero value of the parameter c was required to give satisfactory agreement. Optimised values for reaction with the other anilines are given in Tables 3.8-3.11. Values of parameters obtained are collected in Table 3.15.

Table 3.8

[4-methylaniline]/ mol dm^{-3}	[Dabco]/ mol dm^{-3}	k_{obs}/s^{-1}	k_{calc}/s^{-1}
0.05	0.1	3.46	3.34
0.1	0.1	3.93	3.90
0.15	0.1	4.64	4.48
0.2	0.1	4.95	5.08
0.3	0.1	6.34	6.33
0.1	0.05	3.53	3.54
0.1	0.1	3.93	3.90
0.1	0.15	4.34	4.34
0.1	0.2	4.7	4.79
0.1	0.3	5.5	5.73
(k_{calc}/s^{-1}) calculated from equation 3.14 with		**a** = 95±10	
		b = 2.8±0.2	
		c = 0.04±0.01	
		σ = 0.11	

Table 3.9

[Aniline]/ mol dm^{-3}	[Dabco]/ mol dm^{-3}	k_{obs}/s^{-1}	k_{calc}/s^{-1}
0.03	0.1	1.13	1.00
0.05	0.1	1.14	1.07
0.07	0.1	1.21	1.13
0.1	0.1	1.3	1.24
0.15	0.1	1.45	1.42
0.2	0.1	1.56	1.61
0.3	0.1	1.79	2.00
0.1	0.05	1.08	1.14
0.1	0.08	1.21	1.19
0.1	0.1	1.27	1.24
0.1	0.15	1.38	1.36
0.1	0.2	1.51	1.50
0.1	0.3	1.6	1.77
(k_{calc}/s^{-1}) calculated from equation 3.14 with		**a** = 28±3	
		b = 0.9±0.3	
		c = 0.05±0.01	
		σ = 0.09	

Table 3.10

[4-chloroaniline]/ mol dm^{-3}	[Dabco]/ mol dm^{-3}	k_{obs}/s^{-1}	k_{calc}/s^{-1}
0.05	0.1	0.166	0.156
0.1	0.1	0.197	0.184
0.15	0.1	0.214	0.212
0.2	0.1	0.23	0.242
0.3	0.1	0.306	0.305
0.1	0.05	0.161	0.168
0.1	0.1	0.181	0.184
0.1	0.15	0.202	0.204
0.1	0.2	0.218	0.226
0.1	0.3	0.263	0.269
(k_{calc}/s^{-1}) calculated from equation 3.14 with		**a** = 4.5±1	
		b = 0.13±0.01	
		c = 0.05±0.01	
		σ = 0.008	

Table 3.11

[3-cyanoaniline]/ mol dm^{-3}	[Dabco]/ mol dm^{-3}	k_{obs}/s^{-1}	k_{calc}/s^{-1}
0.1	0.05	0.012	0.012
0.1	0.1	0.013	0.013
0.1	0.15	0.014	0.014
0.1	0.2	0.016	0.015
0.1	0.3	0.018	0.018
0.1	0.1	0.013	0.013
0.15	0.1	0.015	0.015
0.2	0.1	0.016	0.017
0.3	0.1	0.019	0.020
(k_{calc}/s^{-1}) calculated from equation 3.14 with		**a** = 0.25±0.02	
		b = 0.01±0.002	
		c = 0.05±0.01	
		σ = 5×10^{-4}	

Results were also obtained for reactions involving the more sterically hindered anilines **3.2g-i** and are given in Table 3.12-3.14. Although the data here was more limited no clear improvement in fitting the data was obtained by using non-zero values of k_{An}/k_{Dabco}.

The failure of these anilines to contribute to the proton transfer step is likely to be due to steric hindrance to their approach to the reaction centre.

Table 3.12

[Dabco]/ mol dm^{-3}	[2-methylaniline]/ mol dm^{-3}	k_{obs}/s^{-1}
0.1	0.1	0.91
0.1	0.2	1.00
0.1	0.3	1.07
0.1	0.05	0.84

Table 3.13

[Dabco]/ mol dm^{-3}	[2-ethylaniline]/ mol dm^{-3}	k_{obs}/s^{-1}
0.1	0.1	0.653
0.1	0.2	0.741
0.1	0.3	0.829
0.1	0.4	0.908

Table 3.14

[Dabco]/ mol dm^{-3}	[N-methylaniline]/ mol dm^{-3}	k_{obs}/s^{-1}
0.1	0.1	0.174
0.1	0.2	0.181
0.1	0.3	0.209
0.05	0.1	0.142

Table 3.15 Summary of kinetic results.

Anilines	K_1K_{Dabco}[a] / $dm^3\ mol^{-1}$	K_1k_{Dabco} / $dm^6\ mol^{-2}\ s^{-1}$	k_{DabcoH^+}[b] / $dm^3\ mol^{-1}\ s^{-1}$	k_{An}/k_{Dabco}
3.2a	0.43±0.04	380±20	880±30	0.04±0.01
3.2b	0.34±0.06	95±10	280±20	0.04±0.01
3.2c	0.31±0.1	28±3	90±30	0.05±0.01
3.2d	0.35±0.1	4.5±1	13±1	0.05±0.01
3.2e	0.34±0.07	1.2±0.2	3.5±0.1	0.1±0.02
3.2f	0.25±0.09	0.25±0.02	1±0.2	0.05±0.01
3.2g	0.10±0.04	8±1	80±20	0
3.2h	0.13±0.05	8±2	60±10	0
3.2i	0.14±0.05	2.0±0.3	14±2	0

a. $K_1K_{Dabco} = K_1k_{Dabco}/k_{DabcoH^+}$.

b. From $b = k_{DabcoH^+}[DabcoH^+]$.

Values are summarised in Table 3.15. The value of K_1k_{Dabco} and of k_{DabcoH^+} in Table 3.15 show a strong dependence on the nature of the ring substituent.

Hammett plots for **3.2a-3.2f** lead to ρ values of -3.82 and -3.62 respectively as shown in Figures 3.10, 3.11.

The negative ρ value in Figure 3.10 reflect the increase in positive charge on the amino nitrogen on formation of the zwitterion. The negative ρ value in Figure 3.11 corresponds to the increase in positive charge on the amino nitrogen as the anionic adduct **3.3** in Scheme 3.5 is protonated to give the zwitterion.

Figure 3.10 Hammett σ correlation with log K_1k_{Dabco}.

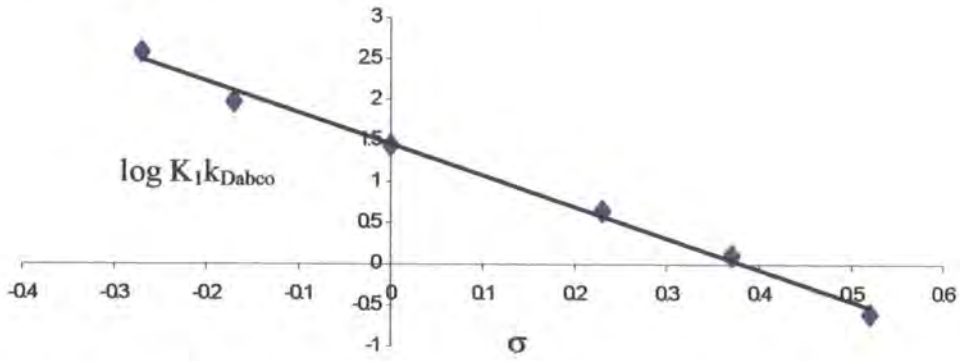

Figure 3.11 Hammett σ correlation with log k_{DabcoH}^{+}.

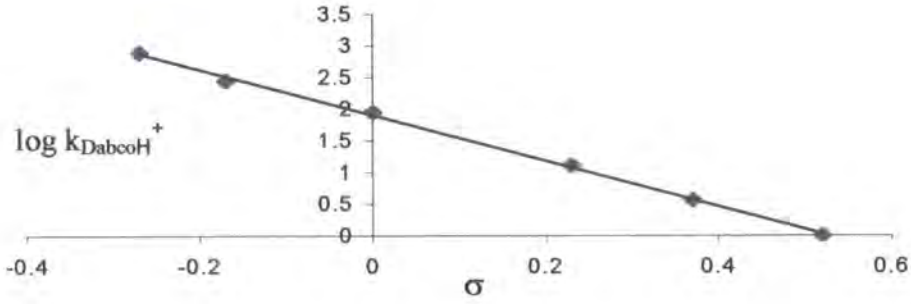

Compensation in the variation of these terms leads to values of (K_1K_{Dabco} = $K_1k_{Dabco}/k_{DabcoH+}$) which show only a small variation with the nature of the substituent. The values obtained from the kinetic data are in reasonable agreement with these obtained from absorbance measurements reported in Table 3.5. The lower values for K_1K_{Dabco} obtained for the 2-substituted anilines and for N-methylaniline are likely to be due to steric hindrance associated with formation of the adducts.

3.2.5 Reaction with Quinuclidine

In order to see the effect of changing the base from Dabco to quinuclidine a small number of experiments were carried out. The UV/visible spectrum of the adduct with λ_{max} =445 and 529 nm was unchanged with the change in base. Kinetic measurements were made with TNB (4×10^{-5} mol dm^{-3}) and quinuclidinehydrochloride (0.01 mol dm^{-3}). Values of rate constants are given in Table 3.16, 3.17 and 3.18 and linear plots according to equation 3.11 gave values for K_1k_{quin} and k_{quinH}^{+} which are collected in Table 3.19.

Comparison with values for reactions involving Dabco in Table 3.15 show that for these two bases values of K_1k_B are independent of the nature of the base, implying that values of k_B are determined by factors other than basicity. Values of k_{BH}^{+} show a direct dependence on the values of the acidity of the conjugate acids (pK_a values, $DabcoH^+$ 9.06; $quinuclidineH^+$, 10.05). This is also shown by the dependence of values of the equilibrium constant, K_1K_B, on the basicity of the base used.

Further discussion of these results will be delayed until results for 4-nitrobenzofuroxan have been given.

Table 3.16

[Quin]/ mol dm^{-3}	[aniline]/ mol dm^{-3}	k_{obs}/s^{-1}
0.01	0.04	0.0862
0.01	0.07	0.0946
0.01	0.10	0.1080
0.01	0.14	0.1190

Table 3.17

[Quin]/ mol dm^{-3}	[4-methoxyaniline]/ mol dm^{-3}	k_{obs}/s^{-1}
0.02	0.025	0.81
0.02	0.04	0.98
0.02	0.07	1.16
0.02	0.10	1.44

Table 3.18

[Quin]/ mol dm^{-3}	[4-chloroaniline]/ mol dm^{-3}	k_{obs}/s^{-1}
0.02	0.05	0.0133
0.02	0.08	0.0146
0.02	0.11	0.0149
0.02	0.14	0.0204

Table 3.19 Summary of results using quinuclidine.

Anilines	K_1K_{quin}/ dm^3 mol^{-1}	K_1k_{quin}/ dm^6 mol^{-2} s^{-1}	k_{quinH}^+/ dm^3 mol^{-1} s^{-1}
3.2a 4-OMe	5±1	350±20	70±10
3.2c H	4.7±1	33±3	7±1
3.2d 4-Cl	3.8±0.8	4.5±0.5	1.2±0.1

3.3 Reaction of 4-Nitrobenzofuroxan (4-NBF) with Aniline in DMSO

3.3.1 Initial Studies

The UV spectrum of 4-NBF in DMSO shows strong absorption at 411 nm ($\epsilon = 1.28\times10^4$ dm^3 mol^{-1} cm^{-1}). Aniline (0.1 mol dm^{-3}) starts to absorb strongly at 340 nm while Dabco (0.1 mol dm^{-3}) does not absorb above 300 nm.

Mixtures of the three components show a new band at 350 nm ($\epsilon=2.8\times10^4$ dm^3 mol^{-1} cm^{-1}), as shown in Figure 3.12. The intensity of the band decreased in the presence of Dabcohydrochloride.

Figure 3.12 Visible spectra of 4-NBF (5×10^{-5} mol dm^{-3}), in DMSO with DabcoH$^+$ (0.01 mol dm^{-3}) and different concentrations of aniline and Dabco.

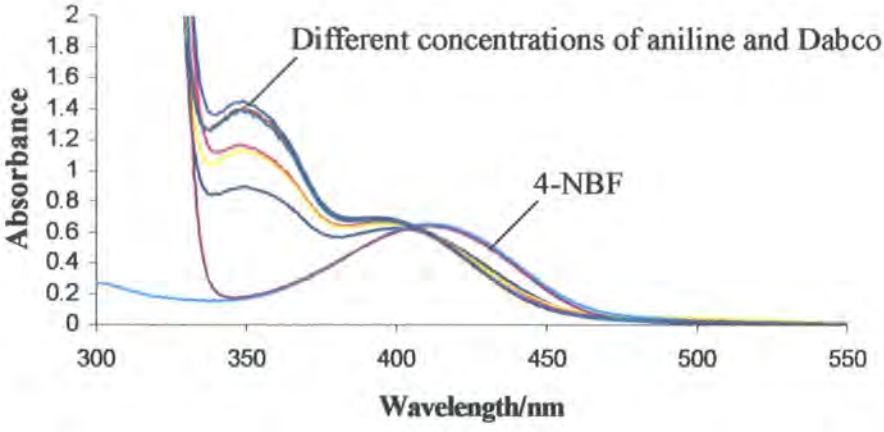

Semi-quantitative measurements of absorbance at 350 nm indicated a value for the equilibrium constant for adduct formation of *ca* 2-3 dm^3 mol^{-1}.

It is known[13] from studies of 4-NBF with aliphatic amines that addition at the 5-position is kinetically preferred but the adducts at the 7-position are thermodynamically more stable. For example for reaction with piperidine $K_{c,5}$ = 27 dm^3 mol^{-1} while $K_{c,7} = 1.8\times10^4$ dm^3 mol^{-1}.

Since aniline is much less reactive than the aliphatic amine it seems probable that the interaction giving the new band at 350 nm is due to formation of the 7-adduct, while the 5-adduct is not observed. Thus if the value of 2-3 $dm^3\ mol^{-1}$ is assigned to formation of the 7-adduct, the value for the equilibrium constant for formation of the 5-adduct would be expected to be $< 0.01\ dm^3\ mol^{-1}$.

Hence the interaction observed may be written as shown in Scheme 3.7.

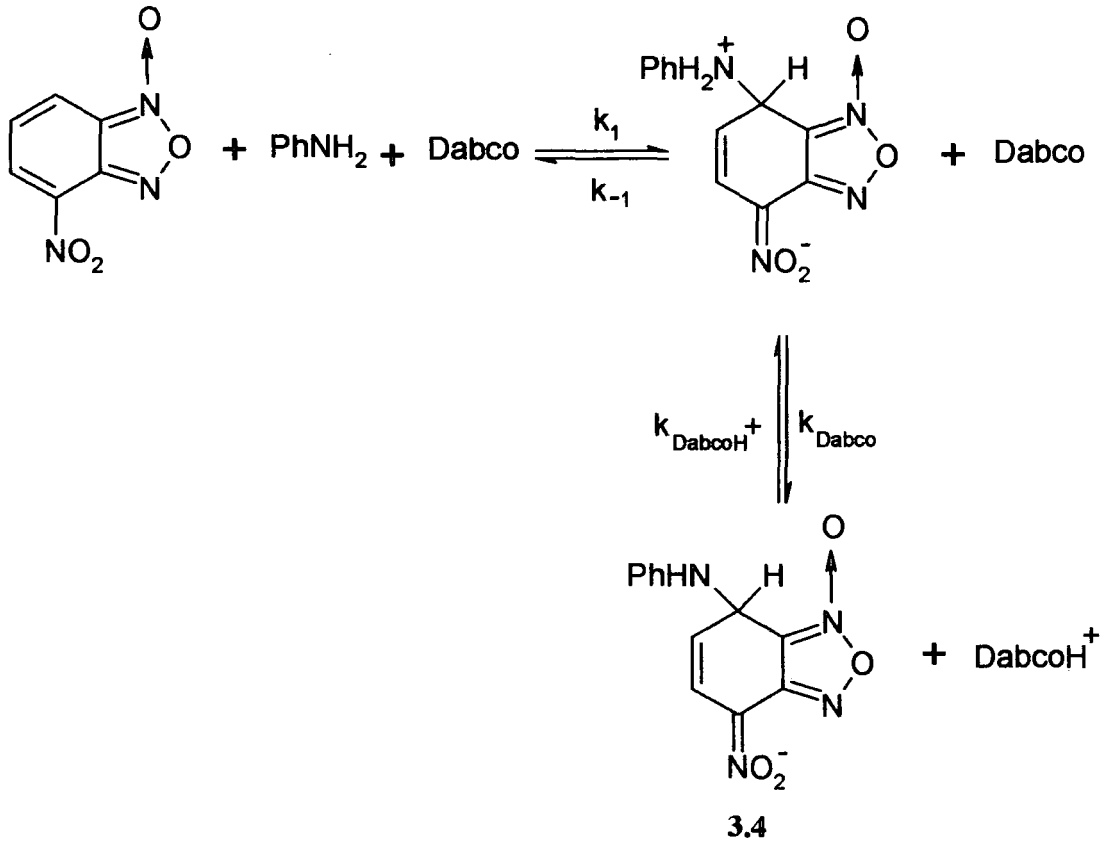

3.4

Scheme 3.7

$$K_{obs} = \frac{[\mathbf{3.4}][DabcoH^+]}{[4-NBF][Aniline][Dabco]}$$

It should also be noted that a slower reaction was also observed leading to irreversible decomposition of the adduct.

3.3.2 ^{1}H NMR Spectra

The spectrum of 4-NBF alone in $^{2}H_6$ DMSO showed bands at (δH_5 = 8.61, H_6 = 7.54, H_7 = 8.14), ($J_{5,6}$ = 7.6, $J_{6,7}$ = 9.2 Hz).

A spectrum for a solution of 4-NBF (0.1 mol dm^{-3}) in the presence of 4-methoxyaniline (0.1 mol dm^{-3}) and Dabco (0.4 mol dm^{-3}) is shown in Figure 3.13 and a spectrum with 4-NBF (0.01 mol dm^{-3}) aniline (0.1mol dm^{-3}) and Dabco (0.1 mol dm^{-3}) is in Figure 3.14.

Figure 3.13 ^{1}H NMR spectrum for adduct **3.4** formed from 4-NBF (0.1 mol dm^{-3}) with 4-methoxyaniline (0.1 mol dm^{-3}) and Dabco (0.4 mol dm^{-3}) in $^{2}H_6$ DMSO.

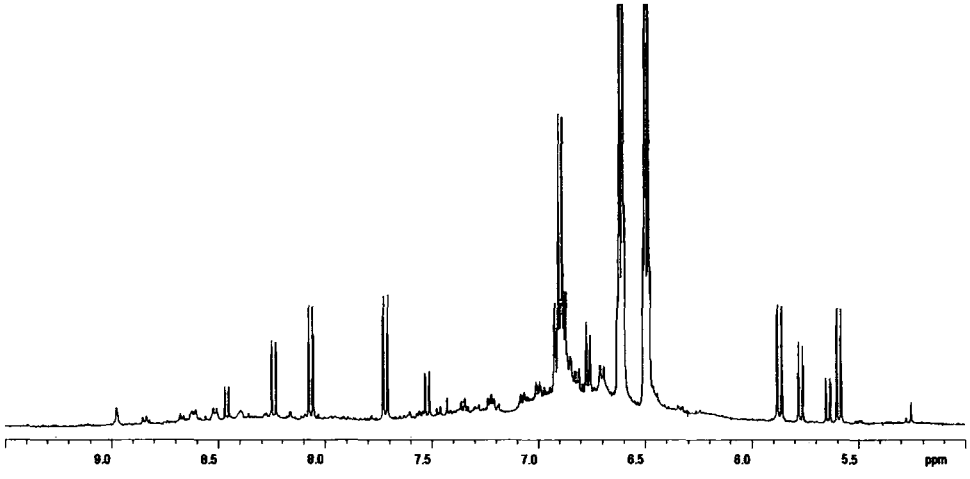

Figure 3.14 ^{1}H NMR spectrum for adduct **3.4** formed from 4-NBF (0.1 mol dm^{-3}) with aniline (0.1 mol dm^{-3}) and Dabco (0.1 mol dm^{-3}) in $^{2}H_6$ DMSO.

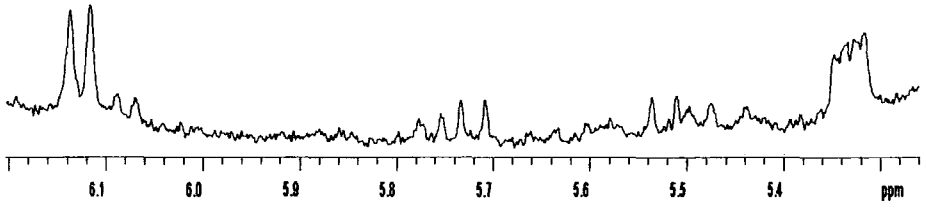

The spectra taken about 15 minutes after mixing indicate that several species are present and are not readily interpretable. This is due to relatively low values of the equilibrium constant for adduct formation and due to the decomposition reactions.

Previous work with aliphatic amines has shown that the ring hydrogens in 7-adducts may be expected at ca δ 7.0, 5.0 and 4.6 ppm.

3.3.3 Kinetic and Equilibrium Studies

Rate and equilibrium measurements were made using stopped-flow spectrophotometry for the initial fast reactions of 4-NBF with anilines **2.3a-e** in DMSO in the presence of Dabco at 25 °C. The absorption maxima of the adducts were at 350 nm, but due to some overlap with the parent anilines at this wavelength some measurements were made at 370 nm.

The 4-NBF concentration was kept at 2.5×10^{-5} mol dm^{-3}. All measurements were made in the presence of $DabcoH^+$ (0.01 mol dm^{-3}). Good first order kinetic plots were obtained. The data are interpreted in terms of Scheme 3.7.

Treating the zwitterion as a steady state intermediate gives equation 3.15, which simplifies to equation 3.16 and 3.17 where $K_1 = k_1/k_{-1}$.

In contrast to the reaction with TNB the results obtained are not compatible with the condition $k_{-1} >> k_{Dabco}[Dabco]$ and can not be fitted using equation 3.11 or 3.13. For example the results in Table 3.22 show that increasing [Dabco] at constant concentration of 4-methoxyaniline causes a decrease in value of k_{obs} while increasing [4-methoxyaniline] at constant concentration of Dabco causes an increase in k_{obs}. Hence the results were fitted to equation 3.17.

Also in contrast to the TNB reactions, no improvement was obtained by including a term representing proton transfer to aniline as the base.

$$k_{obs} = \frac{k_1[PhNH_2]k_{Dabco}[Dabco]}{k_{-1} + k_{Dabco}[Dabco]} + \frac{k_{DabcoH^+}[DabcoH^+]k_{-1}}{k_{-1} + k_{Dabco}[Dabco]} \qquad \textbf{(3.15)}$$

$$k_{obs} = \frac{k_1[PhNH_2]k_{Dabco}[Dabco] + k_{DabcoH^+}[DabcoH^+]k_{-1}}{k_{-1} + k_{Dabco}[Dabco]} \qquad \textbf{(3.16)}$$

$$k_{obs} = \frac{K_1 k_{Dabco}[PhNH_2][Dabco] + k_{DabcoH^+}[DabcoH^+]}{1 + \frac{k_{Dabco}[Dabco]}{k_{-1}}} \quad (3.17)$$

There are three variable parameters in equation 3.17, which were represented as shown below when fitting the experimental data.

$K_1 k_{Dabco} = a$

$k_{DabcoH}^{+}[DabcoH^+] = b$

$k_{Dabco} / k_{-1} = c$

Then equation 3.17 is equivalent to equation 3.18.

$$k_{calc} = \frac{a[PhNH_2][Dabco] + b}{1 + c[Dabco]} \quad (3.18)$$

Representative data for reaction of [4-NBF] = 2.5×10^{-5} mol dm^{-3} with 4-methoxyaniline **3.2a** in the presence of [$DabcoH^+$] = 0.01 mol $dm^{-3}$are in Table 3.20, and data for aniline are in Table 3.21. Values of a,b and c, were varied so as to optimise the fit, judged by the standard deviation σ, between observed and calculated values.

$$\sigma = \sqrt{\frac{\sum (k_{obs} - k_{calc})^2}{n}}$$

All reported data were measured with [4-NBF] = 2.5×10^{-5} mol dm^{-3} and [Dabcohydrochloride] = 0.01 mol dm^{-3}.

It is worth noting that equation 3.17 includes terms involving [Dabco] in both the numerator and denominator. Partial compensation of these terms may lead to the invariance of k_{obs} with [Dabco] seen for example in the lower half of Table 3.21.

Table 3.20

[4-methoxyaniline]/ mol dm^{-3}	[Dabco]/ mol dm^{-3}	k_{obs}/s^{-1}	k_{calc}/s^{-1}	k_{calc}/s^{-1}	k_{calc}/s^{-1}	k_{calc}/s^{-1}	k_{calc}/s^{-1}
0.03	0.1	0.248	0.203	0.207	0.211	0.247	0.220
0.06	0.1	0.327	0.306	0.314	0.323	0.377	0.331
0.1	0.1	0.464	0.443	0.457	0.471	0.550	0.480
0.15	0.1	0.672	0.614	0.636	0.657	0.767	0.666
0.2	0.1	0.894	0.786	0.814	0.843	0.983	0.851
0.05	0.04	0.300	0.295	0.300	0.305	0.339	0.320
0.05	0.07	0.288	0.280	0.286	0.293	0.335	0.304
0.05	0.1	0.298	0.271	0.279	0.286	0.333	0.294
(k_{calc}/s^{-1}) calculated from equation 3.18 with		**a** =	120	125	130	130	130
		b =	0.35	0.35	0.35	0.35	0.38
		c =	25	25	25	20	25
		σ =	4.8×10^{-2}	3.5×10^{-2}	2.4×10^{-2}	6.3×10^{-2}	2.1×10^{-2}

Table 3.21

[Aniline]/ mol dm^{-3}	[Dabco]/ mol dm^{-3}	k_{obs}/s^{-1}	k_{calc}/s^{-1}	k_{calc}/s^{-1}	k_{calc}/s^{-1}	k_{calc}/s^{-1}	k_{calc}/s^{-1}
0.04	0.1	0.018	0.016	0.016	0.016	0.013	0.015
0.07	0.1	0.020	0.022	0.022	0.021	0.018	0.021
0.1	0.1	0.027	0.027	0.027	0.027	0.023	0.026
0.15	0.1	0.036	0.037	0.037	0.036	0.032	0.036
0.2	0.1	0.047	0.047	0.046	0.045	0.040	0.045
0.1	0.04	0.025	0.027	0.027	0.026	0.022	0.026
0.1	0.07	0.024	0.027	0.027	0.026	0.023	0.026
0.1	0.1	0.025	0.027	0.027	0.027	0.023	0.026
0.1	0.15	0.026	0.028	0.028	0.027	0.024	0.027
0.1	0.2	0.028	0.028	0.028	0.027	0.024	0.027
(k_{calc}/s^{-1}) calculated from equation 3.18 with		**a** =	6	5.7	5.5	5	5.7
		b =	0.025	0.025	0.025	0.02	0.025
		c =	21	20	20	20	21
		σ =	1.8×10^{-3}	1.7×10^{-3}	1.43×10^{-3}	3.5×10^{-3}	1.42×10^{-3}

Optimised values for reaction with the other anilines are given in Tables 3.22-3.24. Values of parameters obtained are collected in Table 3.25.

Table 3.22

[4-methylaniline]/ mol dm^{-3}	[Dabco]/ mol dm^{-3}	k_{obs}/s^{-1}	k_{calc}/s^{-1}
0.05	0.03	0.074	0.071
0.05	0.06	0.062	0.067
0.05	0.09	0.060	0.065
0.05	0.12	0.061	0.064
0.05	0.15	0.059	0.063
0.03	0.05	0.055	0.054
0.06	0.05	0.077	0.075
0.09	0.05	0.098	0.095
0.12	0.05	0.117	0.116
0.15	0.05	0.144	0.136
(k_{calc}/s^{-1}) calculated from equation 3.18 with		**a** = 32±5	
		b = 0.08±0.01	
		c = 27±2	
		σ = 4×10^{-3}	

Table 3.23

[4-chloroaniline]/ mol dm^{-3}	[Dabco]/ mol dm^{-3}	k_{obs}/s^{-1}	k_{calc}/s^{-1}
0.03	0.1	0.007	0.007
0.06	0.1	0.008	0.009
0.09	0.1	0.010	0.011
0.12	0.1	0.011	0.013
0.15	0.1	0.013	0.015
0.1	0.03	0.014	0.013
0.1	0.05	0.012	0.012
0.1	0.08	0.011	0.012
0.1	0.1	0.011	0.011
0.1	0.15	0.014	0.011
(k_{calc}/s^{-1}) calculated from equation 3.18 with		**a** = 2±1	
		b =0.014±0.001	
		c = 20±1	
		σ = 1×10^{-3}	

Table 3.24

[3-chloroaniline]/ mol dm^{-3}	[Dabco]/ mol dm^{-3}	k_{obs}/s^{-1}	k_{calc}/s^{-1}
0.03	0.1	0.0024	0.0024
0.06	0.1	0.0033	0.0029
0.09	0.1	0.0038	0.0035
0.12	0.1	0.0042	0.0040
0.15	0.1	0.0043	0.0046
0.1	0.03	0.0035	0.0036
0.1	0.05	0.0035	0.0036
0.1	0.08	0.0035	0.0036
0.1	0.1	0.0035	0.0037
(k_{calc}/s^{-1}) calculated from equation 3.18 with		**a** = 0.37±0.03	
		b=0.0036±0.0001	
		c = 10±2	
		σ = 2.2×10^{-4}	

Results are summarised in Table 3.25. The values of K_1K_{Dabco} were obtained using equation 3.19.

$$K_1K_{Dabco} = \frac{K_1k_{Dabco}}{k_{DabcoH^+}} \qquad (3.19)$$

Values of k_1 were obtained using equation 3.20.

$$k_1 = \frac{K_1k_{Dabco}}{\frac{k_{Dabco}}{k_{-1}}} \qquad (3.20)$$

Table 3.25 Summary of results for 4-nitrobenzofuroxan.

Anilines	K_1K_{Dabco}/ dm^3 mol^{-1}	K_1k_{Dabco} / dm^6 mol^{-2} s^{-1}	k_{DabcoH}^+ / dm^3 mol^{-1} s^{-1}	k_{Dabco}/k_{-1}	k_1/ dm^3 mol^{-1} s^{-1}
3.1a	3.4±0.6	130±10	38±3	25±5	5.2±1.8
3.1b	4±1.3	32±5	8±1	27±2	1.2±0.28
3.1c	2.3±0.7	5.7±0.3	2.5±0.5	20±1	0.3±0.016
3.1d	1.4±0.6	2±1	1.4±0.1	20±1	0.1±0.06
3.1e	1±0.14	0.37±0.03	0.36±0.01	10±2	0.037±0.013

Hammett plots in Figures 3.15-3.18 all have negative ρ values. Formation of the zwitterions (Scheme 3.7) will involve an increase in positive charge on the amino nitrogen. Since values of k_{Dabco} are not expected to change with the nature of the ring substituent, the ρ value for log K_1 is -3.66 corresponding to the positive charge produced. The corresponding value for log k_1 is -3.13 indicating that there is a high degree of charge development in the transition state for the nucleophilic attack. The ρ value of -2.77 for log k_{DabcoH}^{+} is consistent with protonation of the anionic adduct.

The ρ value for log K_1K_{Dabco} is much lower, -0.92, since there is no charge on the amino nitrogen in the anionic adduct.

Figure 3.15 Hammett σ correlation with log K_1K_{Dabco}.

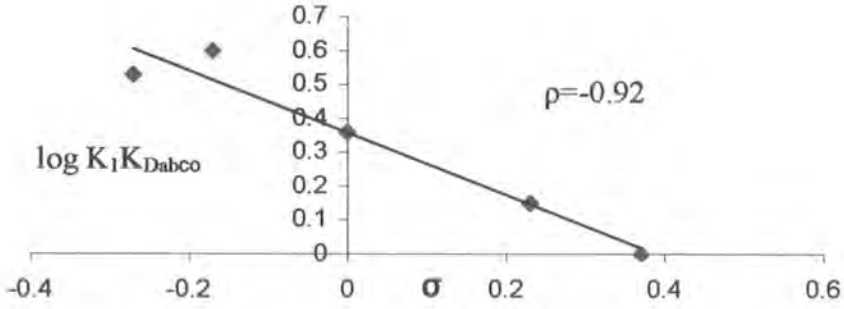

Figure 3.16 Hammett σ correlation with log K_1k_{Dabco}.

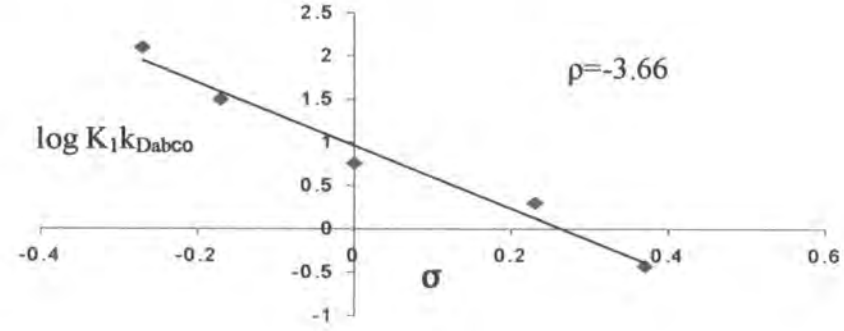

Figure 3.17 Hammett σ correlation with log k_{DabcoH}^{+}.

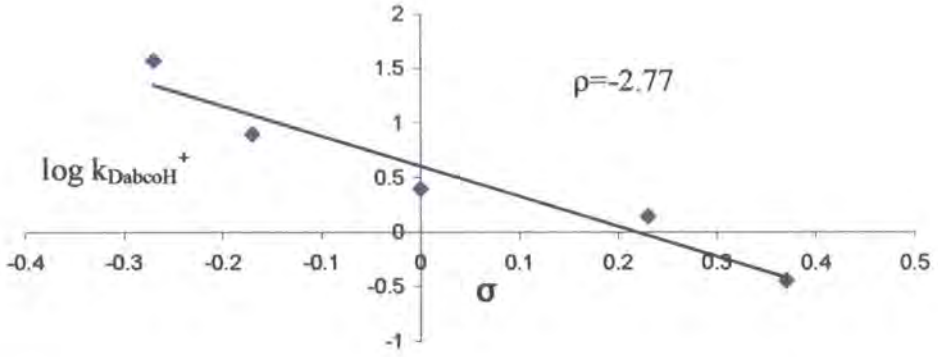

Figure 3.18 Hammett σ correlation with log k_1.

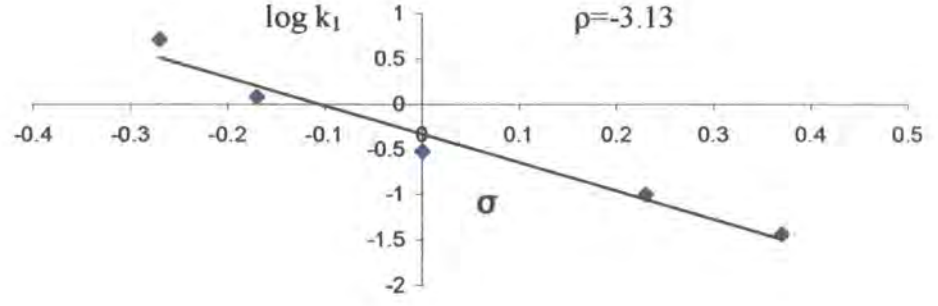

3.4 Conclusions

For the reactions of substituted anilines with TNB and 4-NBF in the presence of Dabco the experimental results lead to the values given in Table 3.26 and 3.27 respectively. These are reproduced here for convenience.

Table 3.26 Reaction with TNB.

Anilines	K_1K_{Dabco}[a] / $dm^3\ mol^{-1}$	K_1k_{Dabco} / $dm^6\ mol^{-2}\ s^{-1}$	k_{DabcoH}^+ / $dm^3\ mol^{-1}\ s^{-1}$	k_{An}/k_{Dabco}
3.1a	0.43±0.04	380±20	880±30	0.04±0.01
3.1b	0.34±0.06	95±10	280±20	0.04±0.01
3.1c	0.31±0.2	28±3	90±30	0.05±0.01
3.1d	0.35±0.1	4.5±1	13±1	0.05±0.01
3.1e	0.34±0.07	1.2±0.2	3.5±0.1	0.1±0.02
3.2f	0.25±0.09	0.25±0.02	1±0.2	0.05±0.01
3.2g	0.10±0.04	8±1	80±20	0
3.2h	0.13±0.05	8±2	60±10	0
3.2i	0.14±0.05	2.0±0.3	14±2	0

a. $K_1K_{Dabco} = K_1k_{Dabco}/k_{DabcoH}^+$.

Table 3.27 Reaction with 4-NBF.

Anilines	K_1K_{Dabco} / $dm^3\ mol^{-1}$	K_1k_{Dabco} / $dm^6\ mol^{-2}\ s^{-1}$	k_{DabcoH}^+ / $dm^3\ mol^{-1}\ s^{-1}$	k_{Dabco}/k_{-1}	k_1 / $dm^3\ mol^{-1}\ s^{-1}$
3.1a	3.4±0.6	130±10	38±3	25±5	5.2±1.8
3.1b	4±1.3	32±5	8±1	27±2	1.2±0.28
3.1c	2.3±0.7	5.7±0.3	2.5±0.5	20±1	0.3±0.016
3.1d	1.4±0.6	2±1	1.4±0.1	20±1	0.1±0.06
3.1e	1±0.14	0.37±0.03	0.36±0.01	10±2	0.037±0.013

3.4.1 Overall Equilibrium Constant

Values of K_1K_{Dabco} for reaction with 4-NBF are between 3 and 10 times higher than those for reaction with TNB. If a statistical correction were applied to take account of the three equivalent ring positions in TNB, then the factors would be three times larger. It is of interest to compare the relative stabilities of TNB and 4-NBF adducts with other nucleophiles.

For the reaction in DMSO of 4-NBF with aliphatic amines[13], which are more reactive than aniline, isomeric attack at the 5-and 7-ring position is observed.

For reaction with n-butylamine the values of K_5 and K_7 are 110 $dm^3\ mol^{-1}$ and 5.6×10^3 $dm^3\ mol^{-1}$ respectively. The corresponding value for reaction with TNB is 1×10^3 $dm^3\ mol^{-1}$. Hence the ratio for 4-NBF (7-position) to TNB for n-butylamine attack is 5.6, similar to the values obtained with aniline.

For reaction with methoxide ions in methanol[20] the values of K_5 and K_7 for reaction of 4-NBF are 475 $dm^3\ mol^{-1}$ and 8000 $dm^3\ mol^{-1}$ respectively, while for the

reaction with TNB, K has a value of 22.3 dm^3 mol^{-1}. Hence the ratio for 4-NBF (7-position) to TNB is 360.

For the reaction with sulfite in water[12] the value corresponding to K_5 is 8×10^6 dm^3 mol^{-1} for 4-NBF and the value for TNB is 290 dm^3 mol^{-1}. Hence the ratio for 4-NBF (7-position):TNB would be expected to be > 3×10^4. The increase in the value of the ratio is likely to be due, at least in part, to a solvent effect. In water the adduct **3.5**, where the charges are localised, will be well solvated, hence leading to an increase in stability. DMSO is better at solvating large polarisable species with delocalised charges.

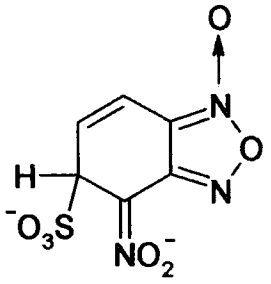

3.5

3.4.2 Rate Constants for Proton Transfer

The experimental results show that in the TNB reaction proton transfer is rate limiting, $k_{-1}>>k_{Dabco}[Dabco]$. However in the 4-NBF reaction there is a balance between nucleophilic attack and proton transfer as the rate limiting step

$k_{-1}\sim k_{Dabco}[Dabco]$. Although it is not possible to obtain values of k_{Dabco} experimentally, the results do give values for k_{DabcoH}^+, the reverse step in Scheme 3.8 and in Scheme 3.5. These show that values of k_{DabcoH}^+ are at least ten times larger in the TNB reaction.

It is interesting to speculate as to the likely values of k_{Dabco} in these systems. This process (Scheme 3.5 and 3.8) represent a strongly thermodynamically favourable proton transfer between nitrogen atoms. Buncel originally proposed a value of 1×10^9 dm^3 mol^{-1} s^{-1}, close to the diffusion controlled limit. However it is now known[4,21] that in DMSO values for such proton transfer may be slowed by hydrogen-bonding to the solvent, as shown in **3.6**.

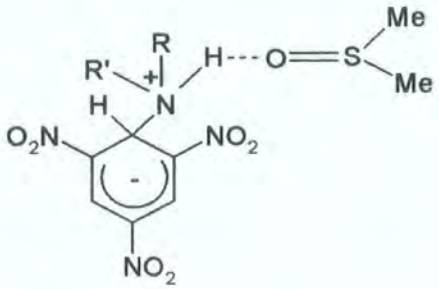

3.6

It is necessary to break the H-bond before the proton may be transferred. Steric congestion at the reaction centre may also reduce proton transfer rates.[3,4]

However, for anilines **2.3a–f** carrying remote substituents, any possible steric effects are likely to be constant. Furthermore, since values of k_{DabcoH}^{+} will also be subject to steric effects, the plot in Figure 3.19 versus pK_a values is informative. The slopes are 0.80 and 0.87 respectively

Figure 3.19 Plots of log k_{DabcoH}^{+} and log K_1k_{Dabco} for the reaction of TNB with anilines versus the pK_a values of the corresponding anilinium ions. Points **g**, **h** and **i** represent 2-methyl-, 2-ethyl- and N-methyl-anilines respectively.

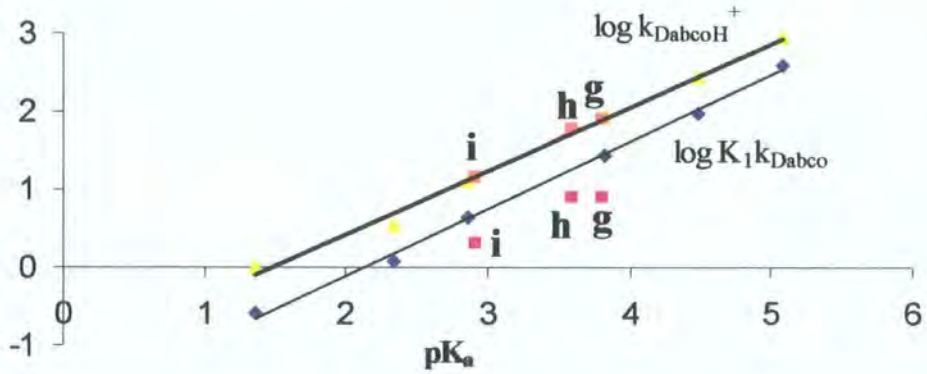

It shows that even for **2.3g–i** the values of k_{DabcoH}^{+} do not deviate from linearity. The implication is that for these primary amines, and even for N-methylaniline, there are no serious steric effects on proton transfer between the zwitterions and anions **3.3**. It should be noted that here proton transfer involves Dabco, which should be relatively unhindered.

Thus it will be assumed that the value of k_{Dabco} is 1×10^{8} dm^3 mol^{-1} s^{-1} reduced below the diffusion limit only by hydrogen bonding to the solvent. The value will be

independent of the aniline nucleophile. The correspondence in values of K_1k_{Dabco} and K_1k_{quin}, for corresponding anilines, in Tables 3.15 and 3.19 indicates that values of k_{Dabco} and k_{quin} are equal. If steric effects on proton transfer are unimportant in reactions of TNB, they are also likely to be unimportant in reactions involving 4-NBF and **3.2a-e**. Hence it is reasonable to assume in this system, too, a value for k_{Dabco} of 1×10^8 dm^3 mol^{-1} s^{-1}.

These values were used to calculate the values given in Table 3.28 and 3.29. These were calculated using.

$$K_{Dabco} = \frac{k_{Dabco}}{k_{DabcoH^+}}$$

$$K'_a = \frac{K^{DabcoH^+}}{K^{AnH^+}} \quad \text{(Using } pK_a \text{ values in Table 2.10).}$$

$$K_{An} = K_{Dabco}K'_a \quad (\equiv \frac{k_{An}}{k_{AnH^+}})$$

For TNB, $\quad k_{An} = (\frac{k_{An}}{k_{Dabco}})1\times10^8$

$$k_{AnH^+} = \frac{k_{An}}{K_{An}}$$

$$K_1 = \frac{K_1K_{Dabco}}{K_{Dabco}}$$

For 4-NBF, $\quad k_{-1} = \frac{k_1}{K_1}$

Table 3.28 Derived values for TNB.

Anilines	K_{Dabco}	$K_a^{'}$	K_{An}	k_{An}/ $dm^3\ mol^{-1}\ s^{-1}$	k_{AnH}^{+}/ $dm^3\ mol^{-1}\ s^{-1}$	K_1/ $dm^3\ mol^{-1}$
4-OMe	1.14×10^{5}	1.05×10^{-4}	12	4×10^{6}	3.3×10^{5}	3.8×10^{-6}
4-Me	3.6×10^{5}	2.64×10^{-5}	9.5	4×10^{6}	4.2×10^{5}	9.5×10^{-7}
H	1.11×10^{6}	5.75×10^{-6}	6.4	5×10^{6}	7.8×10^{5}	2.8×10^{-7}
4-Cl	7.7×10^{6}	6.3×10^{-7}	4.9	5×10^{6}	1×10^{6}	4.5×10^{-8}
3-Cl	2.9×10^{7}	1.90×10^{-7}	5.5	10×10^{6}	1.8×10^{6}	1.2×10^{-8}
3-CN	10×10^{7}	1.99×10^{-8}	1.99	5×10^{6}	2.5×10^{6}	2.5×10^{-9}
2-Me	1.3×10^{6}	5.4×10^{-6}	7.1	/	/	7.7×10^{-8}
2-Et	1.7×10^{6}	4.8×10^{-6}	3.3	/	/	7.6×10^{-8}
N-Me	7.1×10^{6}	7.25×10^{-7}	5.0	/	/	2.0×10^{-8}

Table 3.29 Derived values for 4-NBF.

Anilines	K_{Dabco}	$K_a^{'}$	K_{An}	K_1/ $dm^3\ mol^{-1}$	k_1/ $dm^3\ mol^{-1}\ s^{-1}$	k_{-1}/ s^{-1}
4-OMe	2.6×10^{6}	1.05×10^{-4}	270	1.3×10^{-6}	5.2	4×10^{6}
4-Me	12.5×10^{6}	2.64×10^{-5}	330	3.2×10^{-7}	1.2	3.75×10^{6}
H	40×10^{6}	5.75×10^{-6}	230	5.8×10^{-8}	0.3	5×10^{6}
4-Cl	71×10^{6}	6.3×10^{-7}	45	1.9×10^{-8}	0.1	5×10^{6}
3-Cl	277×10^{6}	1.90×10^{-7}	53	3.6×10^{-9}	0.037	10×10^{6}

3.4.3 Substituent Effects

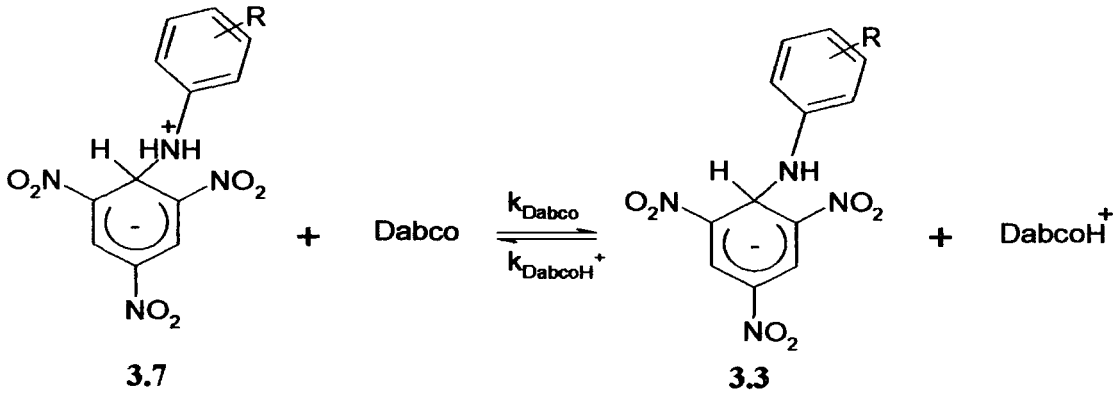

3.7 **3.3**

Scheme 3.8

The results in Table 3.28 show that the value of K_{Dabco} increases by a factor of *ca* 1000 as R changed from 4-OMe to 3-CN. The Hammett ρ value, from Figure 3.11, is +3.62, corresponding to the deprotonation of nitrogen in the zwitterion **3.7**. The corresponding value for the 4-NBF system is 2.77. It is interesting that values of K_{An}, corresponding to the proton transfer process in Scheme 3.9, show only small

variations with the nature of R. This shows that the acidities of the zwitterion, **3.7**, and anilinium ions are affected similarly by the substituents R as might be expected.

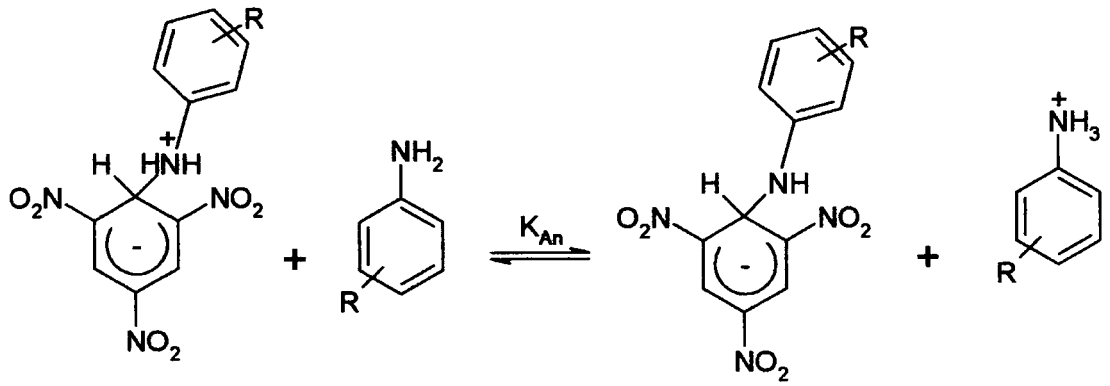

3.7

Scheme 3.9

The results for K_1, Scheme 3.10, show a decrease by a factor of *ca* 1000 on changing R from 4-OMe to 3-CN. The ρ values are -3.82 for TNB (from Figure 3.10) and -3.66 for 4-NBF (from Figure 3.16). The plot, in Figure 3.19, versus pK_a values has a slope of 0.87. It may be significant that the points for 2-methyl, 2-ethyl and N-methylanilines fall before the line defined by remote substitutents. This may indicate some steric hindrance to the formation of the zwitterions in these derivatives leading to reductions in values of K_1. The negative values of ρ correspond to an increase in positive charge at the nitrogen atom (Scheme 3.10).

The K_1K_{Dabco} values show only a small variation with the nature of R due to the compensation of the two factors.

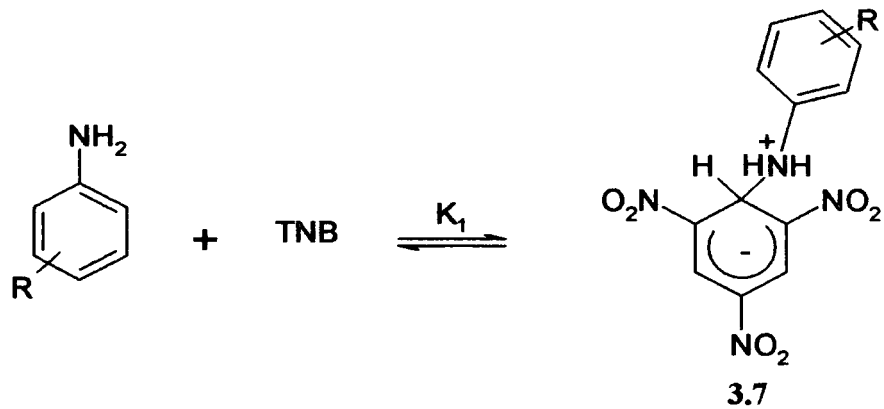

3.7

Scheme 3.10

3.4.4 k_1 and k_{-1} Values

k_1 for 4-NBF has a strong dependence on R. The ρ value is -3.13 while k_{-1} has a little dependence on R. This indicates a product like transition state (T.S) for nucleophilic attack where bonding between the nucleophile and the ring is well-developed (Scheme 3.11).

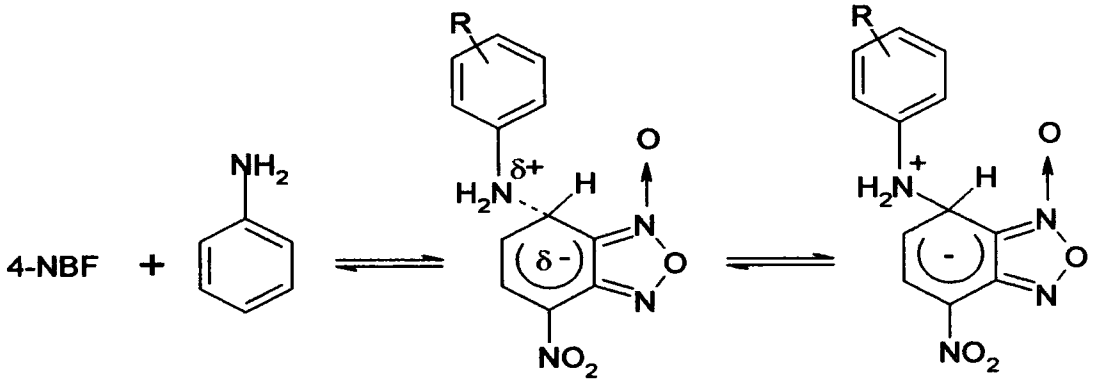

Scheme 3.11

Values of k_1 and k_{-1} for the corresponding reaction of TNB are not observable, since the interconversion of TNB and zwitterion is a rapid equilibrium. However the results show that for TNB, $k_{-1} >> k_{Dabco}[Dabco]$.

If it is estimated that when [Dabco] = 0.3 mol dm^{-3},

$$k_{-1}/k_{Dabco}[Dabco] > 10$$

Then:

$$k_{-1} > 10 \times 1 \times 10^8 \times 0.3$$

$$k_{-1} > 3 \times 10^8 \text{ dm}^3 \text{ mol}^{-1} \text{ s}^{-1}.$$

The value for k_1 for aniline (R = H) may then be estimated to be,

$$k_1 = K_1 k_{-1}$$

$$k_1 > 84 \text{ dm}^3 \text{ mol}^{-1} \text{ s}^{-1}.$$

Comparing these values with those for the corresponding reaction of 4-NBF it is seen that both k_1 and k_{-1} are at least one hundred times larger for TNB.

It is interesting that in the corresponding reaction of aliphatic amines[13] values of k_1 were larger for TNB than for 4-NBF by factors of *ca* 100. This has been attributed to the high intrinsic barrier associated with adduct formation at the 7-position of 4-NBF, due to the extensive delocalisation possible (Scheme 3.12).

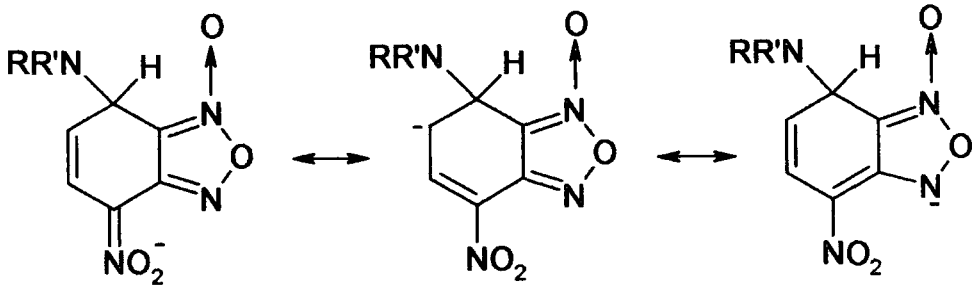

Scheme 3.12

This analysis shows that the reason for the change in the nature of the rate determining step for reactions with TNB and 4-NBF is the higher value for k_{-1} in the case of TNB. This leads to rate determining proton transfer.

3.4.5 K_{Dabco} Values

K_{Dabco}, referring to the process shown in Scheme 3.8 measures the acidity of the zwitterions relative to that of $DabcoH^+$. Comparison of the data in Tables 3.28 and 3.29 showes that for a given aniline values are *ca* ten times higher for zwitterions derived from 4-NBF than from TNB. Similarly values of K_{An}, for the process in Scheme 3.9, are larger in the case of 4-NBF than for TNB.

It is known[4] that the 2,4,6-trinitrohexadienyl ring although negatively charged is electron withdrawing relative to hydrogen. These results indicate that the negatively charged 4-nitrobenzofuroxan ring in **3.8** is more electron withdrawing than the corresponding 2,4,6-trinitrobenzene ring.

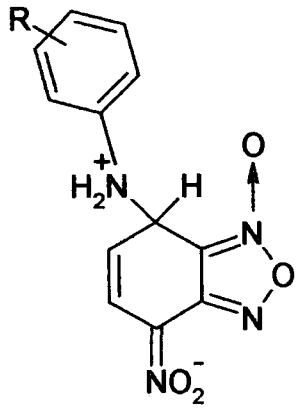

3.8

Some independent support for this idea comes from the observation[22] that the pK_a for **3.9** is 7.68 while that for **3.10** is 8.20. This indicates higher acidity for the 4-nitrobenzofurazan derivative.

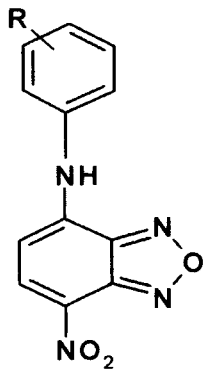

3.9

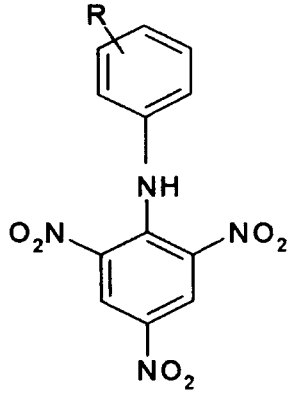

3.10

3.4.6 Energy Diagram

The reactions of TNB with aniline are represented schematically in an energy diagram in Figure 3.20.

Figure 3.20 Schematic energy diagram representing Scheme 3.5. The base B may be aniline, Dabco or quinuclidine.

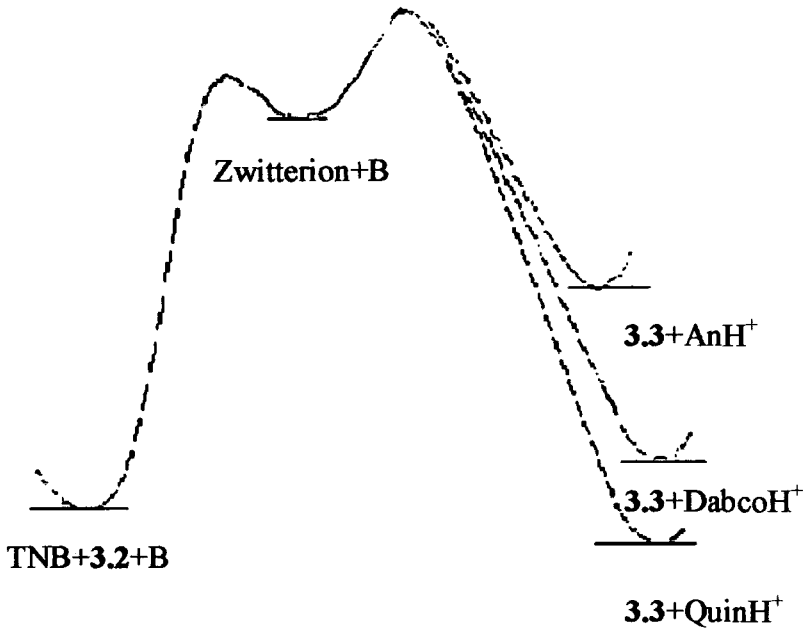

Initially a high energy intermediate, the zwitterion, is formed from TNB and aniline. When B is aniline, a very weak base, the final products are unstable relative to the reactants. The products become increasingly stable as the strength of the base is increased, first with Dabco and more so with quinuclidine.

Values of k_{BH}^{+} depend directly on the acidity of the conjugate acids and are much lower for $QuinH^{+}$ than for AnH^{+}.

In the case of the TNB reaction the energy barrier for the k_{-1} process, expulsion of aniline, is lower than the energy barrier for proton transfer. This barrier reflects diffusion of the base to the zwitterions and breaking of the hydrogen bonds between the zwitterions and the DMSO solvent.

3.5 References

[1] F. Terrier, 'Nucleophilic Aromatic Displacement', 1991, VCH.

[2] M. R. Crampton and V. Gold, J. Chem. Soc., B, 1967, 23.

[3] C. F. Bernasconi, M. C. Muller and P. Schmid, J. Org. Chem., 1979, **44**, 3189.

[4] M. R. Crampton and B. Gibson, J. Chem. Soc., Perkin Trans. 2, 1981, 533.

[5] E. Buncel and J. G. K. Webb, Can. J. Chem., 1972, **50**, 129.

[6] E. Buncel and J. G. K. Webb, Can. J. Chem., 1974, **52**, 630.

[7] E. Buncel and W. Eggimann, J. Am. Chem. Soc., 1977, **99**, 5958.

[8] M. R. Crampton and I. Robotham, Can. J. Chem., 1998, **76**, 627.

[9] E. Buncel, H. Jarrell, H. W. Leung and J. G. K. Webb, J. Org. Chem., 1974, **39**, 272.

[10] F. Terrier, F. Millot, A.-P. Chatrousse, M.-J. Pouet and M.-P. Simonnin, Org. Magn. Reson., 1976, **8**, 56.

[11] E. Buncel, N. Chuaqui-Offermanns, B. K. Hunter and A. R. Norris, Can. J. Chem., 1977, **55**, 2852.

[12] M. R. Crampton, L. M. Pearce and L. C. Rabbitt, J. Chem. Soc., Perkin Trans. 2, 2002, 257.

[13] M. R. Crampton, J. Delaney and L. C. Rabbitt, J. Chem. Soc., Perkin Trans. 2, 1999, 2473.

[14] E. Buncel and J. G. K. Webb, Tetrahedron Lett., 1976, 4417.

[15] E. Buncel and J. G. K. Webb and J. F. Wiltshire, J. Am. Chem. Soc., 1977, **99**, 4429.

[16] C. Boga and L. Forlani, J. Chem. Soc., Perkin Trans. 2, 2001, 1408.

[17] C. Boga and L. Forlani, J. Chem. Soc., Perkin Trans. 2, 1998, 2155.

[18] E. Buncel and W. Eggimann, J. Chem. Soc., Perkin Trans. 2, 1978, 673.

[19] M. R. Crampton and I. A. Robotham, J. Chem. Res. (S), 1997, 22.

[20] F. Terrier, A.-P. Chatrousse and F. Millot, J. Org. Chem., 1980, **45**, 2666.

[21] M. R. Crampton and S. D. Lord, J. Chem. Soc., Perkin Trans. 2, 1997, 369.

[22] J.-C. Halle, M. Mokhtari, P. Soulie and M.-J. Pouet, Can. J. Chem., 1997, **75**, 1240.

Chapter Four:

Reaction of 4-Nitrobenzofurazan Derivatives with Nitroalkane Anions

Chapter Four: Reaction of 4-Nitrobenzofurazan Derivatives with Nitroalkane Anions

4.1 Introduction

As reported in chapter 1 there have been previous studies of the reactions of 1,3,5-trinitrobenzene and also 4,6-dinitrobenzofuroxan with nitroalkane anions. It was thought to be of interest to make measurement with nitrobenzofurazan and some 7-substituted 4-nitrobenzofurazans in order to allow comparison with TNB and DNBF.

Also, and importantly it will be shown in chapter 5 that carbanions formed from benzyl triflones will readily form σ-adducts with 4-nitrobenzofurazan derivatives but not with TNB. Hence these measurement allow comparisons of the reactions of the nitro- and trifluoromethylsulfonyl-activated carbanions.

4.2 1,3,5-Trinitrobenzene (TNB)

As early as 1968, Fyfe[1] reported that addition of triethylamine to TNB dissolved in d_6-DMSO and nitroalkanes resulted in the formation of σ-adducts. The ^{1}H NMR band at δ 9.2 ppm due to TNB was replaced with new bands at δ 8.4 and 5.5 ppm in an intensity ratio 2:1. However the spectra reported, measured at 100 MHz, are not well-defined.

In order to confirm the conclusion and to obtain a detailed spectrum a solution was prepared in d_6-DMSO containing TNB, nitroethane and triethylamine in an approximately 1:1:1 molar ratio and at a concentration of 0.2 mol dm^{-3}. The spectrum obtained at 400 MHz showed bands attributable to the adduct **4.1**.

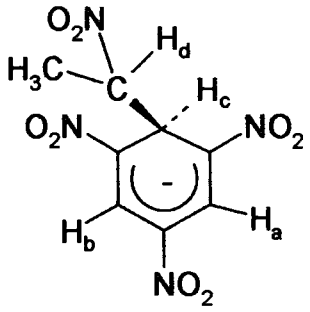

4.1

Interestingly in the spectrum separate resonances, δ 8.35 and 8.38 ppm, J_{ab} = 2.0 Hz, are observed for H_a and H_b which are made diastereotopic due to the asymmetry of the added nitroethane group. The ring-hydrogen, H_c, at the position of attack is observed at δ 5.58 ppm; the large shift to lower frequency compared with the parent is due to the change in hybridisation from sp^2 to sp^3. Spin-coupling is observed with H_a and H_b, J ~ 1.0 Hz and with H_d, J_{cd} = 3 Hz. H_d is observed at δ 4.67 ppm with coupling to H_c, J_{cd} = 3 Hz and to the methyl group, J = 6.8 Hz. The spectrum is unchanged after two hours indicating that the adduct is stable under these condition.

The UV/visible spectra were reported by Fyfe[1] showing maxima at 455 nm, ε = 2.3×10^4 $dm^3\,mol^{-1}\,cm^{-1}$, and 560 nm, ε = 1.2×10^4 $dm^3\,mol^{-1}\,cm^{-1}$.

4.3 4-Nitrobenzofurazan Derivatives, ^{1}H NMR Studies

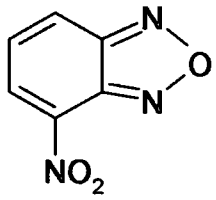

4.2

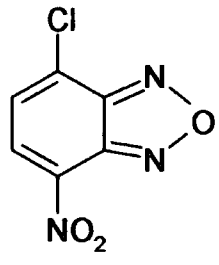

4.3

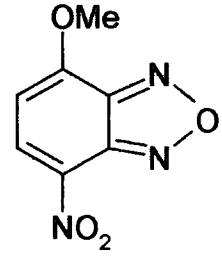

4.4

CH_3NO_2

4.5

$CH_3CH_2NO_2$

4.6

$(CH_3)_2CHNO_2$

4.7

Measurements were made with 4-nitrobenzofurazan **4.2**, 7-chloro-4-nitrobenzofurazan **4.3** and 7-methoxy-4-nitrobenzofurazan **4.4**, with each of the

nitroalkanes, nitromethane **4.5**, nitroethane **4.6** and 2-nitropropane **4.7** in the presence of triethylamine. Typically the parent nitro-compound was at a concentration of *ca* 0.2 mol dm^{-3} with molar ratios of nitro compound:nitroalkane:triethylamine *ca* 1:2:2. ^1H NMR spectra in d_6-DMSO were recorded as soon as possible after mixing, usually about 15 minutes and changes in spectrum with time were observed. The results to be described are in accord with Scheme 4.1 showing the initial formation of adducts **4.8** by reaction at the 5-position of the benzofurazans.

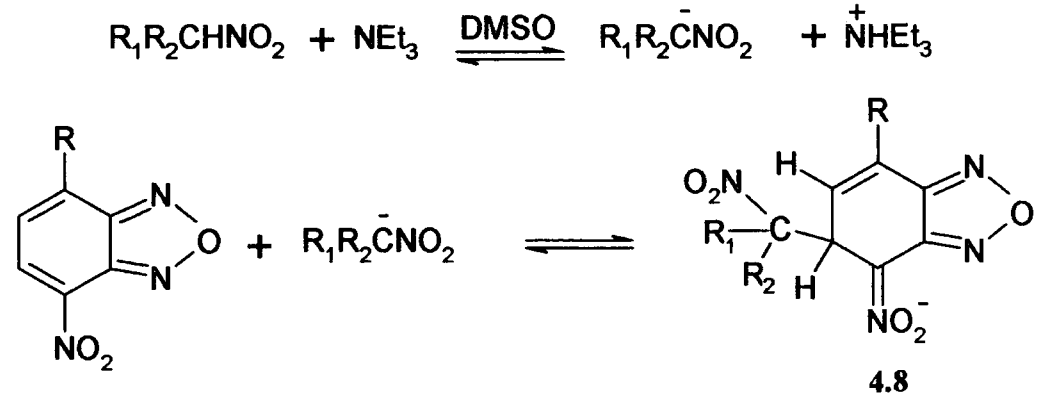

4.8

R=H, Cl, OMe. R_1R_2=H, H; H, Me; Me, Me.

Scheme 4.1

Slower reactions indicate the possibility for **4.2** of isomeric addition to give adducts at the 7-position. Importantly the spectra indicate that base-catalysed elimination of nitrous acid may lead to the formation of alkene derivatives.

The results for the different compounds are sufficiently distinct to merit separate treatment. ^1H NMR data for the parent compounds and for the nitroalkanes are reported in Table 4.1. They are in accord with values previously reported[2].

Table 4.1 ^{1}H NMR data for parent molecules in d_6-DMSO.

Parent molecules	δ H_5	δ H_6	δ H_7	δ Me	J_{56}[a]	J_{67}[a]	J_{57}[a]
4.2	8.70	7.85	8.61	/	7.2	8.8	0.8
4.3	8.68	8.03	/	/	7.6	/	/
4.4	8.75	7.06	/	4.21	8.6	/	/
	δ CH_nNO_2			δ Me	J_{CH-Me}[a]		
4.5	4.43			/	/		
4.6	4.55			1.41	7.2		
4.7	4.76			1.46	6.8		
Triethylamine	CH_2 at δ 2.42			0.93	7.2		

a. J values in Hz.

4.3.1 4-Nitrobenzofurazan with Nitroethane

The ^{1}H NMR spectrum of **4.2** (0.24 mol dm^{-3}) with **4.6** (0.5 mol dm^{-3}) in the presence of triethylamine (0.5 mol dm^{-3}) was recorded as soon as possible after mixing, about 15 minutes. The spectrum shown in Figure 4.1 indicates the formation of two adducts in the intensity ratio 2:1. In addition to bands due to unreacted nitroethane at δ 4.5 and NH^+ at δ 5.3 ppm there are pairs of bands centred at *ca* δ 7.0, 6.3, 5.5 and 4.6 ppm. Addition might be expected at the 5- and/or 7-ring position, so it is necessary to consider the position of attack in the present case. Previous results in related systems[3,4], such as the reactions of **4.2** with aliphatic amines, in d_6-DMSO show that the shift of the hydrogen at the 6-position is diagnostic. When reaction occurs at the 7-position the shift of H_6 is *ca* 5 ppm while for reaction at the 5-position H_6 is observed in the region 6-6.5 ppm. In the present case bands attributable to H_6 are at δ 6.0 and 6.5 ppm indicating that reaction has occurred at the 5-position. The fact that two sets of bands are observed is attributable to the presence of diastereoisomeric adducts resulting from the two chiral centres in the molecule **4.9**.

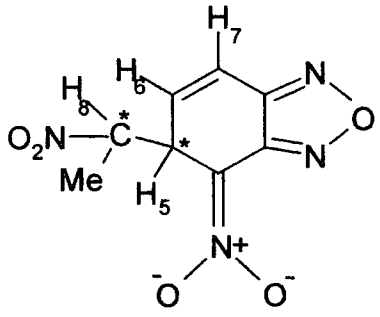

4.9

Figure 4.1 ^{1}H NMR spectrum of **4.2** with **4.6** in the presence of triethylamine (0.5 mol dm^{-3}) in d_6-DMSO.

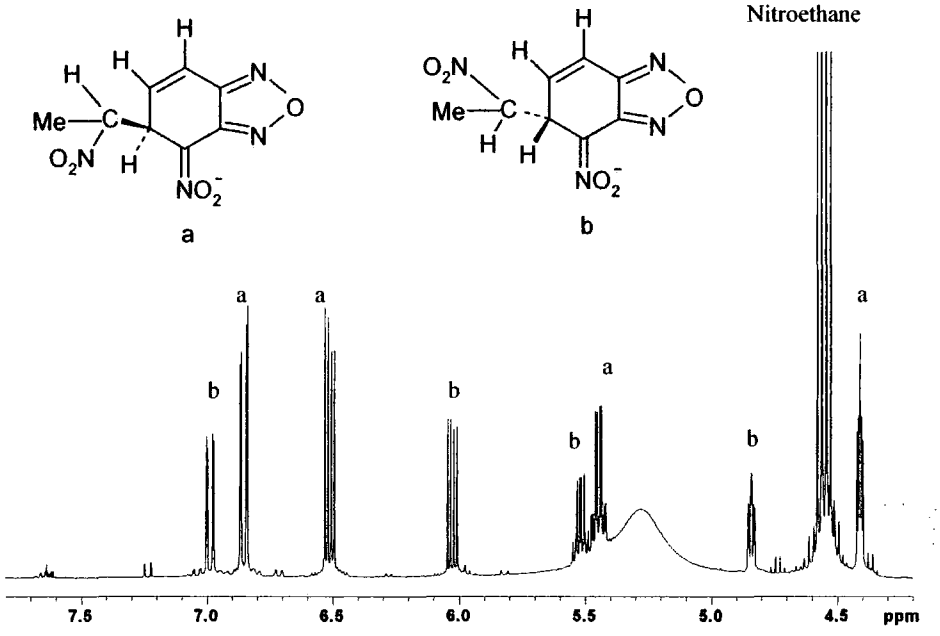

Chemical shifts and coupling constants are collected in Table 4.2. With increasing time one set of bands decreases in intensity, while the other set remains unchanged. The spectrum after 2 hours is shown in Figure 4.2 This shows the appearance of new bands attributable to the product of elimination of nitrous acid as indicated in Scheme 4.2. The new bands are labelled **c**. Bands due to **a** have decreased in intensity relative to the initial spectrum.

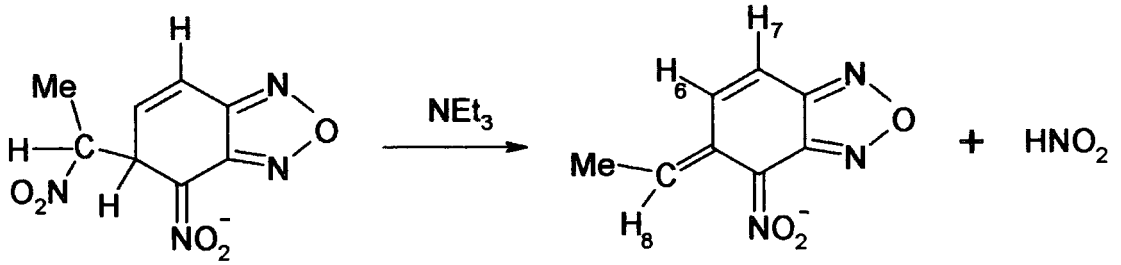

Scheme 4.2

Table 4.2 ^{1}H NMR[b] data for nitrobenzofurazan derivatives **4.2**, **4.3** and **4.4**, with nitroethane to give diastereoisomeric adducts in d_6-DMSO.

a	δ H_5	δ H_6	δ H_7	δ H_8	δ Me	J_{56}[a]	J_{57}[a]	J_{67}[a]	J_{58}[a]	$J_{Me\text{-}8}$[a]
4.2	4.40	6.51	6.85	5.44	1.55	4.8	1.8	10.4	2.8	6.8
4.3	4.54	6.74	/	5.45	1.21	5.2	/	/	4.4	6.8
4.4	4.39	5.51	/	5.39	1.54	5.4	/	/	2.4	6.8
b	δ H_5'	δ H_6'	δ H_7'	δ H_8'	δ Me'	J_{56}'[a]	J_{57}'[a]	J_{67}'[a]	J_{58}'[a]	$J_{Me\text{-}8}$'[a]
4.2	4.83	6.02	6.98	5.51	1.15	4.8	1.4	10.2	4.0	6.8
4.3	4.95	6.24	/	5.46	1.21	5.4	/	/	4.0	6.8
4.4	4.87	4.98	/	5.50	1.12	5.4	/	/	4.0	6.8

a. J values in Hz.

b. For numbering see structure **4.9**.

Figure 4.2 ^{1}H NMR spectrum of **4.2** with **4.6** in the presence of triethylamine in d_6 DMSO after 2 hours.

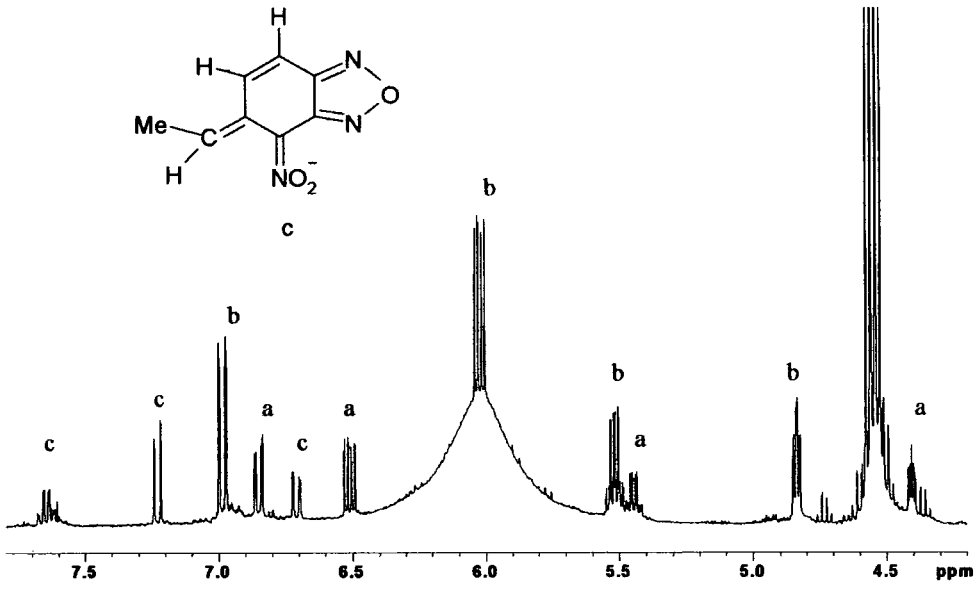

A quartet, J = 6.8 Hz, at δ 7.65 ppm is observed due to H_8, with a doublet at δ 1.91 ppm for the methyl group. Bands at δ 6.71 and 7.23 ppm are attributed to H_6 and H_7 in the alkene.

Measurements with higher concentrations of triethylamine up to 2 mol dm^{-3} showed an increased rate of the elimination showing that the process was base catalysed. The mechanism of the elimination will be discussed later.

4.3.2 4-Nitrobenzofurazan with 2-Nitropropane

The spectrum in the presence of **4.7** and triethylamine indicates that here a mixture of the 5- and 7-adducts is initially formed. The bands for H_6 in the two adducts are at δ 6.29 and 4.96 ppm respectively. The spectrum soon after mixing shows the intensities for the 5-adduct and 7-adduct in the ratio of 1:5. After two hours only bands due to the 7-adduct were observed. After 24 hours decomposition had occurred involving elimination of nitrous acid to give an alkene. These processes are summarized in Scheme 4.3 and shifts are collected in the Table 4.3.

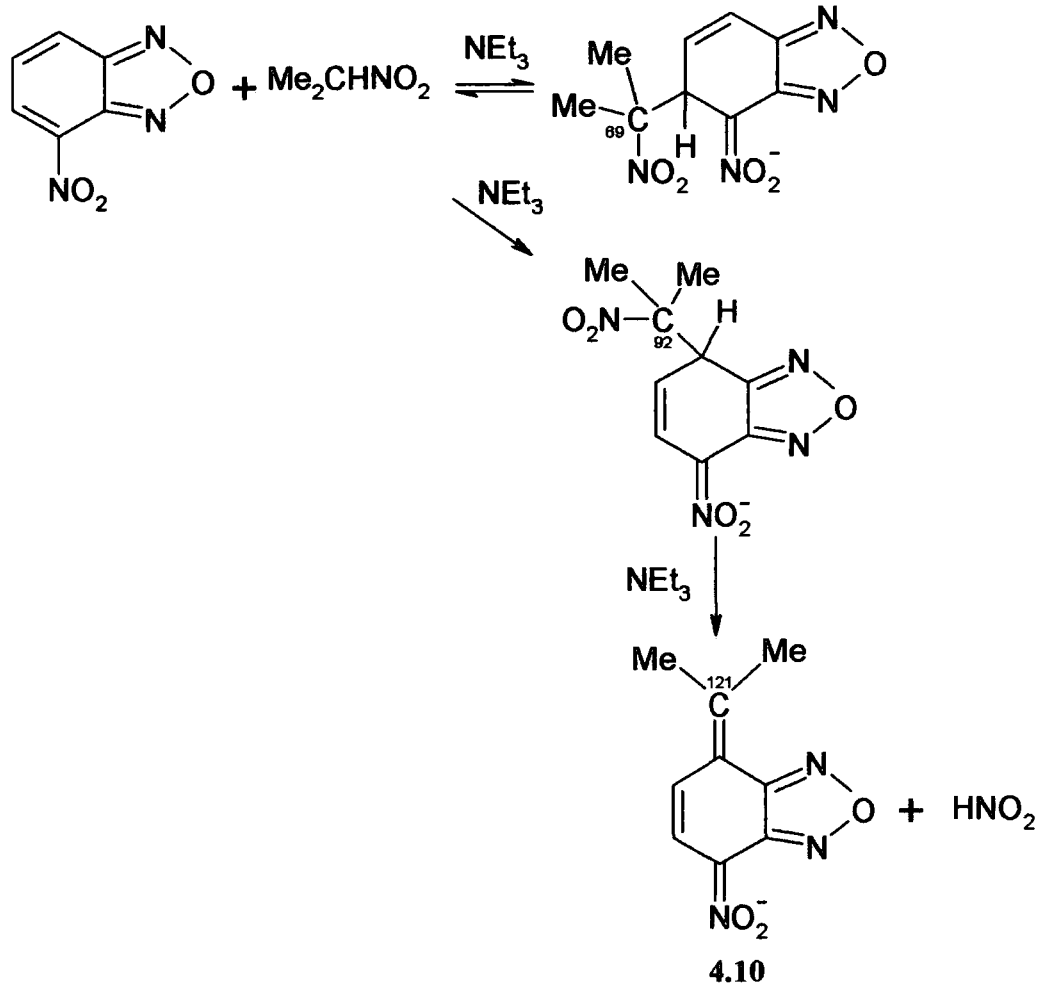

4.10

Scheme 4.3

Table 4.3 ^{1}H NMR data for adducts from nitrobenzofurazan derivatives with 2-nitropropane in d_6-DMSO.

	δ H_5	δ H_6	δ H_7	δ Me_a	δ Me_b	J_{56}[a]	J_{57}[a]	J_{67}[a]
4.2, 5-adduct	4.95	6.29	6.94	/[b]	/[b]	5.6	1.0	10
4.2, 7-adduct	7.09	4.96	4.58	1.51	1.45	10.4	1.6	4.4
4.3	5.03	6.50	/	1.40	1.56	6.0	/	/
4.4	4.94	5.24	/	1.34	1.54	6.2	/	/

a. J values in Hz.

b. Hidden by 2-nitropropane signal.

In the spectrum of alkene **4.10** the two methyl groups are non-equivalent and give singlets at δ 1.99 and 2.26 ppm while the ring hydrogen give bands at δ 6.02 and 6.89 ppm, J = 10.4 Hz.

The presence of **4.10** in the reaction mixture was confirmed by negative electrospray mass spectrometry which showed a peak at m/z = 206 as expected.

In an attempt to isolate the neutral product **4.11** a sample from the NMR tube in DMSO was added to aqueous hydrochloric acid. A precipitate was obtained and the mass spectrum in acetonitrile taken. Under negative electrospray conditions that showed a small peak at m/z = 206 corresponding to M-H. This indicates the likely presence of **4.11** with M.W = 207. However the mass spectrum showed many other bands at higher molecular weights indicating the presence of other species.

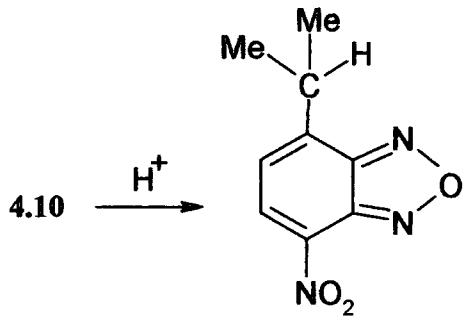

4.11

The results for **4.7** are in general accord with those of Terrier el al[3] who reported that reaction of potassium 2-nitropropenide with **4.2** in d_6-DMSO results in a mixture of the 5- and 7-adducts with the 7-adducts having greater thermodynamic stability. In the absence of added base elimination of nitrous acid was not observed.

However chemical oxidation of the 7-adduct was reported[3] to give a neutral product.

4.3.3 4-Nitrobenzofurazan with Nitromethane

A solution in d_6-DMSO of **4.2** (0.42 mol dm^{-3}), **4.5** (0.37 mol dm^{-3}) and triethylamine (0.5 mol dm^{-3}) gave bands attributable to the 5-adduct **4.12**. Bands are observed due to H_6 and H_7 at δ 6.41 and 6.84 ppm respectively with H_5 at δ 4.55 ppm. Since C_5 is chiral separate bands are observed due to H_a and H_b at δ 4.87 and 5.08 ppm. Since H_5 is spin coupled to four other hydrogens it showed a complex multiplet, while splitting patterns for other hydrogen atoms were more easily interpreted. Values are in Table 4.4. With time rapid irreversible decomposition occurred. Broad bands

were obtained which were not readily interpretable, so this system was not investigated further.

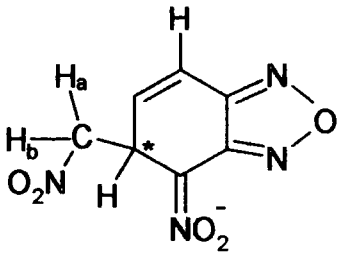

4.12

Table 4.4 ^{1}H NMR data for adducts from nitrobenzofurazan derivatives with nitromethane in d_6-DMSO.

	δ H_5	δ H_6	δ H_7	δ H_a	δ H_b	J_{56}[a]	J_{57}[a]	J_{67}[a]	J_{ab}[a]	J_{a5}[a]	J_{b5}[a]
4.2	4.55	6.41	6.84	4.87	5.08	4.8	1.6	10	12	4	5.6
4.3	4.66	6.63	/	4.86	5.16	5.2	/	/	8.2	3.2	5.6
4.4	4.59	5.42	/	4.84	4.97	5.2	/	/	11.2	4	5.8

a. J values in Hz.

4.3.4 7-Chloro-4-Nitrobenzofurazan with Nitroethane

The spectrum of **4.3** (0.2 mol dm^{-3}) with **4.6** (0.5 mol dm^{-3}) in the presence of triethylamine (0.5 mol dm^{-3}) in d_6-DMSO was recorded as soon as possible. The spectrum shown in Figure 4.3 indicates the formation of two diastereoisomeric adducts in the intensity ratio 1.8:1 corresponding to reaction at the 5-position.

Chemical shifts and coupling constants are collected in Table 4.2. With time one set of bands, these labelled **a** in Figure 4.3, decreases in intensity coupled with the appearance of new bands attributable to the alkene derivative. The process of elimination depended on the triethylamine concentration. The spectrum with high concentration of triethylamine (2 mol dm^{-3}) is shown in Figure 4.4. A quartet, J = 8 Hz, at δ 7.62 ppm is observed due to H_8, with a doublet at δ 1.91 ppm for the methyl group. A singlet band is observed due to H_6 at δ 7.32 ppm in the alkene.

Figure 4.3 ^{1}H NMR spectrum of **4.3** with **4.6** in the presence of triethylamine (0.5 mol dm^{-3}) in d_6-DMSO.

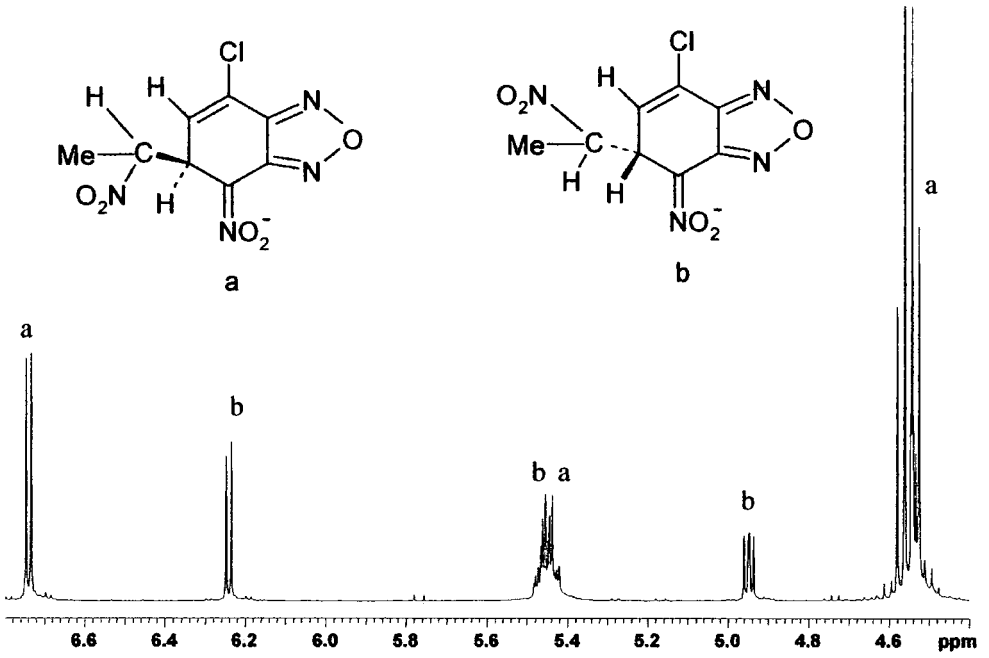

Figure 4.4 ^{1}H NMR spectrum of **4.3** with **4.6** in the presence of triethylamine (2 mol dm^{-3}) in d_6-DMSO

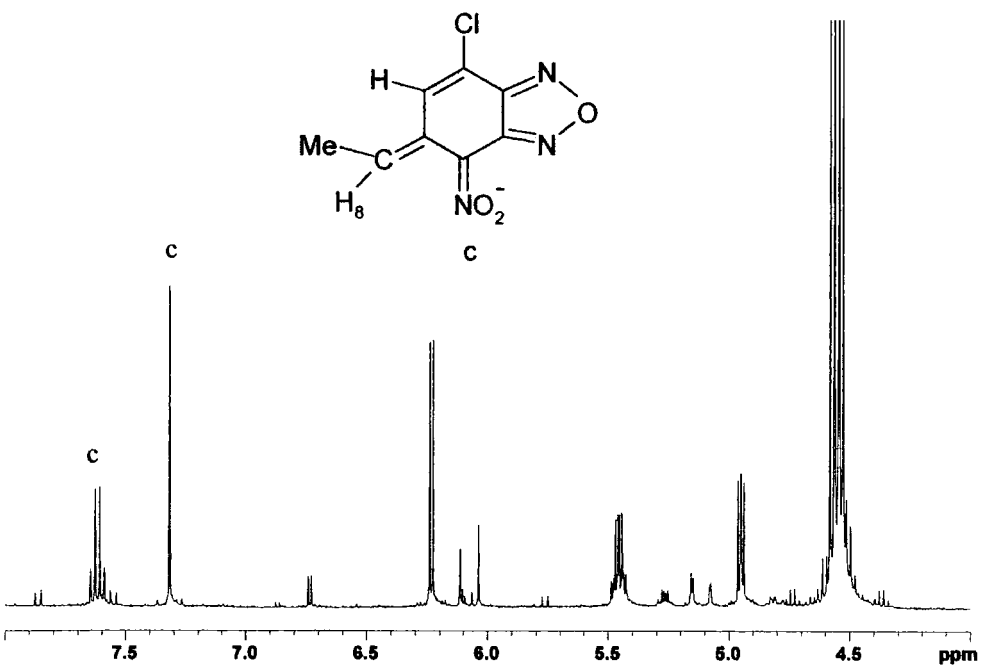

Table 4.5 Variation with time of the intensity[a] of NMR bands due to diastereoisomeric adducts from **4.3** and nitroethane.

Triethylamine/ mol dm^{-3}	Initial			30 minutes			120 minutes		
	a	b	ratio	a	b	ratio	a	b	ratio
0.5	1.49	0.85	1.8	0.83	0.69	1.2	0.13	0.36	0.36
1.0	1.39	0.77	1.8	0.68	0.62	1.1	1.46	6.29	0.23
2.0	0.57	4.17	0.14	0.56	6.4	0.09	/	/	0.00

a. Relative intensities of bands due to H_6 at δ 6.74 (**a**) and 6.24 ppm (**b**) in solutions in d_6-DMSO containing **4.3** (0.2 mol dm^{-3}) and nitroethane (0.5 mol dm^{-3}).

The values in Table 4.5 show the relative intensities of bands due to H_6 in the two diastereoisomeric adducts. Since the individual values depend on the integration settings they are only directly comparable within one spectrum. Hence the values of the ratio of intensities **a/b** is the important result. The data in the Table clearly show that the ratios **a/b** decrease with time indicating the more rapid reaction of isomer **a**, also the rate of change is faster at higher triethylamine concentration indicating a base catalysed process. With lower concentration of triethylamine some decomposition to give the hydroxy[2] derivative was observed giving bands at δ 5.78, 8.25 ppm, J = 10 Hz. However there was no evidence for displacement of chloride by the carbanion.

4.3.5 7-Chloro-4-Nitrobenzofurazan with 2-Nitropropane

NMR measurements for **4.3** (0.2 mol dm^{-3}), **4.7** (0.5 mol dm^{-3}) and triethylamine (0.5 mol dm^{-3}) indicated the formation of the 5-adduct with bands due to H_5 and H_6 at δ 5.03 and 6.50 ppm respectively, J = 6 Hz. Non-equivalence of the methyl groups was observed with singlets at δ 1.40 and 1.56 ppm. The spectrum obtained initially showed the presence of unreacted **4.3**, indicating that the equilibrium constant for adduct formation was lower than that for **4.6**. Spectra measured after one hour, and after five days showed no band around δ 7 ppm as expected for the elimination product.

The failure to find elimination may indicate that the product **4.13** would involve considerable steric strain between the coplanar methyl and nitro-groups.

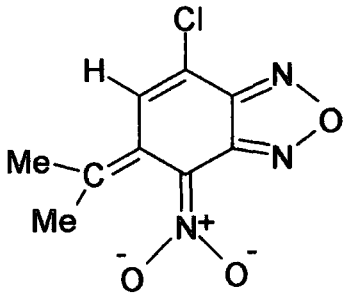

4.13

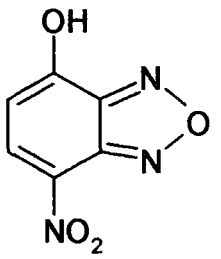

4.14

The spectra with increasing time indicated displacement of the chloride by hydroxide produced from residual water in the solvent to give the hydroxy derivative **4.14**.

Spectra recorded with twice the concentration of triethylamine (1.0 mol dm^{-3}) were generally similar to those detailed above. Differences were that the relative amount of parent **4.3** initially present was reduced and the rate of formation of the hydroxy derivative **4.14** was reduced. This implies that the formation of the hydroxy derivative involves direct reaction of the parent **4.3**.

4.3.6 7-Chloro-4-Nitrobenzofurazan with Nitromethane

With **4.3** (0.2 mol dm^{-3}) **4.5** (0.5 mol dm^{-3}) and triethylamine (0.5 mol dm^{-3}), the spectrum showed bands due to H_5 and H_6 at δ 4.66 and 6.63 ppm attributed to the adduct at the 5-position. Data are in Table 4.4. The bands for H_a and H_b were observed at δ 4.86 and 5.16 ppm. The spectra indicated quite rapid irreversible decomposition but no products could be positively identified.

4.3.7 7-Methoxy-4-Nitrobenzofurazan with Nitroethane

^{1}H NMR spectra were recorded with **4.4** (0.2 mol dm^{-3}) and **4.6** (0.5 mol dm^{-3}) and with triethylamine (0.5 mol dm^{-3}). The spectra indicated reaction at the 5-position to give two diastereoenantiomers in 1:1 ratio. Spectra recorded after 4 hours and after 24 hours indicated no change in the spectrum showing that elimination was not observed. Similarly the spectrum of a solution containing 1.0 mol dm^{-3} triethylamine

again indicated addition at the 5-position with no decomposition observable after 24 hours. Chemical shifts and coupling constant are in Table 4.2.

4.3.8 7-Methoxy-4-Nitrobenzofurazan with 2-Nitropropane

The spectrum of **4.4** (0.2 mol dm^{-3}), **4.7** (0.7 mol dm^{-3}) and triethylamine (0.5 mol dm^{-3}) is shown in Figure 4.5. Spin-coupled bands J = 6.2 Hz are observed at δ 4.94 and 5.24 ppm due respectively to H_5 and H_6. The methoxy signal is at δ 3.68 ppm and two singlets were observed due to the methyl groups at δ 1.34 and 1.54.ppm Interestingly bands due to unreacted **4.4** were seen at δ 8.76, 7.10 and 4.22 ppm. No change in the spectrum occurred after 24 hours.

Figure 4.5 ^{1}H NMR spectrum of **4.4** with **4.7** in the presence of triethylamine (0.5 mol dm^{-3}) in d_6-DMSO

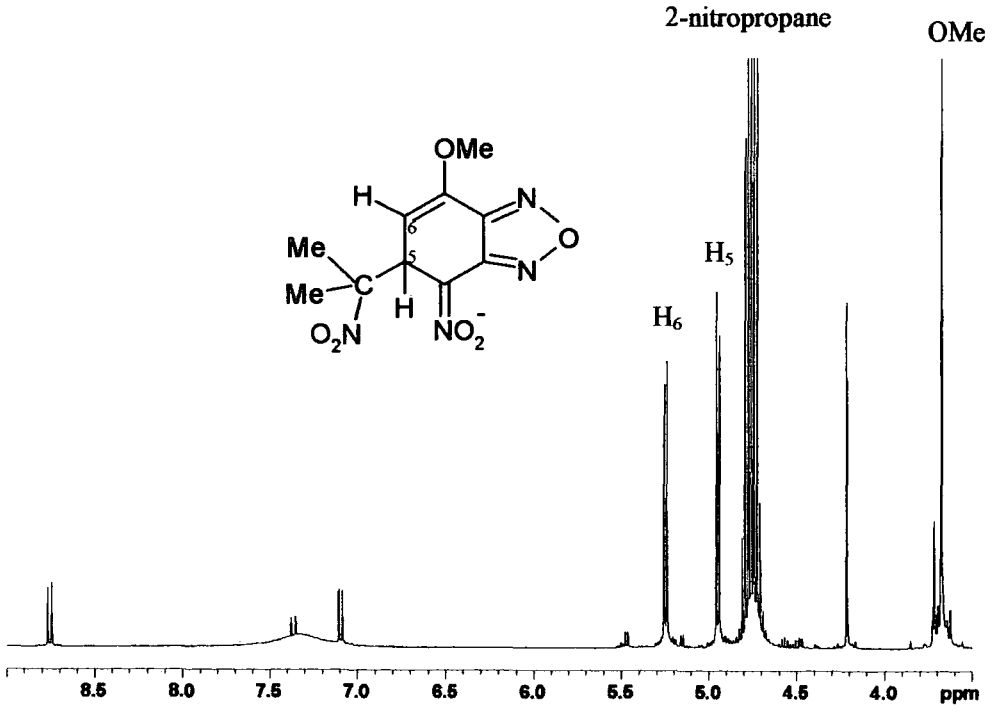

4.3.9 7-Methoxy-4-Nitrobenzofurazan with Nitromethane

The spectrum for **4.4** (0.2 mol dm^{-3}), **4.5** (0.7 mol dm^{-3}) and triethylamine (0.5 mol dm^{-3}) is shown in Figure 4.6. Bands for H_5 and H_6 in the adduct are observed at δ 4.59 and 5.42 ppm respectively. Spin-coupled bands at δ 4.84 and 4.97 ppm are attributed to H_a and H_b respectively with coupling constant J_{ab} = 11.2 Hz, J_{a5} = 4.0 Hz and J_{b5} = 5.8 Hz.

The methoxyl resonance is at δ 3.70 ppm. In addition bands are observed to nitromethane δ 4.43 and triethylamine δ 1.06 and 2.78 ppm. Little decomposition was observed after 24 hours, with no bands visible due to elimination of nitrous acid.

Figure 4.6 ^{1}H NMR spectrum of **4.4** with **4.5** in the presence of triethylamine (0.5 mol dm^{-3}) in d_6-DMSO

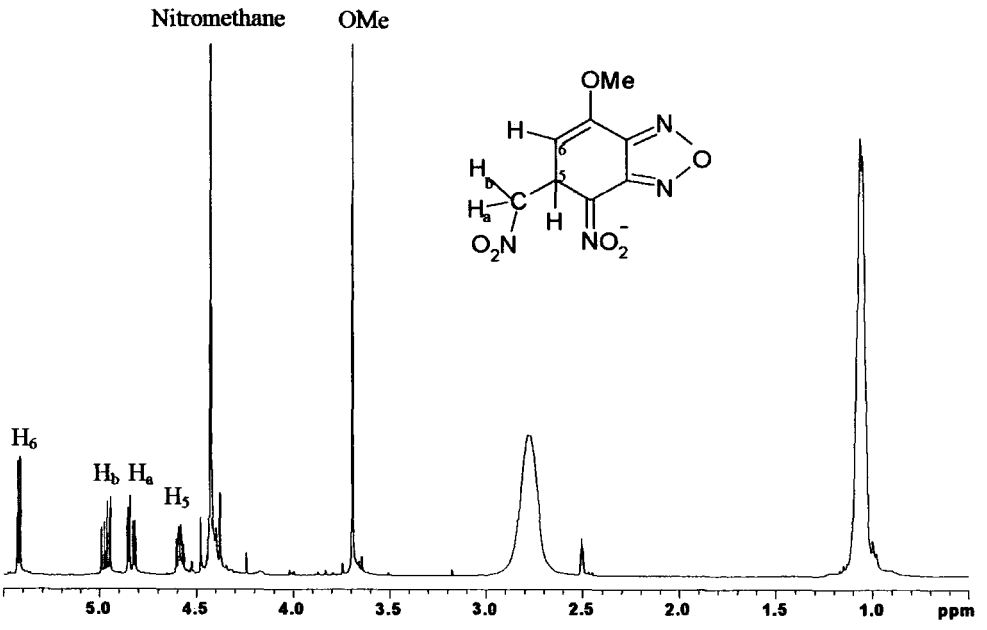

4.4 Kinetic and Equilibrium Studies

4.4.1 Introduction

Previously Terrier et al[5] have reported studies of the reaction of 4-nitrobenzofurazan **4.2**, with methoxide ions in methanol. The parent absorbs at 320 nm and both 5- and 7- adducts had maxima at 330 nm. Kinetic and equilibrium results were given in chapter 1, page 25.

In the present work carbanions were generated from the nitroalkanes by reaction with methoxide ions in methanol. Values of the equilibrium constant, K_1, for this reaction have been reported[8] to be 21 $dm^3\ mol^{-1}$ for nitromethane **4.5**, 500 $dm^3\ mol^{-1}$ for nitroethane **4.6,** and 2600 $dm^3\ mol^{-1}$ for 2-nitropropane **4.7**. Due to the reaction of the 4-nitrobenzofurazans with methoxide it was necessary to reduce the concentration of free methoxide to low values and this was done by working with [nitroalkane]>>[MeO^-] and/or by using buffers to control the methoxide concentration (Scheme 4.4).

$$R_1R_2CHNO_2 + {}^-OMe \underset{}{\overset{K_1}{\rightleftharpoons}} R_1R_2\bar{C}NO_2 + MeOH \qquad (4.1)$$

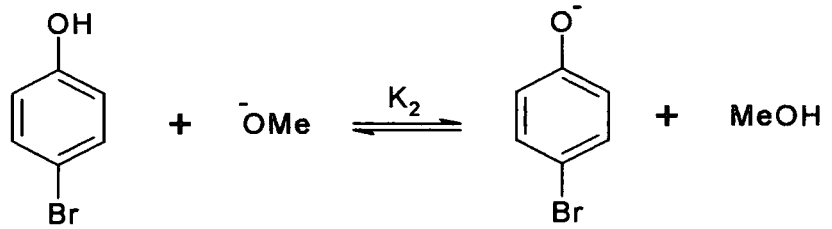

Scheme 4.4

The pK_a value for 4-bromophenol in methanol has been reported[6] to be 13.61. The value of K_2 in Scheme 4.4 will be related to the pK_a value by equation 4.2 where pK_m = 16.92[7] measures the autoprotolysis of methanol (equation 4.3). The value obtained for K_2 is 2040 $dm^3\ mol^{-1}$.

$$\log K_2 = pK_m - pK_a \qquad (4.2)$$

$$MeOH \underset{}{\overset{K_m}{\rightleftharpoons}} MeO^- + H^+ \qquad (4.3)$$

Values of the equilibrium concentration of methoxide ions were calculated using equation 4.4. For example where [PhOH] = 0.09 mol dm^{-3} and [PhO^-] = 0.01 mol dm^{-3}, then [MeO^-] = 5.4×10^{-5} mol dm^{-3}. Since this concentration is buffered it will not be changed on the addition of low concentration of nitroalkanes.

$$[MeO^-] = \frac{[PhO^-]}{[PhOH]}\frac{1}{K_2} \qquad (4.4)$$

4.4.2 4-Nitrobenzofurazan

The UV spectrum of **4.2** (1×10^{-4} mol dm^{-3}) in methanol, shown in Figure 4.7, has a maximum at 320 nm, $\varepsilon = 9.0\times10^{3}$ dm^3 mol^{-1} cm^{-1}. The spectra of solutions made up with **4.2** (6.25×10^{-5} mol dm^{-3}), nitroethane (0.125 mol dm^{-3}) and sodium methoxide (0.0125 mol dm^{-3}), also in Figure 4.7 show that initially there is a shift in the maximum to 340 nm with an increase in absorbance and that a very slow process is observed giving rise to a band at 360 nm. Data are collected in Table 4.6.

Figure 4.7 UV/visible spectra plots for the reaction **4.2** (6.25×10^{-5} mol dm^{-3}) with **4.6** (0.125 mol dm^{-3}) and sodium methoxide (0.0125mol dm^{-3}) in methanol.

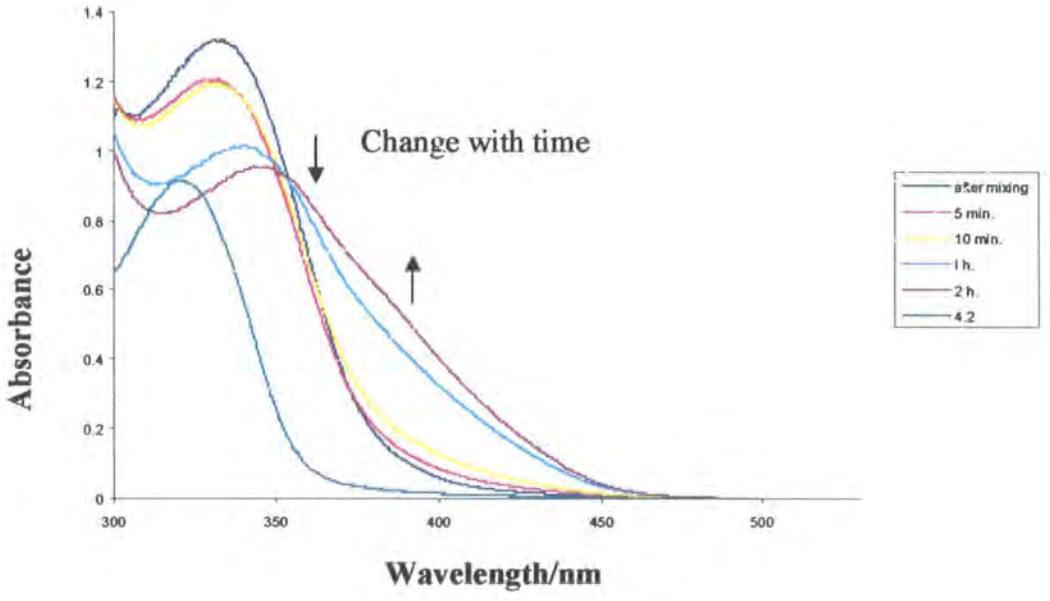

Table 4.6 UV/visible data for **4.2**, **4.3** and **4.4**, with nitroalkanes in methanol.

	Parent		Nitroethane adduct		Alkene product	
	λ_{max}/ nm	$\varepsilon/10^3$ $dm^3\,mol^{-1}\,cm^{-1}$	λ_{max}/ nm	$\varepsilon/10^4$ $dm^3\,mol^{-1}\,cm^{-1}$	λ_{max}/ nm	$\varepsilon/10^4$ $dm^3\,mol^{-1}\,cm^{-1}$
4.2	320	9.0	335	1.6	360	1.3
4.3	337	10.1	340	1.4	380	0.9
4.4	375	9.1	340	1.4	/	/
			Nitropropane adduct		**Alkene product**	
4.2	320	9.0	335	2.0	360	/
4.3	337	10.1	340	1.25	380	/
4.4	375	9.1	340	1.8	/	/
			Nitromethane adduct		**Alkene product**	
4.4	375	9.1	330	1.0	380	1.3

In accordance with the UV spectra, kinetic studies indicate two process whose rate constants are designated k_{fast} and k_{slow} respectively. The faster process was measurable on the stopped-flow timescale and was followed as a colour forming reaction at 350 nm. The slower process was measured as colour forming reaction at 380 nm where the increase in absorbance was greatest

By analogy with the NMR measurements it is likely that the two processes involved are rapid reaction of the carbanions to give an adduct at the 5-position followed by slower elimination of nitrous acid to give the elimination product. These assumptions form a good starting point for the kinetic analysis. All kinetic measurements were made at 25 °C with the concentration of nitroalkane and methoxide in large excess of the concentration of **4.2**. Under these condition all the reactions followed first order kinetics.

4.4.3 Fast Reaction; σ-Adduct Formation

It is known that equilibration of the nitroalkanes with methoxide to give the carbanions is rapid[8], so that the fast process may be written as shown in Scheme 4.5. It may also be necessary to consider competition for **4.2** by methoxide ions. Reaction

here can occur at the 5-position (fast) or 7-position (slow). Reaction at the 5-position is shown in Scheme 4.6.

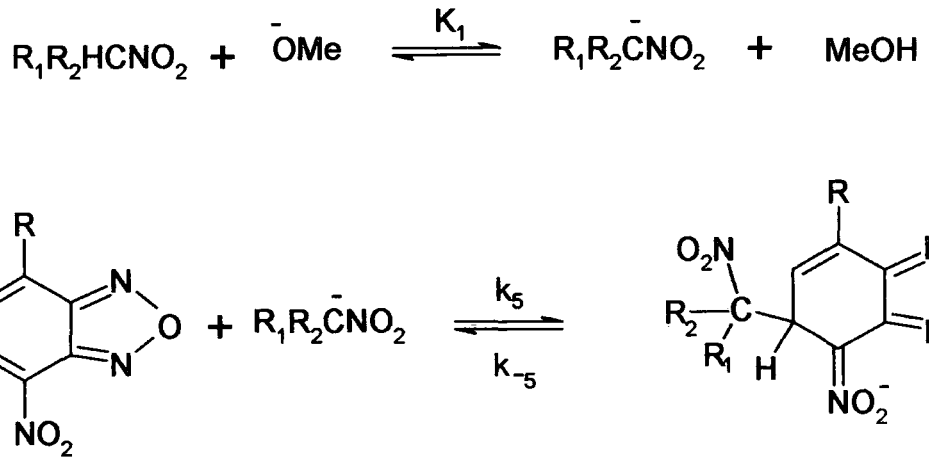

4.15 **4.16**

R=H, Cl, OMe.

R_1R_2=H, H; H, CH_3; CH_3, CH_3.

Scheme 4.5

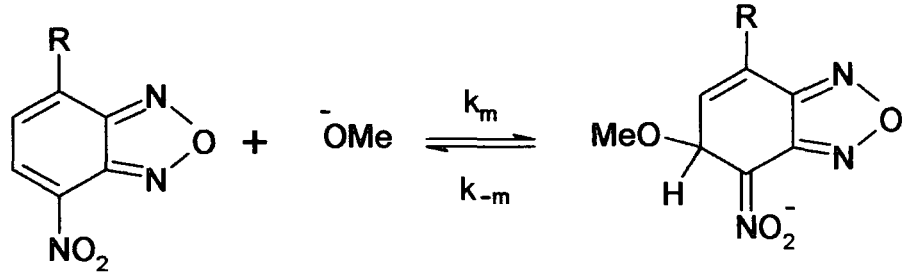

Scheme 4.6

Values of rate and equilibrium constants for reaction of **4.2** with methoxide are known and are quoted in Table 1.2. The value of K_5 for methoxide is 140 dm^3 mol^{-1}, so that at the low equilibrium concentration of methoxide,$<10^{-3}$ mol dm^{-3}, used here this process may be neglected. Although the value of K_7 for reaction of methoxide at the 7-position is higher, K_7 = 3000 dm^3 mol^{-1}, the rate constant for methoxide attack is relatively low, 6 dm^3 mol^{-1} s^{-1}, so that this process does not effectively compete with attack of the carbanions at the 5-position.

Under these conditions it can be shown that the rate constant for the fast process is given by equation 4.5 which is derived below.

$$k_{fast} = k_5[R_1R_2CNO_2^-] + k_{-5} \quad (4.5)$$

Derivation

$$\frac{d[\mathbf{4.16}]}{dt} = k_5[\mathbf{4.15}][R_1R_2CNO_2^-] - k_{-5}[\mathbf{4.16}] \quad (4.6)$$

But:

$$[\mathbf{4.16}]+[\mathbf{4.15}]=[\mathbf{4.15}]_o$$

The sum of the concentrations of **4.16** and **4.15** must always equal, $[\mathbf{4.15}]_o$, the stoichiometric concentration of **4.15**.

Substituting in (4.6).

$$\frac{d[\mathbf{4.16}]}{dt} = k_5[R_1R_2CNO_2^-]([\mathbf{4.15}]_o - [\mathbf{4.16}]) - k_{-5}[\mathbf{4.16}] \quad (4.7)$$

At equilibrium, $[\mathbf{4.16}]_{eq}$, the concentration of **4.16** at equilibrium, is constant.

$$\therefore \frac{d[\mathbf{4.16}]_{eq}}{dt} = 0 = k_5[R_1R_2CNO_2^-]([\mathbf{4.15}]_o - [\mathbf{4.16}]_{eq}) - k_{-5}[\mathbf{4.16}]_{eq} \quad (4.8)$$

Equation 4.7_4.8 gives.

$$\frac{d[\mathbf{4.16}]}{dt} = k_5[R_1R_2CNO_2^-]([\mathbf{4.16}]_{eq} - [\mathbf{4.16}]) + k_{-5}([\mathbf{4.16}]_{eq} - [\mathbf{4.16}]) \quad (4.9)$$

$$\frac{d[\mathbf{4.16}]}{dt} = (k_5[R_1R_2CNO_2^-] + k_{-5})([\mathbf{4.16}]_{eq} - [\mathbf{4.16}]) \quad (4.10)$$

Experimentally it is found that approach to equilibrium is a first order process, where:

$$\frac{d[\mathbf{4.16}]}{dt} = k_{fast}([\mathbf{4.16}]_{eq} - [\mathbf{4.16}]) \qquad (4.11)$$

Hence:

$$k_{fast} = k_5[R_1R_2CNO_2^-] + k_{-5}$$

Results for the reaction involving 2-nitropropane **4.7**, are given in Table 4.7. A plot according to equation 4.5 shown in Figure 4.8 was linear giving values for k_5 = 2.5±0.1 $dm^3\ mol^{-1}\ s^{-1}$ and k_{-5} = (3.3±0.3)×10^{-3} s^{-1}. Combination of these values gave $K_5 = k_5/k_{-5}$, 750±50 $dm^3\ mol^{-1}$.

Table 4.7 Data for **4.2** (5×10^{-5} mol dm^{-3}) with **4.7** and sodium methoxide in methanol.

[4.7]/ mol dm^{-3}	[NaOMe]/ mol dm^{-3}	$[MeO^-]^a_{eq}/10^{-5}$ mol dm^{-3}	$[(CH_3)_2CNO_2^-]^a_{eq}/10^{-3}$ mol dm^{-3}	k_{obs} / s^{-1}
0.05	0.005	3.80	4.94	0.0157
0.025	0.005	7.69	4.99	0.0152
0.05	0.004	2.88	3.74	0.0134
0.05	0.0025	1.92	2.49	0.0098
0.05	0.00125	0.96	1.23	0.0063

a. Calculated from equation 4.1 with a value for K_1 of 2600 $dm^3\ mol^{-1}$.

Figure 4.8 Plot according to equation 4.5 for reaction of **4.2** with 2-nitropropanide anion.

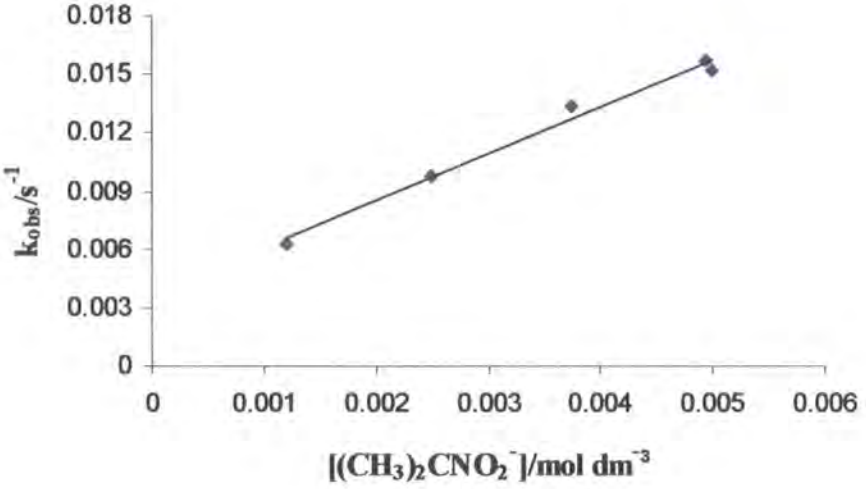

Data for nitroethane **4.6**, are in Table 4.8. They allow the calculation of a value for k_5 of 80±5 $dm^3\ mol^{-1}\ s^{-1}$, but the value of k_{-5} is too small to be accurately determined.

The amplitudes indicate that at these concentrations conversion to adduct is nearly complete. In order to determine the value of k_{-5} measurements were made in buffer solutions (Table 4.9) giving low equilibrium concentrations of methoxide and thus also of nitroethane anion. Extrapolation to zero concentration of carbanion gave a value for k_{-5} of $1.2\times10^{-3}\ s^{-1}$. Combination of the values for k_5 and k_{-5} gives a value for K_5 of $6.7\times10^{4}\ dm^3\ mol^{-1}$ which is in good agreement with that calculated from the amplitudes in the buffer solution.

Table 4.8 Data for **4.2** (5×10^{-5} mol dm^{-3}) with **4.6** and sodium methoxide in methanol.

[4.6]/ mol dm^{-3}	[NaOMe]/ mol dm^{-3}	$[MeO^-]^a_{eq}/10^{-4}$ mol dm^{-3}	$[CH_3CHNO_2^-]^a_{eq}/10^{-3}$ mol dm^{-3}	k_{obs} / s^{-1}	Ampt[b].
0.05	0.005	2.0	4.8	0.375	0.63
0.10	0.005	1.0	4.9	0.419	0.64
0.025	0.005	4.0	4.6	0.382	0.62
0.05	0.0025	1.0	2.4	0.200	0.63
0.025	0.0005	0.4	0.5	0.054	0.52

a. Calculated from equation 4.1 with a value for K_1 of 500 $dm^3\ mol^{-1}$.

b. Amplitudes (Δ Abs) are the relative changes from stopped flow measurement in similar conditions.

Table 4.9 Data for **4.2** (5×10^{-5} mol dm^{-3}) with **4.6** and sodium methoxide in methanol containing the buffered solution.

$[4.6]/10^{-3}$ mol dm^{-3}	$[PhO^-]_{eq}/10^{-3}$ mol dm^{-3}	$[PhOH]_{eq}$/ mol dm^{-3}	$[MeO^-]^a_{eq}/10^{-5}$ mol dm^{-3}	$[CH_3CHNO_2^-]^b_{eq}/10^{-5}$ mol dm^{-3}	k_{obs}/s^{-1}	Ampt.	$K_S^c/10^4$ dm^3 mol^{-1}
1	5	0.045	5.4	2.7	0.0025	0.4	6.4
1.5	5	0.045	5.4	4.0	0.0031	0.45	6.3
2	5	0.045	5.4	5.4	0.0037	0.49	6.5

a. Calculate from equation 4.4.

b. Calculate from equation 4.1.

c. Calculate as $\frac{\text{Ampt.}}{(0.63 - \text{Ampt.})} \frac{1}{[CH_3CHNO_2^-]_{eq}}$.

Table 4.11 Data for **4.2** (5×10^{-5} mol dm^{-3}) with **4.5** and sodium methoxide in methanol containing the buffered solution.

$[4.5]/10^{-3}$ mol dm^{-3}	$[PhO^-]_{eq}/10^{-3}$ mol dm^{-3}	$[PhOH]_{eq}$/ mol dm^{-3}	$[MeO^-]^a_{eq}/10^{-6}$ mol dm^{-3}	$[CH_2NO_2^-]^b_{eq}/10^{-6}$ mol dm^{-3}	k_{obs}/s^{-1}	Ampt.	$K_S^c/10^5$ dm^3 mol^{-1}
1	5	0.045	5.4	1.14	0.0013	0.19	4
1.5	5	0.045	5.4	1.70	0.0018	0.24	4
2	5	0.045	5.4	2.30	0.0022	0.26	3.3

a. Calculate from equation 4.4.

b. Calculate from equation 4.1.

c. Calculate as $\frac{\text{Ampt.}}{(0.60 - \text{Ampt.})} \frac{1}{[CH_2NO_2^-]_{eq}}$.

The data for reaction with **4.5** are in Table 4.10. The values in the Table give $k_5 = 300\pm20$ dm^3 mol^{-1} s^{-1}, but conversion to adduct is too near to completion to allow determination of k_{-5}. Values in the 4-bromophenol buffer, in Table 4.11, give a value for k_{-5} by extrapolation of $(1\pm0.5)\times10^{-3}$ s^{-1}. Combination with the known value of k_5 leads to a value of K_5 *ca* 3×10^5 dm^3 mol^{-1}. This value is in accord with that calculated from the amplitudes given in Table 4.4.

Table 4.10 Data for **4.2** (5×10^{-5} mol dm^{-3}) with **4.5** and sodium methoxide in methanol.

[4.5]/ mol dm^{-3}	[NaOMe]/ mol dm^{-3}	$[MeO^-]^a_{eq}/10^{-4}$ mol dm^{-3}	$[CH_2NO_2^-]^a_{eq}/10^{-3}$ mol dm^{-3}	k_{obs} / s^{-1}	Ampt.
0.30	0.0025	3.3	2.2	0.65	0.58
0.15	0.0025	6.0	1.9	0.62	0.55
0.15	0.0020	4.8	1.5	0.42	0.58
0.15	0.0015	3.6	1.1	0.35	0.59
0.15	0.0010	2.4	0.8	0.24	0.49

a. Calculated from equation 4.1 with a value for K_1 of 21 dm^3 mol^{-1}.

4.4.4 7-Methoxy-4-Nitrobenzofurazan

The UV spectrum of **4.4** (1×10^{-4} mol dm^{-3}) in methanol, shows a maximum at 375 nm, $\varepsilon = 9.1\times10^3$ dm^3 mol^{-1} cm^{-1}. The spectra of solutions made up with **4.4** (1×10^{-4} mol dm^{-3}), **4.7** (0.10 mol dm^{-3}) and sodium methoxide (0.06 mol dm^{-3}) in Figure 4.9, show that initially there is a shift in the maximum to 340 nm, $\varepsilon = 1.0\times10^4$ dm^3 mol^{-1} cm^{-1}. Kinetic measurements were made by following the decrease with time in the absorbance at 380 nm, due to the parent.

Figure 4.9 UV/visible spectra plots for the reaction of **4.4** (1×10^{-4} mol dm^{-3}) with **4.7** (0.10 mol dm^{-3}) and sodium methoxide (0.06 mol dm^{-3}) in methanol.

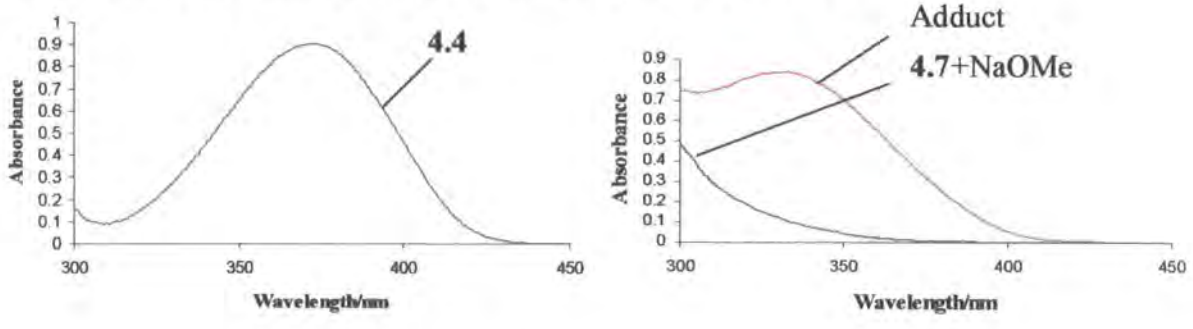

The value of the equilibrium constant[9] for formation of the 5-methoxy adduct from **4.4** is 22 $dm^3 mol^{-1}$ so that at the equilibrium methoxide concentrations used here there is little interference from this process. Methoxide may also add at the 7-position to give a di-methoxy adduct with a rate constant[9], k, of 14.5 $dm^3 mol^{-1} s^{-1}$. However the product of $k[MeO^-]_{eq}$ is much smaller than the values of k_{obs} indicating that attack of the carbanions at the 5-position is the dominant process. Data for reaction with **4.7** are given in Table 4.12. A linear plot of according to equation 4.5 gave values for k_5 = 1.4 $dm^3 mol^{-1} s^{-1}$ and $k_{-5} = 13\times10^{-3}$ s^{-1}. Combination of these values gave $K_5 = k_5/k_{-5}$, 108 $dm^3 mol^{-1}$.

Table 4.12 Data for **4.4** (5×10^{-5} mol dm^{-3}) with **4.7** and sodium methoxide in methanol.

[4.7]/ mol dm^{-3}	[NaOMe]/ mol dm^{-3}	$[MeO^-]^a_{eq}/10^{-4}$ mol dm^{-3}	$[(CH_3)_2CNO_2^-]^a_{eq}/10^{-2}$ mol dm^{-3}	k_{obs} / s^{-1}
0.05	0.03	2.31	2.98	0.057
0.05	0.02	1.51	1.98	0.039
0.05	0.015	1.15	1.49	0.034
0.05	0.01	0.80	0.99	0.028

a. Calculated from equation 4.1 with a value for K_1 of 2600 $dm^3 mol^{-1}$.

Data for **4.6** are shown in Table 4.13. A linear plot gave k_5 = 28 $dm^3 mol^{-1} s^{-1}$, but the value of k_{-5} is too small to be accurately determined. In order to determine the value of k_{-5} measurements were made in buffer solution. Data are in Table 4.14. Extrapolation to zero concentration of carbanion gave a value for k_{-5} of 2.1×10^{-3} s^{-1}.

Combination of the values for k_5 and k_{-5} gives a value for K_5 of 1.3×10^4 dm^3 mol^{-1}.

Results for reaction involving **4.5** are shown in Table 4.15 giving k_5 = 90 dm^3 $mol^{-1} s^{-1}$ but conversion to adduct is too near to completion to allow determination of k_{-5}. Values in buffered solutions (Table 4.16) give a value for k_{-5} by extrapolation of 2.5×10^{-3} s^{-1}, allowing the estimation of $K_5 = 3.6\times10^4$ $dm^3 mol^{-1}$.

Table 4.13 Data for **4.4** (5×10^{-5} mol dm^{-3}) with **4.6** and sodium methoxide in methanol.

[4.6]/ mol dm^{-3}	[NaOMe]/ mol dm^{-3}	$[MeO^-]^a_{eq}/10^{-4}$ mol dm^{-3}	$[CH_3CHNO_2^-]^a_{eq}/10^{-3}$ mol dm^{-3}	k_{obs} / s^{-1}
0.10	0.005	1.0	4.90	0.15
0.10	0.004	0.8	3.92	0.12
0.10	0.003	0.6	2.94	0.09
0.05	0.004	0.8	1.92	0.06
0.10	0.0015	0.3	1.47	0.04
0.10	0.001	0.2	0.98	0.03

a. Calculated from equation 4.1 with a value for K_1 of 500 dm^3 mol^{-1}.

Table 4.14 Data for **4.4** (5×10^{-5} mol dm^{-3}) with **4.6** and sodium methoxide in methanol containing the buffered solution.

$[4.6]/10^{-3}$ mol dm^{-3}	$[PhO^-]_{eq}/10^{-3}$ mol dm^{-3}	$[PhOH]_{eq}$/ mol dm^{-3}	$[MeO^-]^a_{eq}/10^{-5}$ mol dm^{-3}	$[CH_3CHNO_2^-]^b_{eq}/10^{-5}$ mol dm^{-3}	$k_{obs}/10^{-3}$ s^{-1}
1.0	5.0	0.045	5.4	2.7	2.15
1.5	5.0	0.045	5.4	4.0	2.18
2.0	5.0	0.045	5.4	5.4	2.21

a. Calculate from equation 4.4.

b. Calculate from equation 4.1.

Table 4.15 Data for **4.4** (5×10^{-5} mol dm^{-3}) with **4.5** and sodium methoxide in methanol.

[4.5]/ mol dm^{-3}	[NaOMe]/ mol dm^{-3}	$[MeO^-]^a_{eq}/10^{-4}$ mol dm^{-3}	$[CH_2NO_2^-]^a_{eq}/10^{-3}$ mol dm^{-3}	k_{obs} / s^{-1}
0.30	0.0025	3.3	2.2	0.188
0.15	0.0025	6.0	1.9	0.184
0.15	0.0020	4.8	1.5	0.149
0.15	0.0015	3.6	1.1	0.117
0.15	0.0010	2.4	0.8	0.079
0.15	0.0005	1.2	0.4	0.046

a. Calculated from equation 4.1 with a value for K_1 of 21 dm^3 mol^{-1}.

Table 4.16 Data for **4.4** (5×10^{-5} mol dm^{-3}) with **4.5** and sodium methoxide in methanol containing the buffered solution.

$[4.5]/10^{-3}$ mol dm^{-3}	$[PhO^-]_{eq}/10^{-3}$ mol dm^{-3}	$[PhOH]_{eq}$/ mol dm^{-3}	$[MeO^-]^a_{eq}/10^{-5}$ mol dm^{-3}	$[CH_2NO_2^-]^b_{eq}/10^{-6}$ mol dm^{-3}	$k_{obs}/10^{-3}$ s^{-1}
1.0	5.0	0.045	5.4	1.14	2.65
1.5	5.0	0.045	5.4	1.70	2.74
2.0	5.0	0.045	5.4	2.30	2.91

a. Calculate from equation 4.4.

b. Calculate from equation 4.1.

4.4.5 7-Chloro-4-Nitrobenzofurazan

The parent absorbs at 337 nm and reaction with nitroalkane anions resulted in an increase in absorbance but with little change in absorption maximum. Kinetic measurements were made in the range 320-350 nm and values of rate constants were independent of the wavelength of measurement.

The 7-chloro derivative is more reactive than 4-nitrobenzofurazan and the value for the equilibrium constant[9] for methoxide addition at the 5-position is 2800 dm^3 mol^{-1}. In the case of **4.7** it was possible to reduce the equilibrium concentration of methoxide ions to a low level to avoid interference from the methoxide reaction. Data for the reaction with **4.7** are given in Table 4.17. A linear plot of according to

equation 4.5 gave value for k_5 = 10.8 $dm^3 mol^{-1} s^{-1}$ and $k_{-5} = 5\times10^{-3}$ s^{-1}. Combination of these values gave, $K_5 = k_5/k_{-5}$, 2200 $dm^3 mol^{-1}$.

Table 4.17 Data for **4.3** (5×10^{-5} mol dm^{-3}) with **4.7** and sodium methoxide in methanol.

[4.7]/ mol dm^{-3}	[NaOMe]/ mol dm^{-3}	$[MeO^-]^a_{eq}/10^{-5}$ mol dm^{-3}	$[(CH_3)_2CNO_2^-]^a_{eq}/10^{-3}$ mol dm^{-3}	k_{obs} / s^{-1}	Ampt.
0.0625	0.0025	1.54	2.50	0.032	0.14
0.0313	0.0025	3.08	2.50	0.036	0.13
0.0313	0.0020	2.46	1.99	0.026	0.14
0.0313	0.0015	1.85	1.50	0.022	0.14
0.0133	0.0010	1.23	0.99	0.016	0.13

a. Calculated from equation 4.1 with a value for K_1 of 2600 $dm^3 mol^{-1}$.

Data for **4.6** are shown in Table 4.18. Again measurements were made with low concentrations of methoxide, $[MeO^-] \leq 2\times10^{-4}$ mol dm^{-3}. A linear plot according to equation 4.5 gave values for k_5 = 400 $dm^3 mol^{-1} s^{-1}$, but the value of k_{-5} is too small to be accurately determined.

Table 4.18 Data for **4.3** (5×10^{-5} mol dm^{-3}) with **4.6** and sodium methoxide in methanol.

[4.6]/ mol dm^{-3}	[NaOMe]/ mol dm^{-3}	$[MeO^-]^a_{eq}/10^{-4}$ mol dm^{-3}	$[CH_3CHNO_2^-]^a_{eq}/10^{-3}$ mol dm^{-3}	k_{obs} / s^{-1}	Ampt.
0.01	0.005	1.0	4.90	1.80	0.145
0.05	0.005	2.0	3.80	1.93	0.135
0.05	0.004	1.6	3.84	1.49	0.137
0.05	0.003	1.2	2.90	1.09	0.140
0.05	0.002	0.8	1.90	0.70	0.143

a. Calculated from equation 4.1 with a value for K_1 of 500 $dm^3 mol^{-1}$

Data for the reaction with **4.5** are give in Table 4.19. In the case of **4.5** it was not possible to avoid competition with the methoxide reaction. The reactions to be considered are shown in Scheme 4.7.

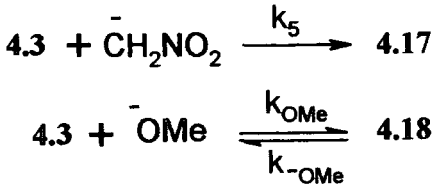

Scheme 4.7

The reaction to give the adduct **4.17** will be essentially irreversible with a low value of the reverse rate constant. However the methoxide addition has been reported to have values for k_{OMe} = 5100 dm^3 mol^{-1} s^{-1} and k_{-OMe} = 1.8 s^{-1}. Since the concentration of methoxide and nitromethane anions do not change in any one kinetic runs. The reactions in the forward direction are first order in [**4.3**]. The reactions shown may be considered as two parallel first order reactions, one of with is reversible. A semi-quantitative kinetic treatment following the methods of Bernasconi[10] gave equation 4.12.

$$k_{fast} = k_5[CH_2NO_2^-] + k_{OMe}[MeO^-] + k_{-OMe}\frac{k_{OMe}[MeO^-]}{k_{OMe}[MeO^-] + k_5[CH_2NO_2^-]} \qquad \textbf{(4.12)}$$

Table 4.19 Data for **4.3** (5×10^{-5} mol dm^{-3}) with **4.5** and sodium methoxide in methanol.

[4.5]/ mol dm^{-3}	[NaOMe]/ mol dm^{-3}	$[MeO^-]^a_{eq}/10^{-4}$ mol dm^{-3}	$[CH_2NO_2^-]^a_{eq}/10^{-3}$ mol dm^{-3}	k_{obs} / s^{-1}
0.15	0.0025	6.0	1.90	6.98
0.15	0.0025	4.8	1.52	6.01
0.15	0.0015	3.6	1.14	4.90
0.15	0.0010	2.4	0.80	3.56
0.45	0.0025	2.4	2.26	4.80
0.30	0.0025	3.5	2.15	5.93
0.15	0.0025	6.0	1.90	7.20
0.05	0.0025	12.4	1.26	9.73

a. Calculated from equation 4.1 with a value for K_1 of 21 dm^3 mol^{-1}.

The data in Table 4.20 was fitted to equation 4.12, allowing variation in each of the three parameters k_5, k_{OMe}, and k_{-OMe}. Some of the calculated values are given in

Table 4.20. The best fit was obtained with values of k_5 = 1500±100 $dm^3 mol^{-1} s^{-1}$, k_{OMe} = 5300±200 $dm^3 mol^{-1} s^{-1}$ and k_{-OMe} = 2±0.4 s^{-1}. The values obtained for k_{OMe} and for k_{-OMe} are close to these previously reported in the literature.

Table 4.20 Data values to equation 4.12 for **4.3** with **4.5** in methanol.

$[MeO^-]_{eq}/10^{-4}$ mol dm^{-3}	$[CH_2NO_2^-]_{eq}/10^{-3}$ mol dm^{-3}	k_{obs}/s^{-1}	k_{calc}/s^{-1}	k_{calc}/s^{-1}	k_{calc}/s^{-1}
6.0	1.90	6.98	7.15	7.24	7.08
4.8	1.52	6.01	6.00	6.02	5.90
3.6	1.14	4.90	4.80	4.77	4.69
2.4	0.80	3.56	3.61	3.51	3.47
2.4	2.26	4.80	5.25	5.41	5.21
3.5	2.15	5.93	5.87	6.00	5.81
6.0	1.90	7.20	7.15	7.24	7.08
12.4	1.26	9.73	10.06	10.12	10.02
			k_{OMe} = 5100	k_{OMe} = 5300	k_{OMe} = 5300
			k_5 = 1500	k_5 = 1600	k_5 = 1500
			k_{-OMe} = 2.4	k_{-OMe} = 2	k_{-OMe} = 2

It should be noted that there is also the possibility of attack by methoxide at the 7-position to give **4.4**. However there was no evidence for this process or for attack of carbanions at the 7-position. The failure of the carbanions to displace chloride may be due to steric hindrance to their attack. The value of the rate constant for methoxide attack at the 7-position is reported[9] to be 7.7 $dm^3 mol^{-1} s^{-1}$, so that at the methoxide concentration used in the present work this process does not compete effectively with the carbanion attack at the 5-position.

4.4.6 Summary of Kinetic and Equilibrium Results for Reaction at the 5-position

Results are summarized in Table.4.21. The values of K_5 increase in the order 2-nitropropane<nitroethane<nitromethane. The order follows that of the pK_a values of the nitroalkanes which measure the proton affinity of the carbanions. The increases in values of K_5 reflect increases in the value of k_5 and smaller decrease in the value of k_{-5}.

Values of K_5 for **4.4** are between 5 and 8 times lower than the corresponding values for **4.2**. This may be attributed to stabilization of the reactant by conjugation between the methoxy- and nitro-groups as shown in **4.19**. This stabilisation will be removed in the adduct **4.16** where the nitro group carries a negative charge.

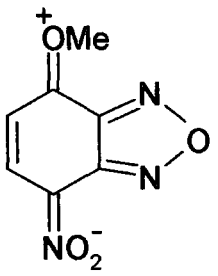

4.19

For **4.3** the value of K_5 for reaction with the anion of **4.7** is 3 times higher than that for **4.2**. Although it was not possible to measure values of K_5 for the anions of **4.6** and **4.5** the values of k_5 are higher than those for corresponding reaction with **4.2**.

These increases for **4.3** are likely to be due to the electron-withdrawing effect of the chlorine which is at the ring position meta to the position of attack (σ_m = 0.37)[11]. The values for **4.2** in Table 4.21 may also be compared with those for corresponding reactions of 1,3,5-trinitrobenzene (TNB). Data for the latter reactions are given in Table 1.1. Values of the ratio K_5/K_1 are *ca* 180 for reactions with **4.7** and with **4.6**, and 4 for reaction with **4.5**. TNB is more sterically demanding than **4.2**, since addition must occur ortho to two nitro groups. A possible explanation for the higher values of the ratio K_5/K_1 for the bulkier nitroalkanes is unfavourable steric interactions in the adducts from TNB.

Table 4.21 Equilibrium and kinetic data for nitrobenzofurazan derivatives **4.2**, **4.3** and **4.4** with **4.5**, **4.6** and **4.7** in methanol.

		4-Nitrobenzofurazan 4.2		
	$k_5/dm^3 mol^{-1} s^{-1}$	$k_5/10^{-3} s^{-1}$	$K_5/dm^3 mol^{-1}$	pK_a[a]
4.7	2.5	3.3	750	13.5
4.6	80	1.2	6.7×10^4	14.2
4.5	300	1.0	3.0×10^5	15.6
		7-Chloro-4-nitrobenzofurazan 4.3		
4.7	10.8	5.0	2200	13.5
4.6	400	/	/	14.2
4.5	1500	/	/	15.6
		7-Methoxy-4-nitrobenzofurazan 4.4		
4.7	1.4	13.0	108	13.5
4.6	29	2.1	1.4×10^4	14.2
4.5	90	2.5	3.6×10^4	15.6

a. pK_a values of nitroalkanes in methanol from reference 8.

4.4.7 Slow Reaction; Elimination

In agreement with the NMR results in DMSO the reaction in methanol showed a slow process, compatible with elimination of nitrous acid as shown in Scheme 4.8.

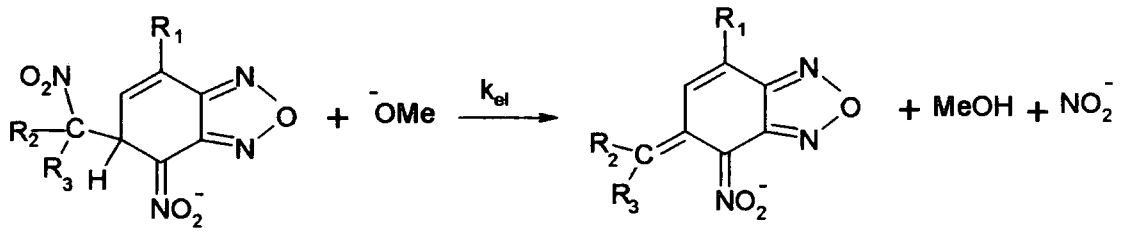

Scheme 4.8

The absorption maximum shifts from *ca* 340 nm for adducts to *ca* 360-380 nm for the elimination products. A spectrum is shown in Figure 4.7. The shift to longer wavelength is consistent with the extended conjugation in the elimination products.

Kinetic measurements for **4.2** were made at 380 nm and gave good correspondence with a first order rate process. Values for reactions involving **4.6** are in Table 4.22.

Table 4.22 Data for **4.2** (1×10^{-4} mol dm^{-3}) with **4.6** and sodium methoxide in methanol.

[4.6]/ mol dm^{-3}	[NaOMe]/ mol dm^{-3}	$[MeO^-]^a_{eq}/10^{-3}$ mol dm^{-3}	$[CH_3CHNO_2^-]^a_{eq}$/ mol dm^{-3}	k_{slow}/ s^{-1}	$k_{slow}/[MeO^-]_{eq}$/ $dm^3\ mol^{-1}\ s^{-1}$
0.050	0.02	1.3	0.02	0.0020	1.6
0.083	0.02	0.6	0.02	0.00080	1.3
0.117	0.02	0.4	0.02	0.00060	1.5
0.167	0.02	0.3	0.02	0.00040	1.6

a. Calculated from equation with a value for K_1 of 500 $dm^3\ mol^{-1}$.

The results show that the value of k_{slow} varies linearly with the equilibrium concentration of methoxide. The concentration of **4.6** anion is sufficiently high to ensure that conversion of **4.2** to the 5-adduct is very nearly complete.

Under this condition equation 4.13 will apply .

$$k_{slow} = k_{el}[MeO^-] \qquad \textbf{(4.13)}$$

Hence the data in Table 4.22 allow the determination of a value for k_{el} of 1.6 $dm^3\ mol^{-1}\ s^{-1}$. It was also noted that there is a very much slower reaction leading to a further increase in absorbance at 380 nm. This process was too slow for convenient measurement. It is known from the NMR results that in one of the two possible diastereoisomers of the 5-adduct elimination occurs very much more rapidly than the other. So these two process may represent the two elimination reactions which occur on different time scales.

Results for the slow reactions with **4.5** anion are in Table 4.23. Measurements here were made at 370 nm. The values lead to $k_{el} = 3.5\ dm^3\ mol^{-1}\ s^{-1}$.

Spectra for **4.3** (1×10^{-4} mol dm^{-3}) in the presence of **4.6** (1.5×10^{-2} mol dm^{-3}) and methoxide (3×10^{-3} mol dm^{-3}) are shown in Figure 4.10. There is an initial rapid increase in absorbance at 340 nm followed by a slower shift to give the elimination product with $\lambda_{max} = 380$ nm. Kinetic data for the slow process which was fast enough to measure on the stopped-flow spectrophotometer are given in Table 4.24. They lead to a value for k_{el} of 12 $dm^3\ mol^{-1}\ s^{-1}$.

Table 4.23 Data for **4.2** (1×10^{-4} mol dm^{-3}) with **4.5** and sodium methoxide in methanol.

[4.5]/ mol dm^{-3}	[NaOMe]/ mol dm^{-3}	$[MeO^-]^a_{eq}/10^{-4}$ mol dm^{-3}	$[CH_2NO_2^-]^a_{eq}/10^{-3}$ mol dm^{-3}	$k_{slow}/10^{-4}$ s^{-1}	$k_{slow}/[MeO^-]_{eq}$/ $dm^3\ mol^{-1}\ s^{-1}$
0.67	0.0011	0.7	1.0	2.6	3.6
0.67	0.0022	1.4	2.0	4.8	3.4
0.95	0.0011	0.5	1.0	1.9	3.8
0.90	0.0020	1.0	1.9	3.8	3.8
0.90	0.0030	1.5	2.8	4.8	3.2

a. Calculated from equation with a value for K_1 of 21 $dm^3\ mol^{-1}$.

Figure 4.10 UV/visible spectra plots for the reaction of **4.3** (1×10^{-4} mol dm^{-3}) with **4.6** (1.5×10^{-2} mol dm^{-3}) and sodium methoxide (3×10^{-3} mol dm^{-3}) in methanol.

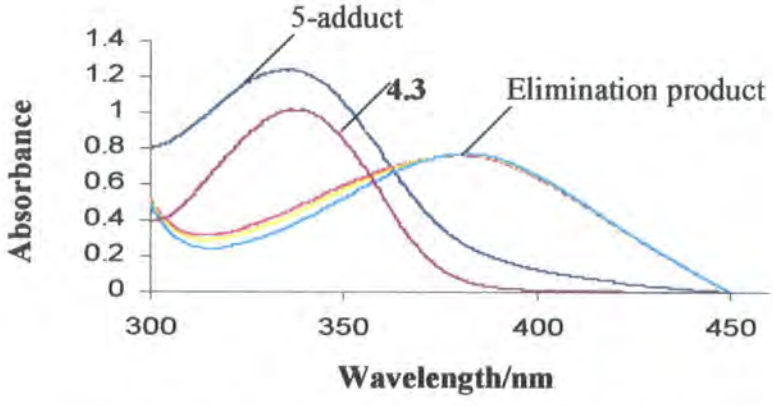

Table 4.24 Data for **4.3** (1×10^{-4} mol dm^{-3}) with **4.6** and sodium methoxide in methanol.

[4.6]/ mol dm^{-3}	[NaOMe]/ mol dm^{-3}	$[MeO^-]^a_{eq}/10^{-4}$ mol dm^{-3}	$[CH_3CHNO_2^-]^a_{eq}/10^{-3}$ mol dm^{-3}	k_{slow}/ s^{-1}	$k_{slow}/[MeO^-]_{eq}$/ $dm^3\ mol^{-1}\ s^{-1}$
0.10	0.005	1.0	4.9	0.0012	12.0
0.05	0.005	2.0	4.8	0.0021	10.3
0.05	0.004	1.6	3.8	0.0018	11.3
0.05	0.003	1.2	2.9	0.0015	12.5
0.05	0.002	0.8	1.9	0.0012	15.0

a. Calculated from equation with a value for K_1 of 500 $dm^3\ mol^{-1}$.

Interestingly acidification with aqueous hydrochloric acid of the solution containing the elimination product resulted in little change in the UV/visible spectrum. This may indicate that protonation occurs at the NO_2^- group rather than at carbon.

Reaction of **4.3** with **4.5** again indicated that elimination was occurring, although kinetic measurements were not made. With **4.7** there was a very slow increase in absorbance at 380 nm and measurements were not attempted.

The UV spectra of **4.4** in the presence of carbanions did not indicate appreciable elimination after two hours.

Table 4.25 Summary of k_{el} values for 4-nitrobenzofurazan derivatives **4.2** and **4.3** with nitromethane **4.5** and nitroethane **4.6** in methanol.

	4.2+4.5	**4.2+4.6**	**4.3+4.6**
k_{el}/ $dm^3\ mol^{-1}\ s^{-1}$	3.3	1.6	12

Results are summarized in Table 4.25. The most likely mechanism for the elimination is an E2 process involving reaction of methoxide with the ring-hydrogen at the 5-position **4.20**. The faster elimination from the adduct with nitromethane than from the adduct with nitroethane is likely to be due to steric interactions. The steric factor might involve difficulty of approach of the methoxide base to the reaction centre or alternatively might be associated with greater steric interference from the ortho-nitro group in the elimination product when R_2 = H, R_3 = Me than when R_2 = R_3 = H.

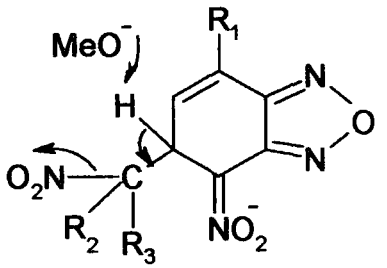

4.20

The faster elimination from the 7-chloro-derivative is likely to be due to the electronic effect of the meta chlorine atom which will help the attack by methoxide.

4.5 Conclusion

The ^1H NMR measurements in d_6-DMSO and the kinetic and equilibrium measurements in methanol complement each other. Despite the change in solvent the general behavior patterns are similar. In the case of 4-nitrobenzofurazan the results indicate that attack by the carbanion at the 5-position occurs rapidly. Isomerisation to the 7-adduct which is thermodynamically more stable is observed in the 2-nitropropane system. The results here parallel these observed with other nucleophiles[4,12,13] which have shown rapid reaction at the 5-position followed by re-arrangement to the more stable 7-isomer. This behavior may be explained[4] by the extent of charge delocolisation possible in the adducts. Comparison of the resonance forms shown in Scheme 4.9 indicates the possibility of greater delocalisation in the 7-adducts. This will result in their greater stability coupled with the higher kinetic barrier to their formation. Thus Bernasconi[14,15] has argued that an increase in charge delocalisation generally results in a higher kinetic barrier to reaction.

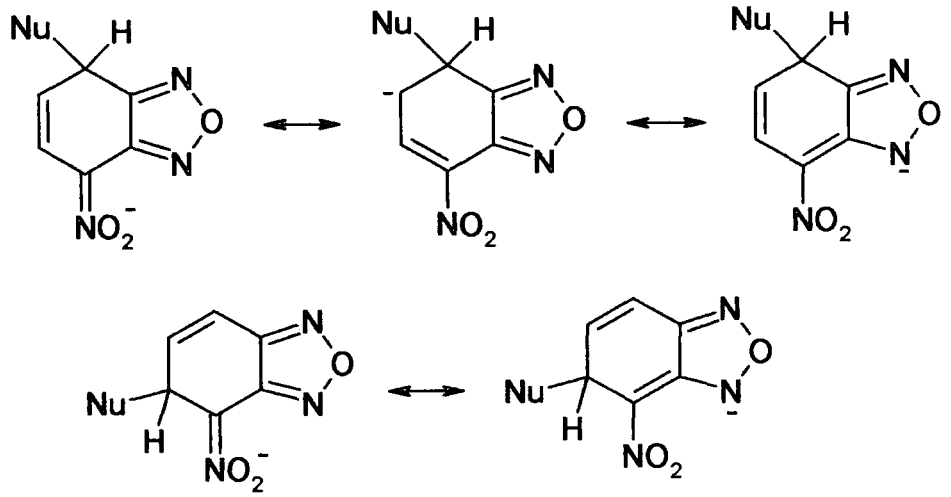

Scheme 4.9

The failure to observe isomerisation of the 5-adducts from nitromethane and nitroethane is likely to be due to the elimination of nitrous acid before re-arrangement can occur. The results show that the elimination process is base catalysed. In the case of the nitroethane adduct one of the possible diastereoisomer eliminates more rapidly than the other. The present results do not give information on the mechanism of the elimination. However results in the literature[16] for elimination of nitrous acid from the

adduct from 4,6-dinitrobenzofuroxan indicate a syn-process, so that this is likely in the present systems as well.

As previously reported in related systems by Terrier et al[3] acidification of the alkenes formed by the elimination process did not give a good yield of the neutral products of substitution of the hydrogen by the carbon species.

For 7-chloro-4-nitrobenzofurazan and 7-methoxy-4-nitrobenzofurazan addition of carbanions again occurred at the 5-position. There was no evidence for displacement of chloride or methoxide by the carbon nucleophiles, presumably due to steric factors, although some displacement of chloride by hydroxide produced from traces of water present in the solvent was observed.

4.6 References

[1] C. A. Fyfe, Can. J. Chem., 1968, **46**, 3047.

[2] M. R. Crampton, R. E. A. Lunn and D. Lucas, Org. Biomol. Chem., 2003, **1**, 3438.

[3] R. Goumont, E. Jan, M. Makosza and F. Terrier, Org. Biomol. Chem., 2003, **1**, 2192.

[4] M. R. Crampton, J. Delaney and L. C. Rabbitt, J. Chem. Soc., Perkin Trans. 2, 1999, 2473.

[5] F. Terrier, A.-P. Chatrousse and F. Millot, J. Org. Chem., 1980, **45**, 2666.

[6] C. H. Rochester and B. Rossall, , J. Chem. Soc., B, 1967, 743.

[7] C. H. Rochester, 'Acidity functions for concentrated solutions of bases', London, New York, 1970.

[8] J. P. L. Cox, M. R. Crampton and P. Wight, J. Chem. Soc., Perkin Trans. 2, 1988, 25.

[9] L. D. Nunno and S. Florio and P. E. Todesco, J. Chem. Soc., Perkin Trans. 2, 1975, 1469.

[10] C. F. Bernasconi, 'Relaxation Kinetics', Academic press, 1976.

[11] H. Maskill, 'Structure and Reactivity in Organic Chemistry', Oxford, New York, 1999.

[12] F. Terrier, F. Millot, A-P. Chatrousse, M-J. Pouet and M-P. Simonnin, Org. Mag. Res., 1976, **8**, 56.

[13] E. Buncel, N. Chuaqui-Qffermanns, B. K. Hunter and A. R. Norris, Can. J. Chem., 1977, **55**, 2852.

[14] C. F. Bernasconi, Pure Appl. Chem., 1982, 2335.

[15] C. F. Bernasconi, Adv. Phys. Org. Chem., 1992, **27**, 119.

[16] F. Terrier, J. Lelievre, A. P. Chatrousse, T. Boubaker, B. Bachet and A. Cousson, J. Chem. Soc., Perkin Trans. 2, 1992, 361.

Chapter Five:

Reaction of 4-Nitrobenzofurazan Derivative and 4-Nitrobenzofuroxan with Carbanions Benzyl Triflones

Chapter Five: Reaction of 4-Nitrobenzofurazan Derivative and 4-Nitrobenzofuroxan with Carbanions Benzyl Triflones

5.1 Introduction

As noted in chapter 1 (section 1.2.5) the strong electron withdrawing effect of the trifluoromethylsulfonyl group is well known[1,2,3], and there is current interest in the acidifying effect of SO_2CF_3 groups on carbon acids[4,5]. However there have been no previous studies of the reactions of carbanions stabilized by SO_2CF_3 groups with aromatic nitro compounds to form σ-adducts. In the present chapter the possible reactions of carbanions derived from benzyl triflones with 1,3,5-trinitrobenzene (TNB), dinitrobenzofuroxan (DNBF) and some nitrobenzofurazan derivatives are examined. Kinetic and equilibrium measurements were made in methanol to allow comparison with the results for the reactions of the nitroalkane anions. Since the pK_a values of the benzyl triflones in this solvent are not known it was necessary to measure them. The benzyl triflones used were **5.1**, **5.2** and **5.3**.

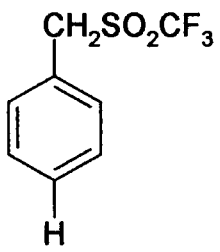

5.1

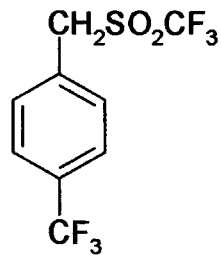

5.2

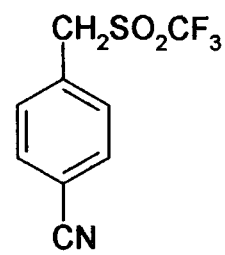

5.3

5.1.1 Synthesis of Benzyl Triflones

The preparation of alkyl triflones has been previously reported[4,6,7] in the literature. A convenient method for the formation of benzyl triflones was found to be by reaction of potassium triflinate with benzyl bromides in boiling acetonitrile.

Potassium triflinate was formed by reaction of trifluoromethanesulfonylchloride with potassium iodide in acetone, equation 5.1. The potassium triflinate formed was reacted for six hours with benzyl bromide in boiling acetonitrile in the presence of iodide ion as catalyst, equation 5.2. Good yields of benzyl triflones were obtained. Information is in Table 5.1.

$$CF_3SO_2Cl + KI \xrightarrow{\text{Acetone}} KSO_2CF_3 + ICl \qquad (5.1)$$

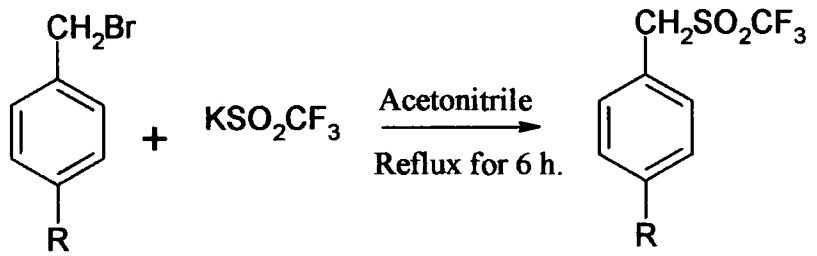

(5.2)

R=H, CF_3, CN.

Table 5.1 Data for benzyl triflones **5.1**, **5.2** and **5.3**.

R	% yield	M.p	NMR
H, 5.1	88	100°	δ 7.47 (C_6H_6) δ 5.25 (CH_2)
CF_3, 5.2	86.5	102°	δ 7.86, $J_{2,3}$ = 8.2 Hz δ 7.72, $J_{5,6}$ = 8.2 Hz δ 5.45 (CH_2)
CN, 5.3	93	119°	δ 8.02, $J_{2,3}$ = 8 Hz δ 7.75, $J_{5,6}$ = 8 Hz δ 5.52 (CH_2)

Preparation of alkyl triflones such as n-butyl triflone by this method was unsuccessful even after refluxing for several days.

5.2 Determination of pK_a Value

It was found that the benzyl triflones **5.1**, **5.2**, **5.3**, showed UV absorbance at *ca* 270 nm in methanol. In the presence of methoxide a strong absorbance was observed with maximum at 290 nm for benzyl triflone **5.1**, 315 nm for 4-trifluoromethylbenzyl triflone **5.2** and 340 nm for 4-cyanomethylbenzyl triflone **5.3**.

This corresponds to ionization to give the carbanions as shown in Scheme 5.1 and the equilibrium constant is given in equation 5.3.

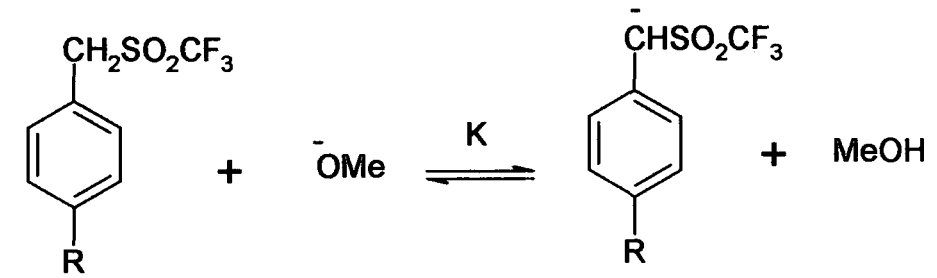

R=H, CF_3, CN.

Scheme 5.1

$$K = \frac{[CHSO_2CF_3^-]}{[MeO^-][CH_2SO_2CF_3]} \qquad (5.3)$$

The acid dissociation constant, K_a, relating to the ionization shown in Scheme 5.2 is related to K and K_m, the autoprotolysis constant of methanol, by equation 5.5.

The value of pK_m is known to be 16.92[8].

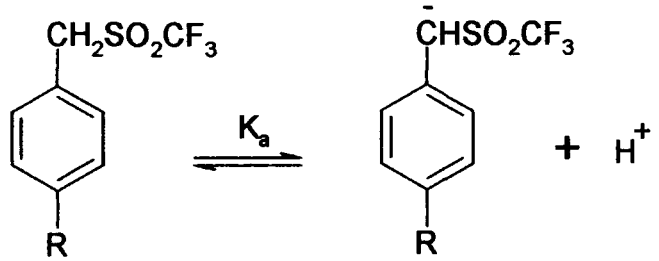

Scheme 5.2

$$MeOH \overset{K_m}{\rightleftharpoons} MeO^- + H^+ \quad (5.4)$$

$$K_a = KK_m \quad (5.5)$$

$$pK_a = pK + pK_m \quad (5.6)$$

In the case of **5.3**, the 4-cyano derivative, ionization could be achieved using solutions of sodium methoxide in methanol. Absorbance measurements are reported in Table 5.2. Since methoxide concentrations up to 0.5 mol dm^{-3} were used, there is deviation from ideal behavior and the basicities can be represented by an acidity function. Both H_M and J_M values are reported in the literature[8] where H_M is related to proton loss and J_M to methoxide addition.

The acid dissociation constant K_a is defined in terms of activities, a, by equation 5.7. Since in concentrated solutions activity coefficients must be included this leads to equation 5.8 and to equation 5.9.

$$K_a = \frac{a_{RC^-}}{a_{RCH}} a_{H^+} \quad (5.7)$$

$$K_a = \frac{[RC^-]}{[RCH]} a_{H^+} \frac{\gamma_{RC^-}}{\gamma_{RCH}} \quad (5.8)$$

$$\log K_a = \log\left(\frac{[RC^-]}{[RCH]}\right) + \log\left(a_{H^+} \frac{\gamma_{RC^-}}{\gamma_{RCH}}\right)$$

$$pK_a = H_M - \log\left(\frac{[RC^-]}{[RCH]}\right) \quad (5.9)$$

Where:

$$H_M = -\log\left(a_{H^+} \frac{\gamma_{RC^-}}{\gamma_{RCH}}\right)$$

The absorbance values in Table 5.2 allow the calculation of values of the ratio $[RC^-]/[RCH]$ and hence, using equation 5.9, to pK_a values.

In the case of **5.1** and **5.2** it was not possible to obtain high conversions into the respective carbanions using methanol alone. Here the basicity of the solution was increased by using methanol-DMSO mixtures. The sodium methoxide concentration was kept constant at 0.025 mol dm^{-3} and the ratio of DMSO to methanol was varied.

The UV spectra obtained for solutions of **5.2** in these media are shown in Figure 5.1. Absorbance data are in Table 5.3. Both H_M and J_M values have been reported[8] for solutions of methoxide in MeOH-DMSO mixtures. The H_M values reported in the literature were measured using amine indicators, while the J_M values were obtained from the reaction, shown in Scheme 5.3, of methoxide ion with α-cyanostilbenes[9]. The latter reaction involves formation of a carbanion which resembles those formed by ionization of the benzyl triflones. Hence these results were used to reflect the basicities of the methanol-DMSO mixtures used in the present work. Values of pK_a were calculated from equation 5.10 and gave a value of 17.5±0.1.

Figure 5.1 UV/visible spectra of **5.2** (4.17×10^{-5} mol dm^{-3}) in solutions containing NaOMe (0.025 mol dm^{-3}) in MeOH-DMSO mixtures corresponding to conditions given in Table 5.3.

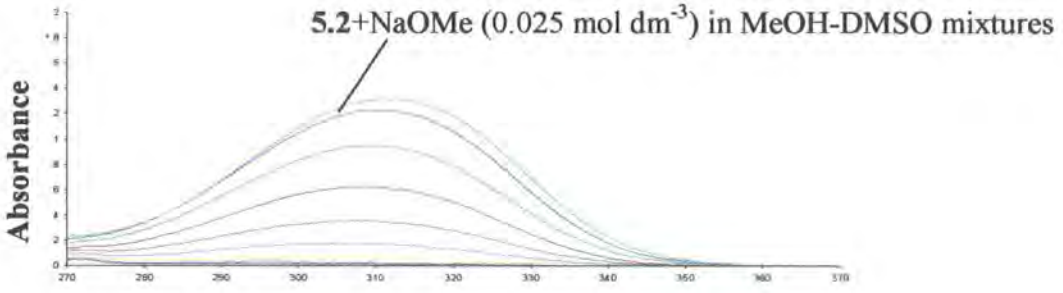

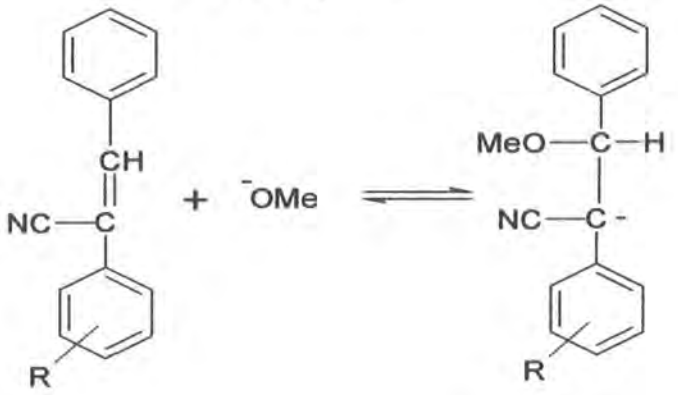

Scheme 5.3

$$pK_a = J_M - \log\frac{[RC^-]}{[RCH]} \qquad (5.10)$$

The lower acidity of **5.1** required the use of solution containing higher proportions of DMSO but the same approach was used as for **5.2**. Absorbance values at 290 nm and the calculated pK_a values are in Table 5.4. The results lead to pK_a=19.5±0.2.

As expected the pK_a values for the benzyl triflones decrease, showing increasing acidity, as the ring substituent is more electron-withdrawing.

Table 5.2 Determination of pK_a value for **5.3** in methanol.

$[MeO^-]$/mol dm^{-3}	Absorbance at 340 nm	H_M[a]	pK_a[b]
0.0167	0.204	15.15	16.04
0.0333	0.384	15.46	16.03
0.0500	0.548	15.66	16.02
0.0833	0.724	15.90	16.07
0.1170	0.953	16.09	16.04
0.1670	1.135	16.32	16.09
0.2500	1.373	16.45	15.94
0.3333	1.493	16.58	15.89

a. H_M values from reference 8.

b. pK_a values calculated from equation 5.9.

Where $\frac{[CHSO_2CF_3^-]}{[CH_2SO_2CF_3]} = \frac{Abs}{1.8 - Abs}$.

The limiting absorbance of high $[MeO^-]$ is 1.8.

Table 5.3 Absorbance values at 315 nm for solutions containing **5.2** (4.17×10^{-5} mol dm^{-3}), sodium methoxide (0.025 mol dm^{-3}) in various MeOH-DMSO mixtures and calculated pK_a values.

Vol. %DMSO	Mol. %DMSO	Absorbance	J_M[a]	pK_a[b]
0	0	0.012	15.32	/
6.66	3.91	0.025	15.70	17.41
13.33	8.07	0.052	16.10	17.48
20.00	12.48	0.159	16.60	17.45
26.67	17.18	0.327	17.10	17.57
33.33	22.19	0.585	17.59	17.51
40.00	27.55	0.902	18.00	/
50.00	36.32	1.191	18.72	/
66.70	53.30	1.297	20.19	/

a. J_M values from reference 9.

b. pK_a values calculated from equation 5.10.

Where $\frac{[RC^-]}{[RCH]} = \frac{Abs}{1.3 - Abs}$.

Table 5.4 Absorbance values at 290 nm for solutions containing **5.1** (6.67×10^{-5} mol dm^{-3}), sodium methoxide (0.025 mol dm^{-3}) in various MeOH-DMSO mixtures and calculated pK_a values.

Vol. %DMSO	Mol. %DMSO	Absorbance	J_M[a]	pK_a[b]
33.33	22.19	0.0156	17.54	19.60
40.00	27.55	0.0292	18.06	(19.80)
46.70	33.30	0.114	18.52	19.69
53.30	39.40	0.520	18.99	19.38
53.30	39.40	0.540	18.99	19.33
60.00	46.10	1.160	19.59	19.34
66.70	53.30	1.590	20.19	/
73.30	61.0	1.790	20.88	/
78.30	67.3	1.760	21.42	/

a. J_M values from reference 9.

b. pK_a values calculated from equation 5.10.

Where $\frac{[RC^-]}{[RCH]} = \frac{Abs}{1.8 - Abs}$.

5.3 Spectroscopic Studies

The reactions of the benzyl triflones with 4,6-dinitrobenzofuroxan **5.4**, 1,3,5-trinitrobenzene **5.5**, and several benzofurazan derivatives were examined spectroscopically.

5.3.1 4,6-Dinitrobenzofuroxan

The spectrum in d_6-DMSO of **5.4** (0.1 mol dm^{-3}) and 4-trifluoromethylbenzyl triflone **5.2** (0.025 mol dm^{-3}) initially showed bands due to the parent molecules together with small bands at δ5.8 and 8.6 which can be attributed[1] to the hydroxyl adduct **5.6**, formed from reaction with trace of water present in the solvent. Gradually with time new bands developed until after six days little unreacted benzyl triflone remained.

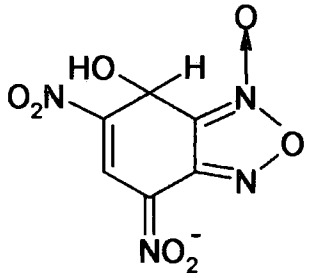

5.6

Two sets of bands were observed due to the two diastereoisomeric forms of the adduct **5.7**. This is shown in Scheme 5.4 and NMR results are in Table 5.5. It is interesting that reaction occurs even in the absence of an added base. This results from the very highly electrophilic nature of **5.4**. Reactions in neutral solution with a variety of carbon acids have previously been reported in the literature[10].

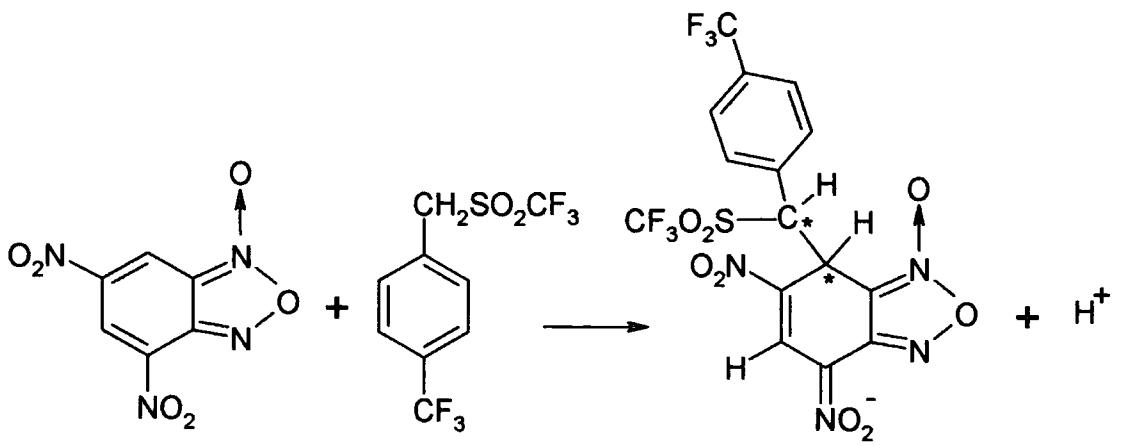

5.4 **5.2** **5.7**

Scheme 5.4

Table 5.5 ^{1}H NMR data for parent molecules and adduct **5.7** in d_6-DMSO.

	δ H_7	δ H_5	J_{57}[a]	δ CH	J_{CH-7}[a]	δ $H_{2,6}$	δ $H_{3,5}$	$J_{2,3}$[a]
5.4	9.26	8.95	2.0	/	/	/	/	/
5.2	/	/	/	5.45	/	7.75	7.86	8.0
5.7(a)	5.40	8.36	<1.0	5.65	2.0	7.49	7.73	8.0
5.7(b)	5.28	8.39	<1.0	5.57	1.6	7.53	7.78	8.0

a. J values in Hz.

In the presence of triethylamine spectra of **5.4** and **5.2** show the immediate formation of **5.7**. A representative spectrum is shown in Figure 5.2. Integration of peak intensities shows that the diastereoisomers **a** and **b** are present in the ratio 1.4:1.

Figure 5.2 ^{1}H NMR spectrum of **5.4** (0.1 mol dm^{-3}) with **5.2** (0.05 mol dm^{-3}) in the presence of triethylamine (0.1 mol dm^{-3}) in d_6-DMSO.

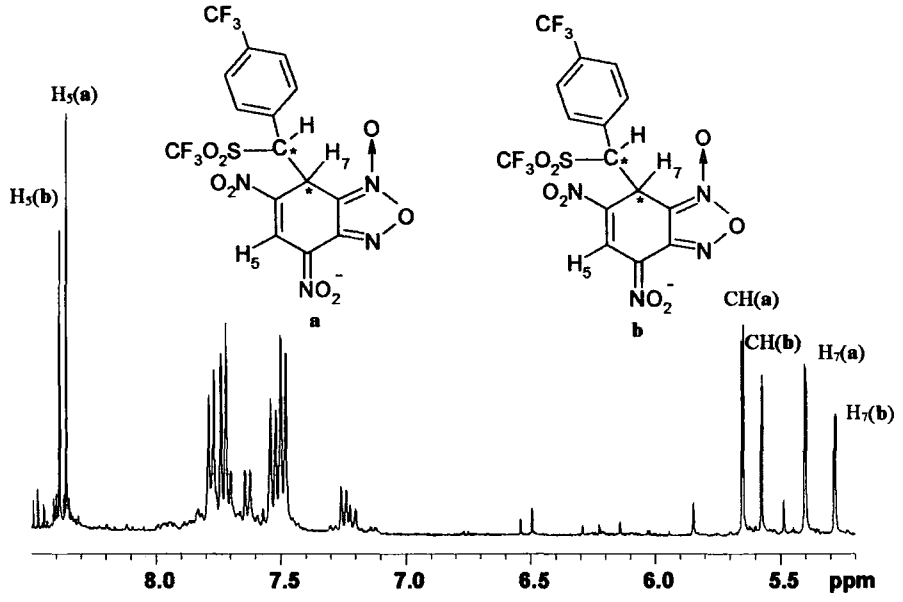

UV/visible measurements of very dilute solutions of **5.4** (1×10^{-4} mol dm^{-3}) in DMSO showed a strong band at 470 nm attributed to the hydroxy-adduct **5.6**.

Addition of benzyl triflone caused a gradual increase in intensity with the maximum shifting to 480 nm which is likely to be due to slow formation of **5.7**.

5.3.2 1,3,5-Trinitrobenzene (TNB)

The ^{1}H NMR spectrum of TNB **5.5**, in d_6-DMSO containing **5.2** and triethylamine showed only the presence of bands due to parent molecules.

The UV/visible spectrum of a solution diluted with DMSO showed very weak bands at 475 and 560 nm but there is no evidence for strong interaction.

The UV/visible spectra of **5.5** with **5.2** and sodium methoxide in methanol showed only bands for the methoxide adduct. In order to increase the concentration of

the carbanion (pK_a for **5.2** is 17.5) measurements were then made in methanol-DMSO mixtures.

The UV/visible spectrum of **5.5** (5×10^{-5} mol dm^{-3}) with **5.2** (5×10^{-3} mol dm^{-3}) and sodium methoxide (1×10^{-3} mol dm^{-3}) was recorded using methanol-DMSO 60/40 (v/v) as solvent. Strong absorbance with maxima at 427 and 570 nm is observed but this results from the direct reaction with methoxide to give the adduct **5.8**. The spectra were similar to that obtained in the absence of benzyl triflone. No change in spectral shape was found after 24 hours.

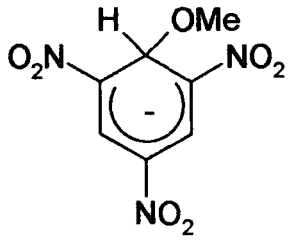

5.8

The failure to observe reaction of TNB with the benzyl triflone may be the result of unfavorable steric interactions in the potential adduct. **5.5** differs from DNBF and the benzofurazan in that addition can occur only at a ring-carbon between two nitro-groups.

5.3.3 Nitrobenzofurazan Derivatives

^{1}H NMR measurements were made with **5.2** mixed with 4-nitrobenzofurazan **5.9**, 4-nitrobenzofuroxan **5.10**, or 7-chloro-4-nitrobenzofurazan **5.11**, in the presence of triethylamine in d_6-DMSO. The spectra with **5.9** and with **5.10** measured within fifteen minutes of mixing showed bands attributable to the products of elimination of HSO_2CF_3 from initially formed σ-adducts. The spectrum of **5.9** (0.04 mol dm^{-3}) with **5.2** (0.05 mol dm^{-3}) and triethylamine (0.1 mol dm^{-3}) is shown in Figure 5.3. Bands for the elimination product **5.13** are observed at δ6.44 (H_6), 7.30 (H_7) and 7.08 (H_8). It is interesting that long-range spin-coupling is observed between H_8 with H_6 and with H_7. The spectrum is unchanged after 2 hours showing that the product is stable in these conditions. In a similar way the spectrum of **5.10** (0.13 mol dm^{-3}) with **5.2** (0.14

mol dm^{-3}) in the presence of triethylamine (0.3 mol dm^{-3}) in d_6-DMSO gave bands indicating the formation of the corresponding elimination product (Scheme 5.5).

Chemical shifts are collected in Table 5.6. Similar measurements with **5.11** were less successful and the spectra showed a large number of bands which could not be readily assigned.

Figure 5.3 ^{1}H NMR spectrum of **5.9** (0.04 mol dm^{-3}) with **5.2** (0.05 mol dm^{-3}) and triethylamine (0.1 mol dm^{-3}) in d_6-DMSO.

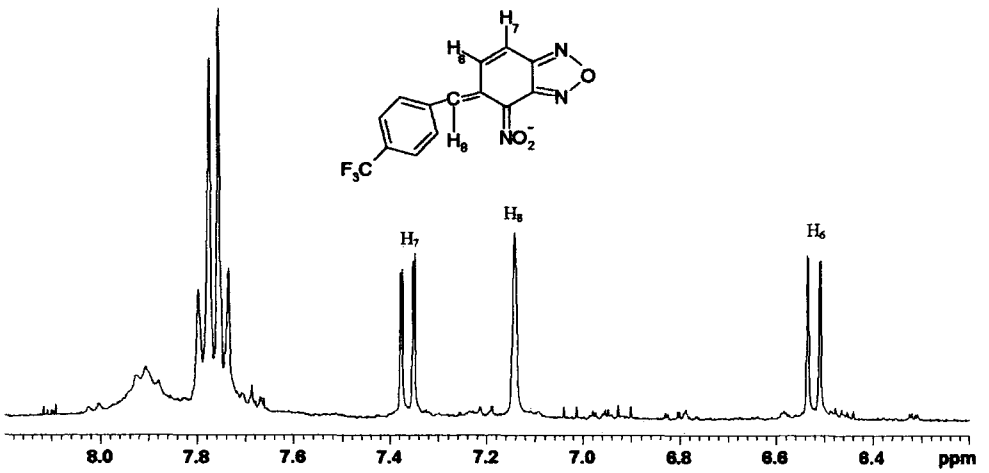

It seems likely that the initial reaction of the nitrobenzofurazan derivative under these condition will yield the σ-adducts **5.12** but here elimination to give the alkene derivatives occurs rapidly.

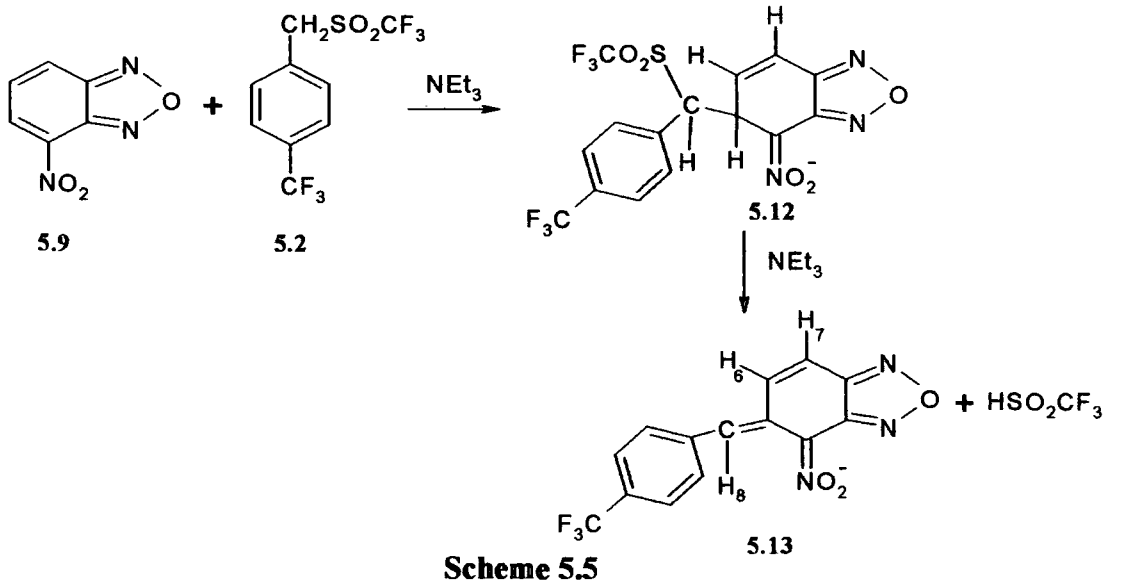

5.9 **5.2** **5.12** **5.13**

Scheme 5.5

Table 5.6 ^{1}H NMR data for elimination products **5.13** formed from **5.9** and **5.10** in d_6-DMSO.

Parent	δ H_6	δ H_7	δ H_8	$J_{6,7}$[a]	$J_{6,8}$[a]	$J_{7,8}$[a]	δ $H_{2,6}$	δ $H_{3,5}$	$J_{2,3}$[a]
5.9	6.44	7.30	7.08	10.4	0.8	1.2	7.70	7.73	8.8
5.10	6.30	7.20	7.44	10.2	0.8	1.2	7.65	7.70	8.0

a. J values in Hz.

UV/visible measurements were made with solutions in methanol of **5.9**, **5.10** and **5.11** (5×10^{-5}-1×10^{-4} mol dm^{-3}) in the presence of benzyl triflones (*ca* 1×10^{-2} mol dm^{-3}) and sodium methoxide (1-2×10^{-3} mol dm^{-3}). The presence of methoxide was necessary to generate the carbanions from the benzyl triflones. However because of the large values of the equilibrium constant for reactions of the benzofurazan derivatives with methoxide[11,12], the initial spectra are compatible with rapid formation of methoxide adducts. Thus the spectrum of **5.10** with benzyl triflone **5.1** and methoxide reported in Figure 5.4 shows initially a band with λ_{max} at 340 nm corresponding to the methoxide adduct. With time a new absorption band forms at 411 nm, which is attributed to the product formed by elimination of HSO_2CF_3 from the addition product of the benzyl triflone. The wavelength and high extinction coefficient, $\varepsilon = 3\times10^4$ dm^3 mol^{-1} cm^{-1}, for the species formed are not compatible with those expected for the σ-adduct. By analogy with the σ-adduct formed from the nitroalkane anions this would be expected to absorb at *ca* 340 nm. It is possible that the initial spectrum may contain some contribution from the carbanion σ-adduct.

Figure 5.4 UV/visible spectra of **5.10** (1×10^{-4} mol dm^{-3}) with **5.1** (1×10^{-2} mol dm^{-3}) in solution containing NaOMe (1×10^{-3} mol dm^{-3}) in MeOH.

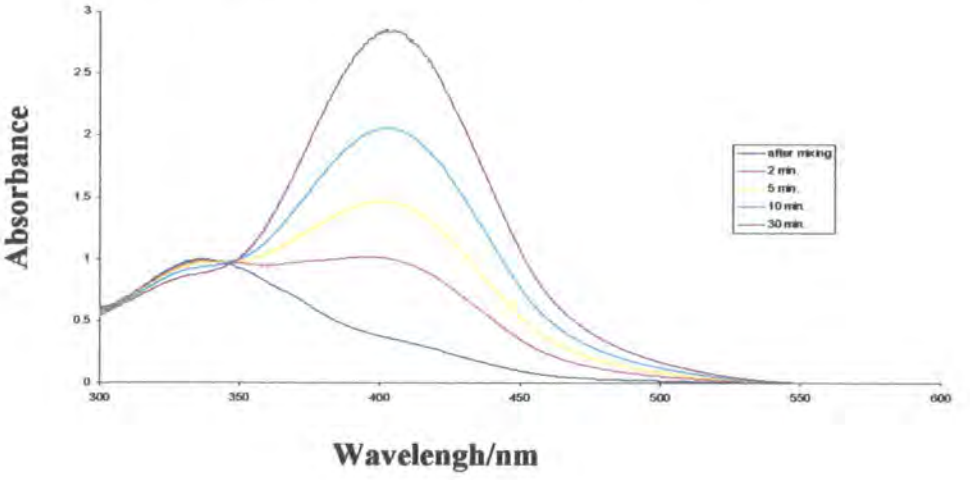

In the case of 7-chloro-4-nitrobenzofurazan **5.11** measurements were made in buffered solutions to allow measurements at very low methoxide concentrations. The spectrum of **5.11** alone shows a band at 337 nm, $\varepsilon = 1.05\times10^{4}$ dm^3 mol^{-1} cm^{-1}. In the buffered solution with methoxide (2.6×10^{-5} mol dm^{-3}) and **5.2** (0.01 mol dm^{-3}) the initial maximum is un changed, but slowly a new band forms at 405 nm, with an excellent isosbestic point at 360 nm. The UV/visible results are summarized in Table 5.7.

Table 5.7 Data absorbance for **5.9**, **5.10** and **5.11**, with benzyl triflone, methoxide in methanol.

	Parent		Methoxide adduct		Final product	
	λ_{max}/ nm	$\varepsilon/10^3$ dm^3 mol^{-1} cm^{-1}	λ_{max}/ nm	$\varepsilon/10^4$ dm^3 mol^{-1} cm^{-1}	λ_{max}/ nm	$\varepsilon/10^4$ dm^3 mol^{-1} cm^{-1}
5.9	320	9.0	340	1.5	409	2.4
5.10	403	11.0	340	1.1	411	3.0
5.11	337	10.5	340	1.6	405	1.5

5.4 Kinetic Measurements

Measurements were made in methanol with **5.9**, **5.10** and **5.11** with each of the three benzyl triflones **5.1**, **5.2** and **5.3** in the presence of methoxide. Due to the high reactivity of the nitrobenzofuroxan with methoxide buffered solution were used for the kinetic measurements. Bromophenol buffers were prepared as described in section 4.4.1, and these allowed measurements in solutions where $[MeO^-]_{eq}\leq5\times10^{-5}$ mol dm^{-3}.

At these low methoxide concentration there is very little interference from their reactions with the benzofurazan. Hence the reaction may be represented by Scheme 5.6 (Page 145).

Kinetic measurements were made at λ_{max} value of the final products. The concentrations of the benzofurazan derivatives ($<1\times10^{-4}$ mol dm^{-3}) were much lower than those of the benzyl triflones and of the buffer components and under these conditions the reactions showed excellent first order behavior. Results for reactions of **5.9** are given in Table 5.8.

Table 5.8 Results for reactions of 4-nitrobenzofurazan **5.9**, with **5.1**, **5.2**, **5.3** and sodium methoxide in methanol containing the buffered solution.

$[MeO^-]_{eq}/10^{-5}$ mol dm^{-3}	[5.1]/ mol dm^{-3}	$[Carbanion]_{eq}/10^{-9}$ mol dm^{-3}	$k_{obs}/10^{-5}$ s^{-1}	$k_5^a/10^4$ $dm^3\ mol^{-1}\ s^{-1}$
5.5	0.053	6.93	9.5	1.4
5.5	0.033	4.35	8.0	1.8
2.6	0.053	3.31	6.1	1.8
$[MeO^-]_{eq}/10^{-5}$ mol dm^{-3}	[5.2]/ mol dm^{-3}	$[Carbanion]_{eq}/10^{-7}$ mol dm^{-3}	$k_{obs}/10^{-4}$ s^{-1}	$k_5^a/10^3$ $dm^3\ mol^{-1}\ s^{-1}$
5.5	0.012	1.50	7.5	5.0
5.5	0.007	0.96	4.9	5.1
2.6	0.012	0.72	3.6	5.0
$[MeO^-]_{eq}/10^{-5}$ mol dm^{-3}	$[5.3]/10^{-4}$ mol dm^{-3}	$[Carbanion]_{eq}/10^{-7}$ mol dm^{-3}	$k_{obs}/10^{-4}$ s^{-1}	$k_5^a/10^3$ $dm^3\ mol^{-1}\ s^{-1}$
5.5	5.7	2.60	3.5	1.3
5.5	3.3	1.52	2.3	1.5
2.6	5.7	1.23	1.9	1.5

a. Calculated as $k_{obs}/[Carbanion]_{eq}$.

The methoxide concentrations were calculated using equation 4.4 storchiametric concentrations were typically 0.04 mol dm^{-3} for bromophenol and 0.004 mol dm^{-3} for methoxide. For example in the first row of the Table 5.8.

$$[MeO^-]_{eq} = \frac{0.004}{0.036}\frac{1}{2040}$$

$$= 5.5\times10^{-5}\ \text{mol dm}^{-3}.$$

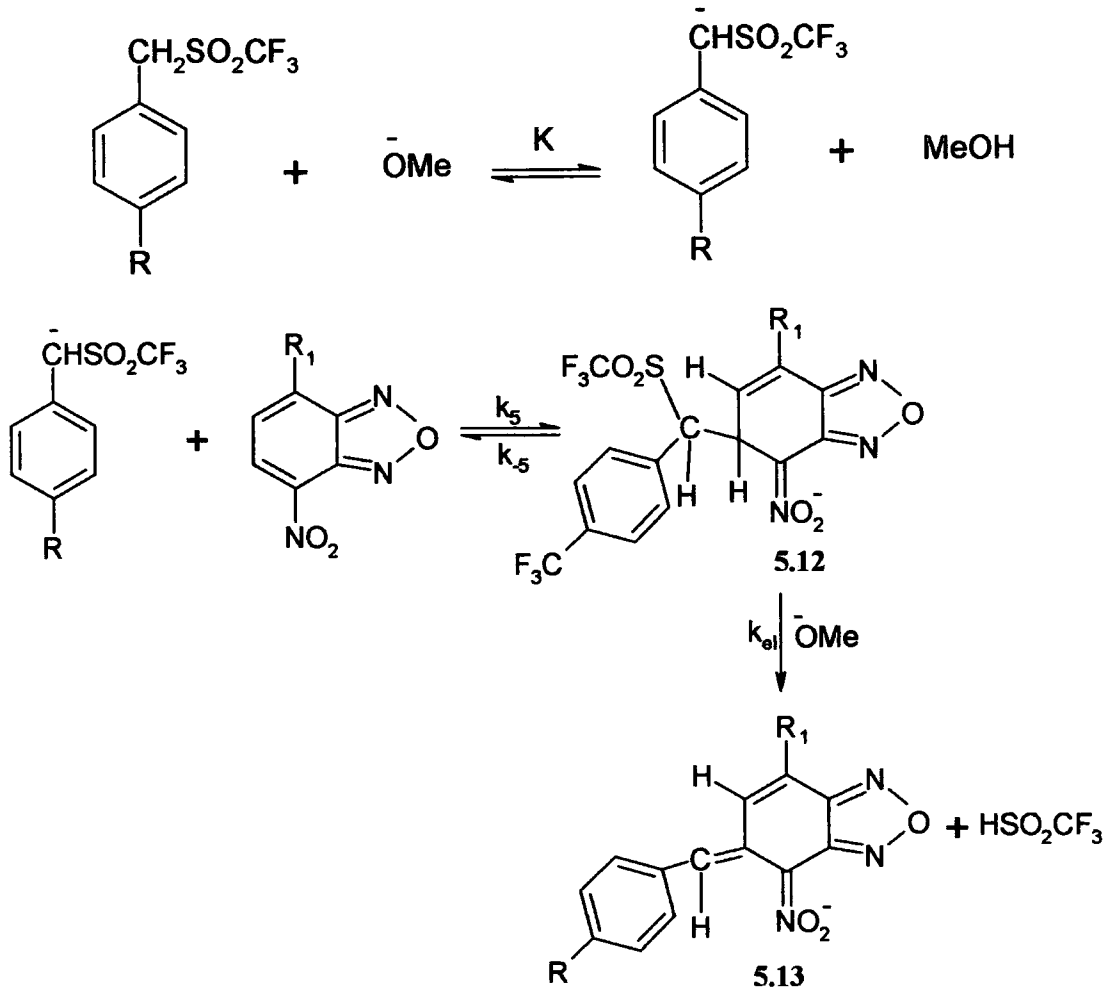

Scheme 5.6

Equilibrium concentrations of the carbanions were calculated using the pK_a values determined previously.

$$K = \frac{[CHSO_2CF_3^-]}{[CH_2SO_2CF_3][MeO^-]} = \frac{K_a}{K_m}$$

The results in the Table show that values of k_{obs} increase linearly with the carbanion concentrations. For each of benzyl triflones the value obtained by dividing k_{obs} by [carbanion] was constant. The general expression for equilibration of benzofurazan and carbanion to give adduct **5.12** is equation 5.9.

$$k_{obs} = k_5[CHSO_2CF_3^-] + k_{-5} \qquad \textbf{(5.9)}$$

The results indicate that values of k_{-5} are too low to measure, so that the measurements give values of k_5. In confirmation of this it was found that the amplitudes of the absorbance changes did not depend on the carbanion concentrations, showing that the reactions went to completion.

There is no spectroscopic evidence for a build-up in concentration of σ-adduct **5.12**. It should be noted that if the elimination step was rate determining then values of k_{obs} would be expected to show dependences on both carbanion concentration and methoxide concentration .

Thus:

$$\text{Velocity} = k_{el}[\mathbf{5.12}][MeO^-]$$

$$K_5 = \frac{[\mathbf{5.12}]}{[\text{Carbanion}][\text{Benzofurazan}]}$$

Hence:

$$\text{Velocity} = k_{el}K_5[\text{Carbanion}][MeO^-][\text{Benzofurazan}]$$

$$\text{Velocity} = k_{obs}[\text{Benzofurazan}]$$

Then:

$$k_{obs} = k_{el}K_5[\text{Carbanion}][MeO^-]$$

The results show that this is not the case. Thus dividing k_{obs} by both [carbanion] and [MeO^-] does not give constant values.

First order dependence on benzofurazan concentration is observed and this shows that formation of the carbanion from the benzyl triflone and methoxide is not rate determining. If this were the case then a zero-order dependence on benzofurazan would be expected.

$$\text{Velocity} = k[\text{Benzyl triflone}][MeO^-]$$

Data for reaction of **5.10** are in Table 5.9. For **5.11** measurements were made only with **5.2** and results are in Table 5.10.

Table 5.9 Results for reactions of 4-nitrobenzofuroxan **5.10**, with **5.1**, **5.2**, **5.3** and sodium methoxide in methanol containing the buffered solution.

$[MeO^-]_{eq}/10^{-5}$ mol dm^{-3}	[5.1]/ mol dm^{-3}	$[Carbanion]_{eq}/10^{-9}$ mol dm^{-3}	$k_{obs}/10^{-3}$ s^{-1}	$k_5^a/10^5$ $dm^3mol^{-1}s^{-1}$
2.6	0.053	3.12	1.47	4.70
2.6	0.033	2.08	0.85	4.10
1.7	0.053	2.08	0.81	3.90
$[MeO^-]_{eq}/10^{-5}$ mol dm^{-3}	[5.2]/ mol dm^{-3}	$[Carbanion]_{eq}/10^{-8}$ mol dm^{-3}	$k_{obs}/10^{-3}$ s^{-1}	$k_5^a/10^4$ $dm^3mol^{-1}s^{-1}$
2.6	0.012	7.23	5.1	7.10
2.6	0.007	4.73	3.6	7.70
1.7	0.012	4.73	3.3	6.95
$[MeO^-]_{eq}/10^{-5}$ mol dm^{-3}	$[5.3]/10^{-4}$ mol dm^{-3}	$[Carbanion]_{eq}/10^{-7}$ mol dm^{-3}	$k_{obs}/10^{-3}$ s^{-1}	$k_5^a/10^4$ $dm^3mol^{-1}s^{-1}$
2.6	5.7	1.23	1.99	1.62
2.6	3.3	0.72	1.18	1.64
1.7	5.7	0.80	1.15	1.43

a. Calculated as $k_{obs}/[Carbanion]_{eq}$.

Table 5.10 Results for reactions of 7-chloro-4-nitrobenzofurazan **5.11**, with **5.2** and sodium methoxide in methanol containing the buffered solution.

$[MeO^-]_{eq}/10^{-5}$ mol dm^{-3}	[5.2]/ mol dm^{-3}	$[Carbanion]_{eq}/10^{-8}$ mol dm^{-3}	$k_{obs}/10^{-3}$ s^{-1}	$k_5^a/10^4$ $dm^3mol^{-1}s^{-1}$
2.6	0.012	7.23	1.23	1.70
2.6	0.007	4.5	0.60	1.30
5.4	0.005	6.6	1.12	1.67

a. Calculated as $k_{obs}/[Carbanion]_{eq}$.

5.5 Conclusion

Overall the spectroscopic and kinetic results indicate that formation of the 5-adducts, the k_5 step, is rate limiting and is followed by rapid elimination of HSO_2CF_3.

Values of k_5 are collected in Table 5.11.

Table 5.11 Summary of k_5 values in units of $dm^3\ mol^{-1}\ s^{-1}$ for **5.9**, **5.10** and **5.11** with benzyl triflones **5.1**, **5.2**, **5.3** in methanol.

	5.9	**5.10**	**5.11**	**pK_a**
5.1	1.8×10^4	4.2×10^5	/	19.5
5.2	5.0×10^3	7.3×10^4	1.4×10^4	17.5
5.3	1.4×10^3	1.6×10^4	/	16.0

For **5.2** the value of k_5 is higher for reaction of 7-chloro-4-nitrobenzofurazan **5.11**, than for 4-nitrobenzofurazan **5.9**. This can be attributed to electron-withdrawing effect of chlorine at a ring position meta to the point of the reaction. Values are higher for 4-nitrobenzofuroxan **5.10**, which is likely to result from the increased electrophilicity with the presence of the N-O group.

The values of k_5 decrease with increasing electron-withdrawal by the para-substituent in the benzyl triflones. The carbanions will be stabilized by the presence of CF_3 and CN groups. Although only three substituents were measured. It is worth drawing Hammett plots. Values of $\log_{10} k_5$ versus σ^- are shown in Figure 5.5 and give ρ values of -1.2 and -1.6 respectively for the benzofurazan and benzofuroxan derivative.

Figure 5.5 Hammett plots. Values of $\log_{10} k_5$ versus σ^- give ρ values of -1.2 and -1.6 respectively for **5.9** and **5.10**.

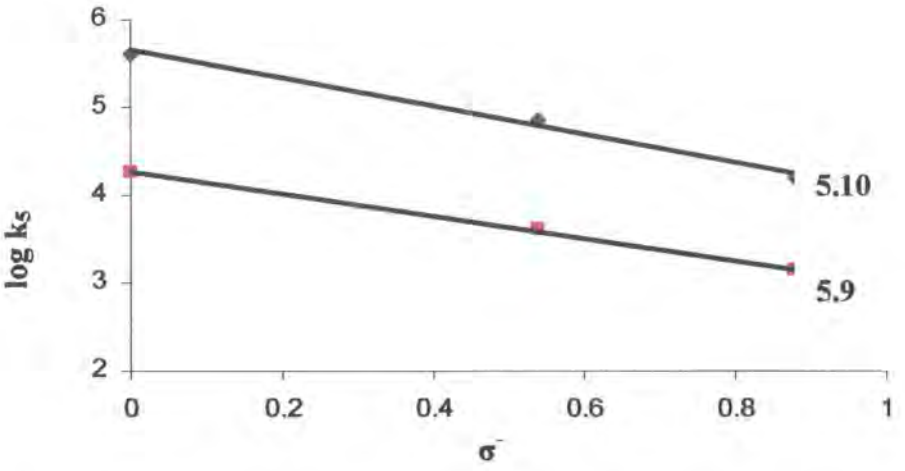

Brønsted plots of $\log_{10} k_5$ versus pK_a values of the benzyl triflones have slopes, β_{nuc}, of 0.3 and 0.4 for the benzofurazan and benzofuroxan respectively.

Figure 5.6 Brønsted plots of $\log_{10} k_5$ versus pK_a values of the benzyl triflones have slopes, β_{nuc}, of 0.3 and 0.4 for **5.9** and **5.10** respectively.

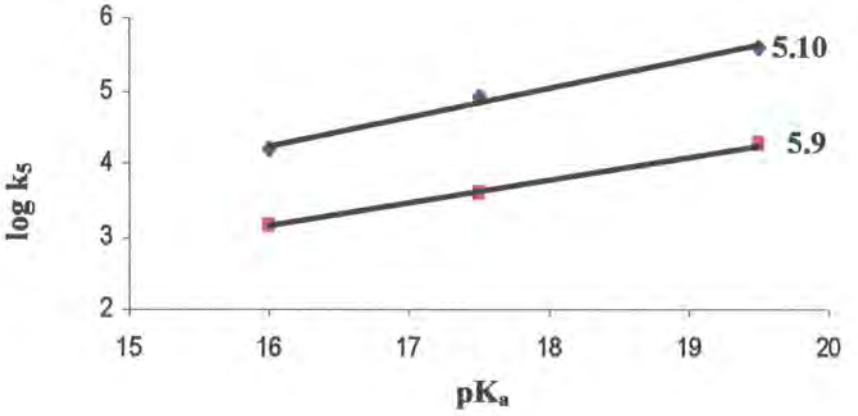

These relatively low values indicate quite a small transfer of negative charge from the carbanion to the benzofurazan in the transition state **5.14**.

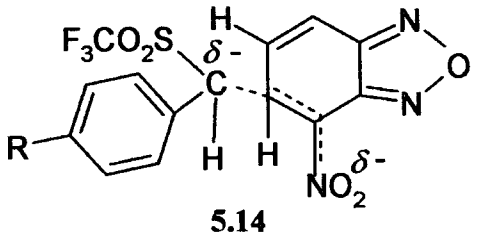

5.14

It is also worth noting that the values obtained for k_5 are considerably lower than those for the corresponding reactions of ring substituted benzyl cyanide anions with 4-nitrobenzofuroxan **5.10**. For example[13] the value of the rate constant for formation of **5.15** in methanol is 1.4×10^8 dm^3 mol^{-1} s^{-1} which is close to the diffusion limit.

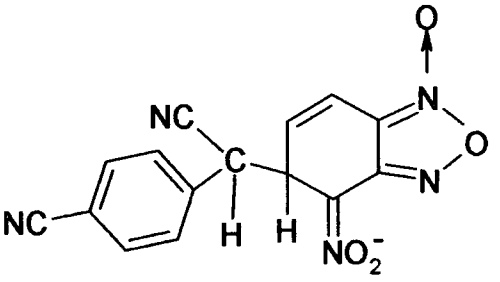

5.15

The lower reactivity of the benzyl triflone carbanions may result from their large bulk which will sterically inhibit their approach to the reaction centre. The low values obtained for β_{nuc} are compatible with a steric affect with large separation of reactants in the transition state.

The steric interactions in the σ-adduct will be higher for reaction with 1,3,5-trinitrobenzene (TNB) where attack must occur at a ring-position between two nitro-groups. It is significant that the carbanions from benzyl triflones did not form σ-adducts with TNB whereas carbanions from benzyl cyanides react readily with TNB[13].

The rapid elimination of HSO_2CF_3 from the σ-adducts formed from the nitrobenzofurazan derivatives may result from unfavorable steric interactions in the initially formed σ-adducts. These steric effects may be reduced in the alkenes formed after elimination (Scheme 5.7).

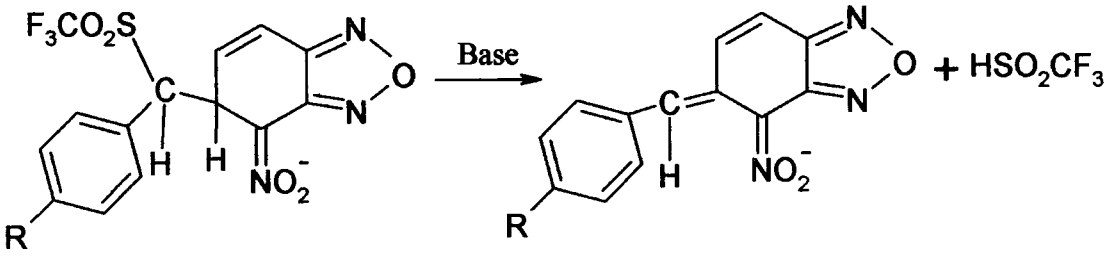

Scheme 5.7

5.6 References

[1] E. Buncel, M. R. Crampton, M. J. Strauss and F. Terrier, 'Electron Deficient Aromatic and Heteroaromatic-Base Interactions', 1984, Elsevier.

[2] F. Terrier, Chem. Rev., 1982, **82**, 77.

[3] F. Terrier, A. P. Chatrousse, E. Kizilian, V. N. Ignatev and L. M. Yagupolskii, Bull. Soc. Chem. Fr., 1989, 627.

[4] R. Goumont, E. Kizilian, E. Buncel and F. Terrier, Org. Biomol. Chem., 2003, **1**, 1741.

[5] F. Terrier, E. Magnier, E. Kizilian, C. Wakselman and E. Buncel, J. Am. Chem. Soc., 2005, **127**, 5563.

[6] R. Goumont, N. Faucher, G. Moutiers, M. Tordeux, C. Wakselman, Synthesis, 1997, 691.

[7] J. B. Hendrickson, A. Giga, J. Wareing, J. Am. Chem. Soc., 1974, **96**, 2275.

[8] C. H. Rochester, 'Acidity functions for concentrated solutions of bases', London, New York, 1970.

[9] R. Stewart and D. J. Kroeger, Can. J. Chem., 1967, **45**, 2163.

[10] F. Terrier, M.-J. Pouet, J.-C. Halle, S. Hunt, J. R. Jones and E. Buncel, J. Chem. Soc., Perkin Trans. 2, 1993, 1665.

[11] F. Terrier, A.-P. Chatrousse and F. Millot, J. Org. Chem., 1980, **45**, 2666.

[12] L. D. Nunno and S. Florio and P. E. Todesco, J. Chem. Soc., Perkin Trans. 2, 1975, 1469.

[13] J. H. Atherton, M. R. Crampton, G. L. Duffield and J. A. Stevens, J. Chem. Soc., Perkin Trans. 2, 1995, 443.

Chapter Six:

Experimental

6.1.3 Benzyl Triflones

The potassium triflinate (0.85 g) formed was heated under reflux with benzyl bromide (0.85 g, 1 equivalent) in acetonitrile for six hours, with potassium iodide (0.2 g) as catalyst[2]. The mixture was cooled and filtered and the product was obtained from the filtrate by rotary evaporation (Scheme 6.2).

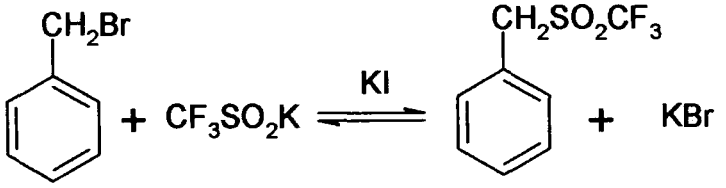

Scheme 6.2

Ring substituted benzyl triflones were prepared similarly. Analytical data are in Table 5.1.

Reaction of n-butyl bromide with potassium triflinate under similar condition did not give butyl triflone even after refluxing for several days.

6.1.4 Dabcohydrochloride

Solutions of Dabcohydrochloride (0.1 mol dm^{-3}) were prepared by taking 10 cm^3 of a solution of Dabco (1 mol dm^{-3}) in DMSO and adding one equivalent of concentrated aqueous hydrochloric acid (0.81 cm^3, 12.35 mol dm^{-3}). The solution was made up to 100 cm^3 with DMSO. Hence the solvent composition was *ca* 99/1 (v/v) DMSO/H_2O. To test for equivalence a volume of 0.5 cm^3 of the stock solution was diluted to 5 cm^3 with water and the pH was measured using a pH meter. The pK_a value of protonated Dabco in water is known[3] to be 8.82, hence the expected pH is 5.4 as shown by equation 6.1.

$$DabcoH^+ \rightleftharpoons Dabco + H^+$$

$$K_a = \frac{[Dabco][H^+]}{[DabcoH^+]}$$

Chapter six: Experimental

6.1 Materials

1,3,5-Trinitrobenzene (TNB) was a commercial sample. 4-nitrobenzofurazan and 4-nitrobenzofuroxan (NBF) were available from previous work and had been prepared by nitration of benzofurazan and benzofuroxan respectively. Other chemicals not described below used were the purest available commercial materials.

The solvent DMSO used was ACS spectrophotometric grade≥99.9%. AnalaR grade methanol was used.

6.1.1 7-Methoxy-4-Nitrobenzofurazan

To a solution of 7-chloro-4-nitrobenzofurazan (1.12 g, 5.622×10^{-3} mol) in methanol (50 cm^3) was added 1 mol dm^{-3} sodium methoxide solution (5.62 cm^3, 5.62×10^{-3} mol). The mixture was heated at 40 °C for 1 hour and then cooled and added to iced water when 7-methoxy-4-nitrobenzofurazan precipitated; m.p. = 113 °C, literature[1] 115 °C. ^1H NMR spectrum in d_6 DMSO, $\delta H_5 = 8.75$, $\delta H_6 = 7.06$, δ OMe = 4.21, $J_{56} = 8.6$ Hz.

6.1.2 Potassium Triflinate

Potassium triflinate was prepared, as previously described in the literature[2], by addition of trifluoromethanesulfonylchloride (4.5 g) over a ten minutes period to potassium iodide (8.9 g, 2 equivalents) slurried in cold acetone. The solvent was removed by rotary evaporation. The solid was washed with dichloromethane to remove iodine. Washing with ethyl acetate dissolved the potassium triflinate leaving solid potassium chloride. Evaporation of the ethyl acetate gave the product (Scheme 6.1), m.p. = 180 °C, literature[2] 180 °C.

$$CF_3SO_2Cl + KI \rightleftharpoons CF_3SO_2K + I_2 + KCl$$

Scheme 6.1

$$[H^+] = \sqrt{K_a[DabcoH^+]} \qquad (6.1)$$

A tolerance of 4.5<pH<6.5 was judged to be acceptable, corresponding to less than 1 % excess of Dabco or acid. If the value was not within these limits very small volumes of either Dabco solution or acid were added to the original stock solution in DMSO.

6.2 Instruments Used

6.2.1 UV/visible Spectrophotometry

Two UV/visible spectrophotometers were used, Shimadzu UV-2101 PC and Perkin-Elmer Lambda 2 instruments. The system basically consists of a UV/visible light source, wavelength selector, sample chamber, photomultiplier and data interpreter/display unit.

All spectrophotometric work was at 25 °C using thermostatted 1 cm path length quartz cuvettes. Absorption spectra were usually scanned between the wavelengths of 300 nm to 600 nm. The reference cell used for each spectrum contained the appropriate solvent and spectrophotometers were zeroed against this, prior to reaction.

6.2.2 NMR Spectroscopy

NMR spectroscopy was used in order to confirm the structures of substrates and to obtain structural information about intermediate and products.

Before any experimentation took place the ^1H NMR spectra of all the starting materials were recorded. This was to ensure that the compounds to be used were reasonably pure and also to provide reference chemical shifts when analyzing the spectra of intermediates and final products formed.

^{1}H spectra were recorded using a Bruker Avance-400 MHz instrument; spectra were generally recorded immediately after the solutions were made. All spectra were obtained with d_6 DMSO as the solvent.

6.2.3 Stopped-flow Spectrophotometry

An Applied photophysics SX-17 MV instrument was used. This instrument is extremely useful in kinetic studies because it has the ability to measure the rate constants of fast reactions with half lives as low as 2 ms. It is necessary for there to be a change in absorption in the UV/visible region during the reaction.

The two reactants, solution A and B are injected into the mixing chamber (M) in equal volumes. The mixing time is approximately 2 ms. The reaction mixture then flows into a thermostatted quartz cell (O), which is also connected to a third syringe.

The third syringe is pushed out and hits the microswitch on the backstop.

Monochromatic light of the required wavelength is passed by a fibre optic cable through the quartz cell and to a photomultiplier which measures changes in the absorption of light in the reacting solution and converts these into voltage reading. The voltage is then amplified and converted into absorbance data by computer.

The concentrations of all solutions prepared for use in the stopped-flow spectrophotometer were double the desired concentrations. This is due to the equal mixing of the two solutions. A schematic diagram of a stopped-flow spectrophotometer is shown in Figure 6.1[4].

Figure 6.1 Schematic diagram of a stopped-flow spectrophotometer.

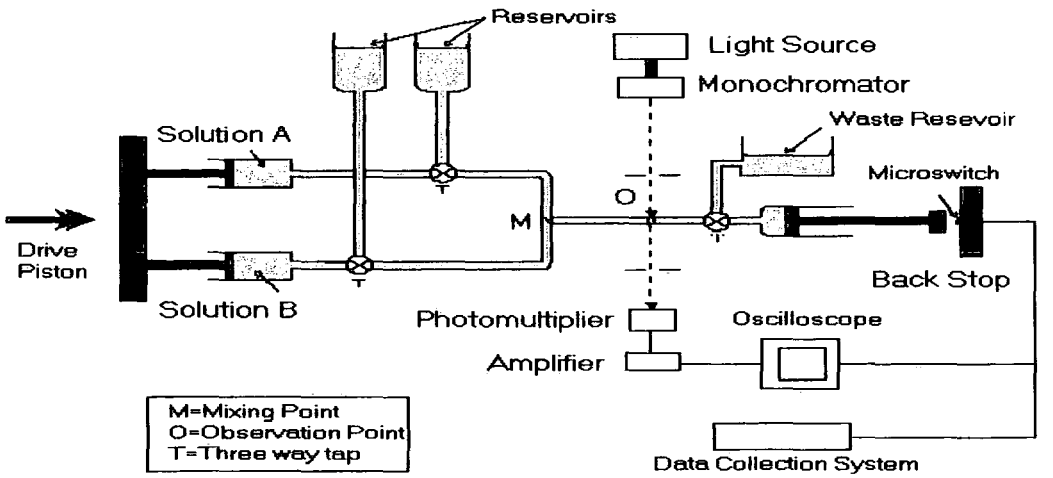

6.2.4 Mass Spectrometry

Mass spectrometry was used to confirm the alkene elimination product using a THERMO FINNIGAN (LTQ) negative electrospray mass spectrometer.

6.3 Data Fitting and Errors in Measurements

All UV/visible and stopped flow experiments were carried out under pseudo first order conditions. The rate constants were obtained by fitting the data to a single exponential model using the Scientist® computer package[5] in the case of conventional UV/visible is measurements, or by using the stopped-flow software for the measurements taken on the apparatus. Data collected from conventional spectrophotometers were converted to an ASCII format and processed using Microsoft Excel® prior to rate constant determination.

For reactions at equilibrium, such as that represented in Scheme 6.3, when one reactant, B, is in excess to the other, A, the reaction becomes first order and the rate is defined by equation 6.2.

$$A + B \underset{k_b}{\overset{k_f}{\rightleftharpoons}} C$$

Scheme 6.3

$$-\frac{d[A]}{dt} = k'_f[A] - k_b[C] \qquad \textbf{(6.2)}$$

where:

$$k'_f = k_f[B] \qquad \textbf{(6.3)}$$

Considering $[A]_e$ and $[C]_e$, the concentrations of A and C at equilibrium respectively, and x, the distance of these concentrations from equilibrium:

$$[A] = [A]_e + x \tag{6.4}$$

$$[C] = [C]_e - x \tag{6.5}$$

where:

$$x = [A] - [A]_e = [C]_e - [C] \tag{6.6}$$

Hence substitution in equation 6.2 gives:

$$-\frac{d([A]_e + x)}{dt} = (k'_f + k_b)x + (k'_f[A]_e - k_b[C]_e) \tag{6.7}$$

At equilibrium the rates of the forward, $k'_f[A]_e$, and reverse reactions, $k_b[C]_e$, are equal thus equation 6.7 can be expressed as:

$$-\frac{d[x]}{dt} = (k'_f + k_b)x \tag{6.8}$$

Hence the first order rate constant, k_{obs}, can be expressed as equation 6.9.

$$k_{obs} = k'_f + k_b \tag{6.9}$$

Thus the relation between [B] and k_{obs} is:

$$k_{obs} = k_f[B] + k_b \tag{6.10}$$

Hence plots of k_{obs} versus [B] are linear with k_f corresponding to the slope and k_b to the intercept.

Such plots were fitted using the linear regression tool of the data analysis function built into Microsoft Excel®. The software allowed calculation for both the gradient and the intercept as well as errors.

6.4 References

[1] L. D. Nunno and S. Florio and P. E. Todesco, J. Chem. Soc., Perkin Trans. 2, 1975, 1469.

[2] R. Goumont, N. Faucher, G. Moutiers, M. Tordeux, C. Wakselman, Synthesis, 1997, 691.

[3] D. D. Perrin, 'Dissociation Constants of Organic Bases in Aqueous Solution', Butterworths, London, 1972.

[4] B. G. Cox, 'Modern Liquid Phase Kinetics', Oxford University press Inc., New York, 1994.

[5] Micromath® Scientist® for Windows®, Version 2.02.

Appendices

Appendices

Appendix I

Derivation (page 60)

$$A + PhNH_2 \underset{k_{-1}}{\overset{k_1}{\rightleftharpoons}} Z \underset{k_{BH^+}[BH^+]}{\overset{k_B[B]}{\rightleftharpoons}} C$$

A = 1,3,5-trinitrobenzene (TNB), B = Dabco

$$\frac{d[C]}{dt} = k_B[B][Z] - k_{BH^+}[BH^+][C] \tag{7.1}$$

$$\frac{d[Z]}{dt} = k_1[PhNH_2][A] + k_{BH^+}[BH^+][C] - (k_{-1} + k_B[B])[Z] \tag{7.2}$$

$$\frac{d[Z]}{dt} = 0$$

$$[Z] = \frac{k_1[PhNH_2][A] + k_{BH^+}[BH^+][C]}{k_{-1} + k_B[B]} \tag{7.3}$$

Substituting in (7.1)

$$\frac{d[C]}{dt} = \frac{k_1[PhNH_2][A]k_B[B] - k_{BH^+}[BH^+]k_{-1}[C]}{k_{-1} + k_B[B]} \tag{7.4}$$

But:

$[A]_o = [A]+[Z]+[C]$
$[Z] = 0$
then, $[A] = [A]_o-[C]$, Substituting in (7.4)

$$\frac{d[C]}{dt} = \frac{k_1[PhNH_2][A]_0 k_B[B] - k_{Dabco}[Dabco]k_1[PhNH_2][C] - k_{BH^+}[BH^+]k_{-1}[C]}{k_{-1} + k_B[B]} \tag{7.5}$$

$\frac{d[C]}{dt} = 0$ and $[C]=[C]_{eq}$

$$0 = \frac{k_1[PhNH_2][A]_0 k_B[B] - k_B[B]k_1[PhNH_2][C]_{eq} - k_{BH^+}[BH^+]k_{-1}[C]_{eq}}{k_{-1} + k_B[B]} \tag{7.6}$$

Substracting from (7.5)

$$\frac{d[C]}{dt}\frac{1}{[C]_{eq}-[C]}=\frac{k_1[PhNH_2]k_B[B]+k_{BH^+}[BH^+]k_{-1}}{k_{-1}+k_B[B]} \quad (7.7)$$

Beer's low

$$Abs = \varepsilon[C]L \quad (7.8)$$

At equilibrium

$$Abs_{eq} = \varepsilon[C]_{eq}L \quad (7.9)$$

Substracting (7.9) from (7.8)

$$Abs_{eq} - Abs = \varepsilon([C]_{eq} - [C]) \quad (7.10)$$

$$\frac{dAbs}{dt} = \varepsilon\frac{d[C]}{dt} \quad (7.11)$$

Dividing (7.11) by (7.10)

$$\frac{dAbs}{dt}\frac{1}{(Abs_{eq}-Abs)}=\frac{d[C]}{dt}\frac{1}{([C]_{eq}-[C])} \quad (7.12)$$

k_{obs} is defined thus,

$$k_{obs}=\frac{dAbs}{dt}\frac{1}{(Abs_{eq}-Abs)} \quad (7.13)$$

Comparison between (7.7), (7.12) and (7.13) give

$$k_{obs}=\frac{k_1[PhNH_2]k_B[B]+k_{BH^+}[BH^+]k_{-1}}{k_{-1}+k_B[B]}$$

$$k_{obs}=\frac{k_1[PhNH_2]k_B[B]}{k_{-1}+k_B[B]}+\frac{k_{BH^+}[BH^+]k_{-1}}{k_{-1}+k_B[B]}$$

Appendix II

First year courses passed (October 2003-March 2004):

1-Fast reactions in solution.

2-Physical organic chemistry.

3-Practical spectroscopy.

4-Sepration methods.

Conferences attended during the course of the PhD:

Reaction Mechanisms VII (4th-8th July 2004).
University College Dublin, Dublin, Ireland.
Poster: "Kinetic and Equilibrium Studies of the Reactions of 1,3,5-Trinitrobenzene and 4-Nitrobenzofuroxan with Substitute Anilines in DMSO".

Physical Organic Chemist Residential Meeting (24th-25th July 2006), organised by RSC Organic Reaction Mechanisms Group, Losehill Hall, Castleton, Hope Valley.
Poster: "Carbanion Reactivity: Reactions of Carbanions from Nitroalkanes and Benzyl Triflones with Aromatic Nitro-Compounds".

Presentations:

Second year (9th April 2005).
"Rate-limiting Proton Transfer in the Reaction of 1,3,5-Trinitrobenzene and Anilines".

Final year (15th May 2006).
"Kinetic Studies of the Reactions of Some Aromatic Nitro-Compounds with Nitrogen and Carbon Nucleophiles".

Publication:

Rate-limiting Proton-transfer in the σ-Adduct Forming Reactions of 1,3,5-Trinitrobenzene and 4-Nitrobenzofuroxan with Substituted Anilines in Dimethyl Sulfoxide.

Basim H. M. Asghar and Michael R. Crampton, Org. Biomol. Chem., 2005, **3**, 3971.